

DOT/FAA/AR-99/2

Office of Aviation Research
Washington, D.C. 20591

Probabilistic Design Methodology for Composite Aircraft Structures

June 1999

Final Report

This document is available to the U.S. public
through the National Technical Information
Service (NTIS), Springfield, Virginia 22161.



U.S. Department of Transportation
Federal Aviation Administration

DTIC QUALITY INSPECTED 4

19990720 042

NOTICE

This document is disseminated under the sponsorship of the U.S. Department of Transportation in the interest of information exchange. The United States Government assumes no liability for the contents or use thereof. The United States Government does not endorse products or manufacturers. Trade or manufacturer's names appear herein solely because they are considered essential to the objective of this report. This document does not constitute FAA certification policy. Consult your local FAA aircraft certification office as to its use.

This report is available at the Federal Aviation Administration William J. Hughes Technical Center's Full-Text Technical Reports page: www.tc.faa.gov/its/act141/reportpage.html in Adobe Acrobat portable document format (PDF).

1. Report No. DOT/FAA/AR-99/2		2. Government Accession No.		3. Recipient's Catalog No.	
4. Title and Subtitle PROBABILISTIC DESIGN METHODOLOGY FOR COMPOSITE AIRCRAFT STRUCTURES				5. Report Date June 1999	
				6. Performing Organization Code 80378	
7. Author(s) M. W. Long and J. D. Narciso				8. Performing Organization Report No. 2-51410/7R-001	
9. Performing Organization Name and Address Northrop Grumman Commercial Aircraft Division P.O. Box 655907 Dallas, TX 75265-5907				10. Work Unit No. (TRAIS)	
				11. Contract or Grant No. FAA Grant No. 95G 0036	
12. Sponsoring Agency Name and Address U.S. Department of Transportation Federal Aviation Administration Office of Aviation Research Washington, DC 20591				13. Type of Report and Period Covered Final Report September 1995-October 1997	
				14. Sponsoring Agency Code AIR-100	
15. Supplementary Notes The Federal Aviation Administration William J. Hughes Technical Center COTR was Donald W. Oplinger.					
16. Abstract <p>Probabilistic structural analysis methods provide a means to quantify the inherent risk of a design and assess the sensitivities of design variables. This report is intended to introduce the subject of probabilistic analysis to engineers in the aerospace industry as well as act as a reference to guide those applying this technology. The current (deterministic) structural analysis approach is described, and its shortcomings are pointed out. The evolution of probabilistic analysis is presented, and the basic theory is discussed and explained via examples. Aerospace industry method development is described in detail, along with associated aerospace applications. An in-depth explanation of one industry method (Northrop Grumman) is given, along with an example run of their computer program. The report concludes with a consensus of potential benefits as well as potential issues of concern that must be addressed by those using these analysis methods.</p>					
17. Key Words Aircraft, Composites, Stress, Probabilistic methods				18. Distribution Statement This document is available to the public through the National Technical Information Service (NTIS) Springfield, Virginia 22161.	
19. Security Classif. (of this report) Unclassified		20. Security Classif. (of this page) Unclassified		21. No. of Pages 138	
				22. Price	

ACKNOWLEDGEMENTS

The authors wish to extend thanks to Mr. Donald Oplinger and Mr. Peter Shyprykevich of the FAA and Dr. Michael Shiao formerly of Galaxy Scientific Corporation for performing a thorough review and providing helpful comments to improve the content and readability of this document.

In addition, thanks to Mr. Rick Fucik of Northrop Grumman Commercial Aircraft Division, Mr. Joseph Soderquist of the FAA, and Dr. William Corley of the University of Texas at Arlington for providing overall direction and oversight for the effort.

Finally, thanks to Dr. Kuo-Feng Chung of the University of Texas at Arlington for his research efforts to acquire and review the hundreds of technical reports, papers, and presentations that provided the majority of the content of chapters 2 through 4.

TABLE OF CONTENTS

	Page
EXECUTIVE SUMMARY	xi
1. INTRODUCTION	1-1
1.1 Current Deterministic Structural Design Approach	1-1
1.2 Need for a Different Approach	1-1
1.3 Philosophy of Probabilistic Analysis	1-2
1.4 General Concept	1-3
2. HISTORY OF PROBABILISTIC DESIGN	2-1
2.1 Probabilistic Methodology Development	2-1
2.2 History of the Safety Factor	2-2
2.3 Historical Aspect of Acceptable Probability of Failure	2-4
3. GENERAL THEORY AND APPROACH	3-1
3.1 Basic Approach	3-1
3.2 General Steps to Probabilistic Analysis	3-2
3.3 Step 1—Identify Potential Failure Modes	3-2
3.4 Step 2—Define Acceptable Probability of Failure	3-2
3.5 Step 3—Develop Models for Stress and Strength	3-3
3.6 Step 4—Statistically Characterize Design Variables	3-3
3.6.1 Random Variable Definition	3-3
3.6.2 Continuous Random Variable Definition—The Probability Density Function and Its Associated Cumulative Distribution Function (CDF)	3-4
3.6.2.1 Normal Distribution	3-5
3.6.2.2 Lognormal Distribution	3-6
3.6.2.3 Weibull Distribution	3-7
3.6.2.4 Beta Distribution	3-7
3.6.2.5 Uniform Distribution	3-8
3.6.3 Discrete Random Variables and Poisson Distribution	3-9
3.6.4 Considerations for Composite Material Properties and Sample Size for Material Testing	3-10
3.7 Step 5—Structural Reliability Assessment	3-11
3.7.1 Single-Variable Failure Probability Determination	3-14

3.7.2	Two-Variable Probability of Failure Determination	3-15
3.7.2.1	Adjustment of PDF Parameters	3-15
3.7.2.2	First-Order Reliability Method	3-16
3.7.2.3	Lognormal-Lognormal Case	3-17
3.7.2.4	Other Two-Variable Cases	3-17
3.7.2.5	Two-Variable Example Problems	3-18
3.7.2.5.1	Scenario 1 (Normal-Normal Case)	3-19
3.7.2.5.2	Scenario 2 (Lognormal-Lognormal Case)	3-19
3.7.2.5.3	Scenario 3 (Lognormal-Normal Case)	3-20
3.7.2.5.4	Two-Variable Example Problem Summary	3-21
3.7.2.6	Probability of Failure With More Than Two Variables	3-22
3.7.3	Monte Carlo Simulation	3-22
3.7.3.1	Accuracy and Number of Required Trials	3-23
3.7.3.2	Generating Random Numbers From PDFs	3-24
3.7.3.3	Correlated Random Variables	3-25
3.7.3.4	Simulation Efficiency Improvement Approaches	3-25
3.7.3.5	Summary and General Discussion	3-25
3.7.3.6	Monte Carlo Example Problem	3-26
3.7.4	Response Surface Approximation Method	3-28
3.7.4.1	Step 1—Analyze Structure at Chosen Values	3-29
3.7.4.2	Step 2—Develop Regression Equation	3-30
3.7.4.3	Step 3—Develop Response Variable PDF	3-30
3.7.4.4	Step 4—Evaluate Probability of Failure	3-31
3.7.4.5	Response Surface Method Example Problem	3-31
3.7.5	Limit State Approximation	3-33
3.7.5.1	Most Probable Point Methods	3-33
3.7.5.1.1	Step 1—Transform Variables	3-34
3.7.5.1.2	Step 2—Identify Most Probable Point	3-35
3.7.5.1.3	Step 3—Develop g-Function and Determine Failure Probability	3-35
3.7.6	General Discussion of Limit State Approximation Methods	3-36
3.7.7	Limit State Approximation Example Problem	3-36

3.8	Step 6—Determine System Probability of Failure	3-39
4.	SUMMARY OF INDUSTRY EFFORTS: 1980 THROUGH 1996	4-1
4.1	Discussion and Explanation of Industry Efforts	4-1
4.2	Air Force	4-1
4.2.1	F-16 Risk Assessment	4-4
4.2.2	T-38 Risk Assessment	4-5
4.3	NASA Lewis	4-5
4.3.1	Integrate Probabilistic Analysis of Composite Structures (IPACS)	4-6
4.3.2	Integrated Composite Analyzer (ICAN)	4-8
4.3.3	Probabilistic Integrated Composite Analyzer (PICAN)	4-8
4.3.4	Adaptive Importance Sampling (AIS)	4-8
4.3.5	Probabilistic Fault Tree Analysis (PFTA)	4-8
4.3.6	Multifactor Interaction Equation (MFIE or TMFIE)	4-8
4.3.7	Parallel Virtual Machine (PVM)	4-9
4.3.8	Blade Assessment for Ice Impact (BLASIM)	4-9
4.3.9	Recent Work by NASA Lewis	4-9
4.4	Southwest Research Institute (SwRI)	4-9
4.4.1	Probabilistic Methods in NESSUS	4-11
4.4.2	Performance Functions in NESSUS	4-11
4.4.3	Recent Work	4-12
4.5	Jet Propulsion Laboratory (JPL)	4-13
4.5.1	PFA Methodology	4-13
4.5.2	NASA Marshall Conclusions and Recommendations	4-14
4.6	Rockwell International Corporation	4-15
4.6.1	SSME Turbopump Blade Application	4-15
4.6.2	Probabilistic Analysis Methodology Development Efforts	4-16
4.7	NYMA, Inc.	4-17
4.8	Aerospatiale	4-17
4.9	Pratt & Whitney	4-19
4.9.1	Methodology	4-20
4.9.2	Box-Behnken Experimental Design Procedure	4-21
4.9.3	Summary and Discussion of Pratt & Whitney Method	4-22
4.10	General Electric (GE)	4-23

4.11	NASA Marshall Flight Center (MSFC)	4-23
4.11.1	Probabilistic Methods Documentation	4-23
4.11.2	Proposed First-Order Method	4-24
4.11.3	Recent Work at NASA Marshall	4-24
4.12	Thiokol Corporation	4-24
4.13	NASA Langley	4-25
4.14	Grumman Aerospace	4-27
4.15	The Central Aero-Hydrodynamic Institute (TsAGI)	4-27
4.15.1	General Input Requirements to the Software	4-27
4.15.2	ProDeCompos Methodology	4-28
4.16	Nanchang Aircraft Manufacturing Group	4-29
4.17	Alpha STAR Corporation	4-30
5.	NORTHROP GRUMMAN METHODOLOGY THEORY	5-1
5.1	Historical Overview	5-1
5.2	NGCAD Probabilistic Design Methodology Overview	5-1
5.2.1	Design Process	5-3
5.2.2	Material Production	5-3
5.2.3	Manufacturing Process and Operations	5-3
5.3	Detailed Description of NGCAD Methodology	5-4
5.4	Additional Probability Calculations	5-18
5.5	Description of Program Output	5-18
5.5.1	Failure Probability Summary	5-18
5.5.2	Defect Summaries	5-19
5.6	Example Problem	5-20
5.6.1	Theoretical Background	5-20
5.6.2	Solution	5-23
6.	BENEFITS OF PROBABILISTIC ANALYSIS	6-1
7.	GROUND RULES, CONSIDERATIONS, AND LIMITATIONS	7-1
8.	REFERENCES	8-1

Appendix A—NGCAD Program Output

LIST OF ILLUSTRATIONS

Figure	Page
3-1 Probabilistic Analysis Concept	3-1
3-2 The Normal Distribution	3-6
3-3 The Lognormal Distribution	3-6
3-4 The Weibull Distribution	3-7
3-5 The Beta Distribution	3-8
3-6 The Uniform Distribution	3-8
3-7 The Poisson Distribution	3-10
3-8 Simplified (2-Dimensional) Formulation	3-12
3-9 Three-Dimensional Representation of Problem	3-12
3-10 17-7PH Steel Bar Loaded in Tension	3-13
3-11 Failure Probability Determination: One Variable	3-14
3-12 Transforming a U(0,1) Pick to Random Variable	3-24
3-13 17-7PH Steel Bar Loaded in Tension	3-26
3-14 Monte Carlo Simulation for Example Problem	3-27
3-15 RSM Procedure Using Three Levels of Design Variables	3-29
3-16 Transformation to Standard Normal Space	3-34
3-17 Original Parameter Space With Variables R and S	3-37
3-18 Reduced Coordinates Parameter Space With Variables R and S	3-38
3-19 Probabilistic Fault Tree Analysis Methodology	3-39
4-1 Integrated Probabilistic Analysis of Composite Structures	4-6
4-2 NASA Lewis Composites Probabilistic Analysis (IPACS)	4-7
4-3 NESSUS Features and Capabilities	4-10
4-4 NESSUS Probabilistic Fatigue Crack Growth Algorithm	4-12
4-5 Probabilistic Failure Assessment Methodology	4-14
4-6 SSME HPFTP Second Stage Turbine Blade FE Model	4-15
4-7 NESSUS CDF Results for Locations A and B	4-16
4-8 Febrel-MSC/NASTRAN Code Structure	4-17
4-9 Inspection Criteria and Probability Levels	4-19
4-10 Structure of Pratt & Whitney Probabilistic Design System	4-21
4-11 TsAGi Probabilistic Methodology	4-28
5-1 Overview of NGCAD Probabilistic Design Model	5-2
5-2 NGCAD Probabilistic Design Model Flowchart	5-5
5-3 Conversion of n_z Exceedance Data to $n_{z \max}$ Per Flight PDF	5-6
5-4 Typical Moisture Absorption Response	5-14
5-5 Effect of Temperature and Moisture on Compression Strength	5-14
5-6 Basic Stress and Material Strength Probability Density Functions	5-21
5-7 Applied Stress PDF and Material Strength CDF	5-21
5-8 Integrand: Product of Applied Stress PDF and Material Strength CDF	5-21
5-9 Maximum Stress and Component Strength PDFs	5-26
5-10 Integrand for Outcome No. 1: No Gust, No Defect	5-26

LIST OF TABLES

Table	Page
2-1 U.S. Aviation Fatal Accident Rates: 1983-1992	2-5
2-2 Normalized Risk Comparison	2-5
2-3 U.S. Major Airline Structural Failures	2-5
3-1 Probability Distribution Descriptions	3-5
3-2 Limit State Formulations Used in Aerospace Structure Design	3-13
3-3 Probability Distribution Transformations	3-16
3-4 Combining Normal Distributions	3-16
3-5 Probability of Failure Expressions for PDF Combinations	3-18
3-6 Two-Variable Example Summary (Significant Overlap)	3-21
3-7 Two-Variable Summary Illustrating Tail Sensitivity	3-22
3-8 Monte Carlo Simulation Results	3-26
3-9 Box-Behnken Experimental Design Matrix	3-30
3-10 Probability Distribution Definition for Hoop Stress Determination	3-31
3-11 Low, Nominal, and High Definitions for Variables	3-32
3-12 Three-Level Box-Behnken Design Test Matrix	3-32
3-13 Results of FEM for Given Input Variable Levels	3-32
4-1 Probabilistic Methods Publications—Academia	4-1
4-2 Aerospace Companies With Published Probabilistic Methods Articles	4-2
4-3 Box-Behnken Design of Experiments Parameters	4-22
5-1 Probability Distribution Transformations	5-2
5-2 Lear Fan 2100 Curve Fitting Optimization	5-7
5-3 Operational Damage; Source: Two U.S. Airlines (1993)	5-12
5-4 Example Probability of Failure Listing	5-18
5-5 Manufacturing Defect Summary	5-19
5-6 Failure Probabilities Associated With Outcomes	5-24
5-7 Results Corresponding to the Four Outcomes	5-25
5-8 Failure Probabilities Associated with M.C. Trials	5-25
5-9 Trapezoidal Rule Calculation (No Gust, No Defect)	5-27

EXECUTIVE SUMMARY

It appears inevitable that the aerospace industry, as well as many other industries, will eventually incorporate probabilistic analysis methods to some degree. Probabilistic structural analysis methods, unlike traditional methods, provide a means to quantify the inherent risk of a design and to quantify the sensitivities of design variables. The degree to which these methods are successfully applied depends on addressing the issues and concerns discussed in this report. Certainly, one issue is to disseminate familiarity and basic understanding of this technology.

This report is intended to introduce the subject of probabilistic analysis (also known as probabilistic design) to engineers in the aerospace industry as well as act as a reference to guide those applying this technology. The level of mathematical complexity is aimed at those with limited statistical training; numerous references are given throughout that point to more elaborate details of the methods.

Section 1 of this report explains shortcomings of the current structural analysis approach and the potential for improvement via incorporation of probabilistic analysis methods. The evolution of probabilistic analysis is given in section 2, dating back to the 1940's when A.G. Pugsley first proposed correlating loads and strengths with structural accident rates. The basic theory of probabilistic analysis is discussed and explained via examples in section 3, and the four major techniques (integration, simulation, response surface, and limit state approximation) for assessing structural reliability are introduced.

Section 4 tells who has been using the probabilistic approach and lists specific design analysis applications. An in-depth look at one industry method (Northrop Grumman Commercial Aircraft Division) is given in section 5. A consensus on the benefits and limitations of the probabilistic approach from numerous authors who have published technical reports in the field is presented in sections 6 and 7, respectively.

1. INTRODUCTION.

Knowing the inherent risk of failure in any design is becoming increasingly important to both the manufacturer and the customer. Designers and management must concern themselves with the ability to assess risk, identify parameters which drive risk, and minimize the risk given other program constraints. Analysis of aircraft structure using probabilistic methods provides a tool for meeting these needs.

This section begins with an overview of the current structural analysis approach, expounding on its shortcomings and listing potential dilemmas in applying the approach to future aerospace designs. The general probabilistic analysis approach is then explained, with discussion on how it can address these problems.

1.1 CURRENT DETERMINISTIC STRUCTURAL DESIGN APPROACH.

At each location in the structure, a most severe state of stress occurs from some applied load condition. This stress is referred to as a limit stress, and the load causing it is a limit load. The "factor of uncertainty" (formerly known as the factor of safety) multiplies limit loads or stresses to obtain design loads or stresses and is used to account for the possibility that an actual load will exceed a predicted load or that the actual strength will be less than the expected strength. This factor, discussed in detail in section 2.2, has evolved from experience and operation of aerospace vehicles.

The design criteria for a structure also specifies allowable strengths for the various materials used. Authorized mechanical properties of materials having a prescribed statistical basis are presented in MIL-HDBK-5 for metals and MIL-HDBK-17 for composites. The allowable structural strength is determined from test data, either from a representative structure or from tests on functionally similar structure.

Analysis performed by applying ultimate load to the structure modeled with the allowable strengths yields "margins of safety" values at each location, which are usually optimized to positive values close to zero. A margin of safety of zero implies the ultimate load (1.5 x design limit load) creates a stress that is equal to the resistive strength of the component. Once the analysis shows these margins to be acceptable, the deterministic design analysis is labeled a success. Static and fatigue tests are normally performed on the full structure to verify the structure will not catastrophically fail under ultimate load and will endure a specified amount of time under repeated or cyclical loading.

1.2 NEED FOR A DIFFERENT APPROACH.

Current aerospace design analysis methods do not directly account for the random nature of most input parameters. The result of treating parameters such as material properties, geometry, environment, and loads as singly determined (deterministic) values is a design of unknown reliability, or conversely, unknown risk.

Risk is defined as the chance of encountering harm or loss. Virtually all activities, including air travel, contain risk, but we are willing to accept the risk levels, given our life experience. When

we elect to participate in these activities, we accept the risk, either overtly or tacitly. The minimization of risk of aircraft structural failure has been handled in the design phase by the application of factors of uncertainty and the use of judicious material properties. The number of aircraft accidents attributable to structural airframe component failure has been very low in the past 30 years. Yet a design process yielding unknown risk poses the following problems for future designs:

- As designs grow more critical and competitive, there is a need to quantitatively assess and optimize reliability (or minimize risk), given other program constraints. Recent military guidelines are emphasizing the importance of reliability on par with performance and cost. With an ever-increasing emphasis on warranties, both commercial and military, quantified reliability is an essential feature.
- New aircraft developments (e.g., reusable launch vehicle, high-speed civil transport) are departing dramatically from traditional environments. Application of historical uncertainty factors may not be sufficient to provide adequate safety. Conversely, the trend to design to all possible unfavorable events occurring simultaneously could produce an unacceptable weight.
- The aerospace industry has seen a steady rise in the percentage of composite airframe structures. These materials have more intrinsic variables than metals due to their heterogeneity and are subjected to more manufacturing process sources of variation. To account for uncertainties, relatively large knockdown factors are employed, which reduce the material allowable. This results in a substantial weight increase without a quantifiable increase in structural reliability.

1.3 PHILOSOPHY OF PROBABILISTIC ANALYSIS.

All design parameters are treated as variables and the basic result from the analysis is a probability of failure, or risk¹. The effect of realistic variability of the design input parameters can thus be obtained. Specifically, given the structural analysis methodology in conjunction with statistical characterization of applied loading, geometry, material behavior, and expected environment, the probabilistic structural analysis methodology is capable of producing:

- Safety (risk) quantification
- Design variable sensitivity analysis
- Cost/weight reduction scenarios
- Optimum inspection intervals

¹ In this handbook, no distinction is made between the terms "probability of failure" and "risk." Actually, there is a difference, in that probability of failure is associated with the quantitative measure of reliability, whereas risk includes economic consequences of failure. Because these considerations will not be addressed in the handbook, the terms will be used interchangeably.

Obviously, statistical definition of the design parameters must be developed very carefully, as this is the crux of the analysis. There must be a thorough understanding of the range and variability of input values, particularly those which are risk sensitive, i.e., producing significant changes in risk. Statistical definition of these must be reviewed from the perspective of a wide range of technologies.

Knowing each design parameter's contribution to overall risk enables the engineer to know where to look to improve reliability. Manufacturing process controls can be tailored to focus on parameters that have the most payoff in terms of overall reliability. Of particular interest to aircraft manufacturers is the ability to optimize weight of components for a given risk level.

1.4 GENERAL CONCEPT.

The foundation of probabilistic design involves basing design criteria on reliability targets instead of deterministic criteria. Design parameters such as applied loads, material strength, and operational parameters are researched and/or measured, then statistically defined. A probabilistic analysis model is developed for the entire system and solutions performed to yield failure probabilities.

The solution includes a number of locations and failure modes. Each location requires corresponding applied stress and material strength distributions. The applied stress is usually obtained from finite element modeling, coupled with conventional structural mechanics approaches. Mathematically, the applied stress and material strength distributions are generally assumed to be independent. The general concept is to integrate the joint probability of applied stress and material strength over the region where stress exceeds strength. The result of this integration is the probability of structural failure.

Sensitivity analysis and/or optimization can be performed once the probabilistic model has been established. The concept is that once design driver contributions are identified, the design can be optimized for the given constraints, while maintaining the overall failure probability at an acceptable level. Sensitivity analysis reveals the major contributors to risk; this allows the analyst to vary the design parameters to produce acceptable reliability at minimum weight, for example.

2. HISTORY OF PROBABILISTIC DESIGN.

One author [1] suggests "the revolutionary concept separating modern times from the past is the mastery of risk: the notion that the future can be at the service of the present, and not a whim of the gods." Serious study of risk began in the mid-1600s, when a French nobleman with a taste for both gambling and mathematics challenged famed mathematician Pascal to solve a puzzle: how to divide stakes of an unfinished game of chance (dice) when one player was ahead. Pascal turned to fellow mathematician Fermat and the outgrowth of their collaboration was the discovery of probability theory. For the first time, one could make decisions and forecast the future with the help of numbers. During the next 100 years, mathematicians such as Bernoulli and Gauss developed probability theory into a powerful instrument for organizing and applying information.

Probability has always carried a double meaning, one looking into the future and the other interpreting the past; one concerned with our opinions and the other concerned with what we actually know. Oftentimes, what we think we know from the past is no longer applicable to the present. We are never certain, always ignorant to some degree, never knowing for sure how good our sample is. Given this, we must still strive to generate sample data in which we have high confidence and is an accurate indicator of future behavior.

Today, the challenge to aircraft designers and analysts is to accurately define what data is obtainable, assess the degree of confidence to which these data apply to the current situation, statistically define the data, and predict performance. One must accept the notion that there is a finite (however small) probability of component failure. A scientist who developed the Saturn 5 rocket put it this way: "You want a valve that doesn't leak and try everything possible to develop one. But the real world provides you with a leaky valve. You must determine how much leaking you can tolerate." Similarly, we must determine levels of aircraft component failure we can tolerate, in concert with manufacturing, economic, performance, etc., constraints.

2.1 PROBABILISTIC METHODOLOGY DEVELOPMENT.

The concept of probabilistic aircraft structural risk assessment has been around for quite some time. In 1942, A. G. Pugsley [2] (Great Britain) published "A Philosophy of Aeroplane Strength Factors" to propose correlating loads and strengths with recorded structural accident rates. He states "By adopting the principle that neither design loads nor safety factors and permissible stresses should be specified arbitrarily, it will be possible to not only eliminate inadequate design, but frequently to achieve considerable economy."

The following quotes are from Alfred Freudenthal (Civil Engineering professor) in his 1945 paper [3] The Safety of Structures: "The true character of the safety factor is disclosed by the introduction of a statistical concept of physical qualities, according to which the individual properties composing strain and resistance are represented by frequency distributions, instead of by individual values... By application of the theory of probability, the concept of safety can be rationalized." Freudenthal's paper sparked international interest in structural safety; structural reliability theory was discussed and formulations presented in papers [4] from British, French, Spanish, and Swedish authors during the early 1950s. The theory was fueled by Weibull's success (1951) in developing robust statistical representations of material strength.

In 1954, Freudenthal [5] published "Safety and the Probability of Structural Failure" in which he expanded the discussion of failure probability. He realized a problem which still may exist to a degree today: "...the concept of safety is deeply rooted in engineering design, whereas the notion of finite (no matter how small) probability of failure is repulsive to a majority of engineers." In discussions at the end of reference 5, Jose Corso and Larry Lawrence, fellow civil engineers, carried the math one step further by simplifying the calculation of failure probability for the case of normally distributed stress and strength. This approach was the foundation of the First-Order Reliability Method yielding the Safety Index and will be further discussed in section 3.

In 1956, the Task Committee on Factors of Safety, American Society of Chemical Engineers, supported by the Office of Naval Research, Air Force Materials Laboratory, and Advanced Research Projects Agency, was commissioned to (1) clearly define the term factor of safety; (2) survey the field as to currently used factors; and (3) recommend forms and values of these factors to be used in the future. At the end of 10 years, the final report [6] conveyed a sense of frustration: "although the committee has not been successful in its efforts to resolve the 'factor of safety' question, it is believed that the probability approach deserves considerably more study than it has received."

This final report defined the following needs of successful structural reliability analysis: (1) improve load sequence representation; (2) describe failure conditions more realistically; (3) define statistical variation of load and resistance (strength) with more confidence; and (4) define design criteria taking reliability concepts into account. Thus the exhortation was made to conduct more research.

Although research continued during the 1960s, lack of acceptance seemed to be caused by the perceived lack of a problem with using conventional methods. The durability and damage tolerance approach was recognized in the 1960s and adopted in the mid-1970s, based on fatigue crack growth prediction laws; this seemed to allay safety concerns. Probabilistic methods were thought to require a mountain of data, and the payoff was not convincing. One author stated "Employing statistics and probability theory seemed to carry an aura of mystery for many practicing engineers."

In 1967, C.A. Cornell [7] proposed a second-moment format for evaluation of structural reliability. This approach generates a "safety index" calculated from the means and variances (the variance is the second moment of a distribution) of the parameter distributions. The safety index is considered to be a measure of reliability, and is an alternative to numerically integrating the joint probability density function to determine a probability of failure. In 1973, Lind [8] demonstrated that Cornell's safety index could be used to derive safety factors on applied loads and resistance. This was a milestone; reliability analysis was at long last related to accepted (civil engineering) methods of design. Subsequent refinements were made by Hasofer and Lind [9], whose method (1974) is considered to be the foundation of probabilistic design theory.

2.2 HISTORY OF THE SAFETY FACTOR [10].

As stated in section 1, the concept of the factor of safety is to provide a safe operating margin between an operational level and a design level of strength. Just how safe is unknown, however,

because of the uncertainty in structural loads, design analysis, materials, operation, and environment.

By the early 1930s, a factor of safety philosophy had evolved but had not been formalized. Airplanes were flying at two-thirds of ultimate, it was agreed that permanent set was not desirable, and permissible limit loads were being pushed as high as possible. Introduction of the V-G (velocity-acceleration) diagram, which establishes a relationship among design load factor, maximum aerodynamic maneuver capability, and operational maneuver limits, helped rationalize criteria for utilizing the factor of safety. In March 1934, the 1.5 factor of safety became a formal requirement of the Air Corps. There was some thought that the 1.5 factor was derived from a ratio of aluminum ultimate to yield stress, but this is just a coincidence which tended to support the selection of 1.5.

This factor did not evolve as the result of some concentrated effort to derive a useful factor. Rather, it evolved together with other design requirements as part of an overall desire to rationalize structural design criteria. Its use is accepted by most engineers without question. When problems have arisen or structural failures have occurred, changes were made to design specifications, load prediction techniques, manufacturing techniques, etc., but the factor of safety value has never been changed.

The 1.5 factor is rational because it is based on what were considered to be representative ratios of design to operating maneuver load factors experienced during the 1920s and 1930s. Yet at the same time it is arbitrary because we do not know the exact design, manufacturing, and operating intricacies and variations it protects against or how to quantify them. Neither can the degree of inflight safety provided by the 1.5 factor be quantified; but its successful history cannot be lightly dismissed.

Interest in replacing the factor of safety approach with probabilistic interpretations of structural safety initiated in the late 1950s. The continued application of the factor of safety approach is challenged by some engineers, but there is reluctance to undergo a major change in design philosophy, especially one which could encourage legal entanglements. The factor of safety still covers many unknown contingencies, and for this reason, some engineers believe there will always be a need for some such factor.

Recently, the factor of safety was renamed to "factor of uncertainty." A draft (June 1995) of the Joint Service Structures Specification Handbook states "The selection of the factor of uncertainty, formerly called the factor of safety, should be made by assessing the factors that have been used on similar air vehicles performing similar missions. The value for manned aircraft has been 1.5.... The selected value of the factor of uncertainty should be increased to account for above normal uncertainty in the design, analysis, and fabrication methods when the inspection methods have reduced accuracy or are limited by new materials and fabrication methods and where the usage of the air vehicle is significantly different.... The use of reduced factors of uncertainty needs to be carefully defined and justified."

If variability in design, manufacturing, and operating environments can be reduced, then a reduction of the 1.5 factor of uncertainty could be justified. If, however, the introduction of new

material systems (for example) actually increases the variability, then the 1.5 factor may be unconservative and have to be increased. In either case, probabilistic analysis can be used to quantify these effects, hence serving a useful purpose. It would not necessarily replace the factor of safety as a design criterion, but would help to establish the optimum factor of uncertainty level.

2.3 HISTORICAL ASPECT OF ACCEPTABLE PROBABILITY OF FAILURE.

A.G. Pugsley's book "The Safety of Structures" (1966) refers to acceptable structural accident rate, developed from British military flight data during the late 1930s, as being in the region of 1 per 10^7 flight hours. "Under war conditions," he states, "this rate rose somewhat, primarily due to changes in loading and usage; by the time it reached 5 in 10^7 flight hours, pilots and crews began to regard the type as structurally dangerous, and wanted design changes.... Post-wartime civil airline experience has confirmed this tendency to react against structural failure very strongly, ...and has lead to the belief in airline operation that the structural accident rate should not exceed 1 in 10^7 hours."

In his 1954 paper [5], A.M. Freudenthal, concerning civil engineering structures, addressed the subject of acceptable probability of failure, stating "The choice of the specification of probability of failure depends on the importance and cost of the structure as well as on the consequences and cost of failure." Concerning aviation, he referred to "...the usually accepted design value (risk) of 2 in 10^7 flying hours."

Released in 1990, the United States Air Force general specification for aircraft structures (AFGS 87221A) states that when probabilistic methods are used to design airframe structures, the maximum acceptable frequency of structural failure leading to the loss of the aircraft is 1×10^{-7} occurrences per flight (or 1 occurrence in 10^7 flights).

Table 2-1 shows accident rates from U.S. aviation in the period from 1983 to 1992, along with the 10-year average. Only one of these accidents is known to have resulted from structural failure. The rates for structural incidents are in need of further study at this time. Table 2-2 gives a summary of the risk of different activities put in appropriate units: deaths per person, per hour of exposure. This shows the relative risk of aviation accidents compared to risks encountered in everyday life. These aviation accident rates were taken from 1985 to 1994 data [11].

A study of U.S. major airline structural incidents during 1985-1994 was performed using data from the FAA Incident Database in the FAA Internet Website. Nearly 5,500 incidents were identified, representing approximately 10^8 flights. After individual review and subsequent screening, 62 of the 5,500 incidents resulted from structural failure. Of the 62 U.S. major airline structural incidents, one resulted in a fatal accident, namely the Aloha Airlines accident in 1988. Resulting rates are presented in table 2-3.

TABLE 2-1. U.S. AVIATION FATAL ACCIDENT RATES: 1983-1992

	Fatal Accident Rates Per Million Flights										
	1983	1984	1985	1986	1987	1988	1989	1990	1991	1992	Avg.
Scheduled Service ⁽¹⁾	0.57	0.17	0.66	0.29	0.41	0.27	0.69	0.38	0.40	0.26	0.41
Nonscheduled Service ⁽¹⁾	0	0	8.40	3.65	0	0	5.32	0	0	0	1.74
Commuter Carriers ⁽²⁾	0.43	2.61	2.37	0.71	3.56	0.69	1.77	0.95	2.94	2.43	1.85
On-Demand Taxis ⁽³⁾	11.4	8.10	13.6	11.5	11.3	10.6	8.3	12.5	11.6	10.8	11.0
General Aviation ⁽⁴⁾	19.4	18.7	17.5	17.5	16.5	16.8	15.3	15.6	15.2	15.0	16.8
Total Rate	15.1	14.4	13.7	12.8	12.2	12.1	11.4	11.5	11.2	11.0	12.5

(1) Includes accidents involving deregulated all-cargo air carriers and commercial operators of large aircraft during scheduled 14 CFR 121 operations.

(2) Includes accidents involving all-cargo air carriers during scheduled 14 CFR 135 operations.

(3) Includes accidents involving all air carriers during scheduled 14 CFR 135 operations. Assumed 1 hr/ft

(4) All operations other than those operating under 14 CFR 121 or 14 CFR 135. Assumed 1 hr/ft.

TABLE 2-2. NORMALIZED RISK COMPARISON

Cause	Number of Deaths	Death/(Person-Hour Exposure)
Motor Vehicle Accident ¹	43,000	0.49×10^{-6}
Home Accident ¹	26,700	0.03×10^{-6}
Work Accident ¹	5,000	0.02×10^{-6}
Aviation Accident ²		
- Major Airlines	169	0.21×10^{-6}
- Commuter Airlines	30	0.99×10^{-6}

1—Based on 1994 data. National Safety Council "1995 Accident Facts" publication

2—Based on average from 1985-1994 data. FAA Statistical Handbooks of Aviation, 1985-1994

TABLE 2-3. U.S. MAJOR AIRLINE STRUCTURAL FAILURES
Incidents and Accidents per Flight

Type	Number (1985-1994)	Incidents (Accidents) Per Flight
Total Incidents	5,497	5.5×10^{-5}
Structural Incidents	62	6.2×10^{-7}
Structural Accidents	1	1×10^{-8}

3. GENERAL THEORY AND APPROACH.

This section will present the fundamental theory and concepts behind probabilistic methods and list the general steps involved in performing a probabilistic structural analysis. A list of six general steps is given, followed by a detailed discussion of each step in sections 3.3 to 3.8. In section 3.7, the four main approaches to probabilistic analysis (integration, Monte Carlo simulation, response surface approximation, and limit state approximation) are explained. Simple example problems are shown, starting with one variable, then two variables (integration) with normal/normal, lognormal/lognormal and lognormal/normal distributions. A three-variable case is presented, leading into discussion of Monte Carlo simulation, response surface, and limit state approximation methods; there are accompanying example problems illustrating these methods.

3.1 BASIC APPROACH.

The basic probabilistic approach can be summarized as the statistical definition of all input variables required for structural analysis methods, statistical definition of the resulting stress and strength of the structure associated with predicted failure modes, and evaluation of the resulting probability of structural failure. Figure 3-1 illustrates this process. The left-hand side shows the input data to determine the applied stress distribution, with each having a statistical distribution, while the right-hand side depicts the various capabilities of the structure. The middle shows the output of the process, that being an applied stress and resistive component strength distribution, per failure mode, with an associated probability of failure.

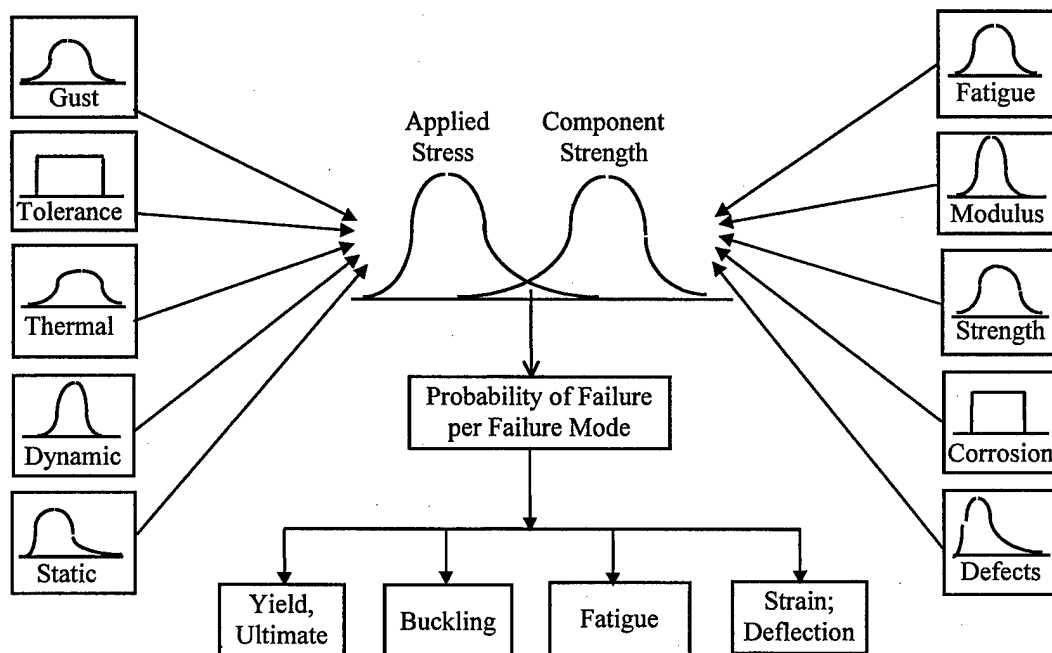


FIGURE 3-1. PROBABILISTIC ANALYSIS CONCEPT

3.2 GENERAL STEPS TO PROBABILISTIC ANALYSIS.

1. Potential failure modes of the structure under anticipated loading conditions are identified.
2. An acceptable probability of failure (or minimum reliability) is established for each failure mode and/or location on the structure.
3. Existing structural analysis methods are used to model the internal response (stresses) of the structure to applied loads and to model the stiffness of the structure.
4. Random design variables affecting both stress and strength are statistically defined.
5. Probabilistic analysis methods are applied to determine the probability of failure at predetermined locations.
6. System probability of failure is modeled as a function of individual location failure probabilities and comparison is made to the acceptable probability of failure.

3.3 STEP 1—IDENTIFY POTENTIAL FAILURE MODES.

The engineer must understand the general behavior of the structure being analyzed. The failure mode can change from location to location on the structure, with some areas being subject to more than one failure mode. This is where engineering know-how is essential.

Causes of structural failure are usually grouped into two broad categories: static failure, which is usually breakage or buckling, and cyclic failure, characterized by fatigue and crack growth. Probabilistic methods have been developed to assess structural failure probability for both static and fatigue scenarios. Failure under static loading (steady or steadily increasing) can be caused by either overstress resulting from the applied load exceeding the load-bearing capacity of the structure or fracture resulting from a combination of applied load and an existing crack growing to critical length.

Structures subjected to cyclic (repeated) loadings can be life-limited by many factors such as the presence of manufacturing defects (e.g., cracks, voids, and delaminations) or cyclic operating temperatures, pressures, and loads. Metallic structural cyclic failure is usually associated with the growth of cracks, whereas composite cyclic failure (although not fully understood) has been modeled assuming cyclic delamination growth and/or cracking of the matrix material.

3.4 STEP 2—DEFINE ACCEPTABLE PROBABILITY OF FAILURE.

The acceptable probability of failure is the criterion to which the results of the probabilistic analysis will be compared to determine if the design is acceptable. Specification of this acceptable, or target, probability of failure for the total structure is a complex issue that generally will not be decided upon by the engineer performing the probabilistic analysis. Legal, technical, and socioeconomic considerations are involved. The agency certifying the structure should be responsible for setting this overall specification for the structure. Proposed failure probability

values seen most often in literature range from 1×10^{-7} to 1×10^{-9} per flight, but this issue remains unresolved at the present time.

If an engineer is performing a probabilistic analysis on only a portion of the structure, there exists the challenge to set a target probability of failure for that component, given the total system target level. Depending on the complexity (and dependency) of the structural components, this task could range from being straightforward (e.g., all components are equally critical and independent) to requiring use of fault tree analysis methods to account for redundant load paths. Modeling system probability is discussed further in this section.

3.5 STEP 3—DEVELOP MODELS FOR STRESS AND STRENGTH.

It is important to note that traditional structural analysis and finite element theory are not being supplanted, but rather are an integral part of the probabilistic design process. The probabilistic structure must be built around the existing structural analysis process. Optimally, probabilistic analysis codes should be interfaced to these structural analysis programs and procedures so that the structural analysis output can be directly fed to the probabilistic program and vice-versa.

3.6 STEP 4—STATISTICALLY CHARACTERIZE DESIGN VARIABLES.

In most probabilistic applications, the two desired probability density functions (PDFs) from which structural reliability is determined represent the maximum stress the structure will experience and the material strength of the structure to resist this maximum applied stress. Unfortunately, these PDFs are not directly available and must be generated from test data and/or analysis.

A common procedure to accomplish this consists of a goodness-of-fit test between the theoretical distribution and the actual data. In some instances, a goodness-of-fit test will not reject several types of distributions, so the engineer must choose among them. The calculated probability of failure is sensitive to the underlying form of the distribution if the probability is sensitive to the tails of the distribution, which is usually the case for aircraft structural reliability. Therefore choice of the appropriate distribution is very important. This section is intended to give considerations for identifying appropriate distributions of design variables. Two excellent references for identifying appropriate distributions are (1) a book entitled *Statistical Distributions*, by M. Evans [12] and (2) a technical paper entitled "Statistical Characterization of Life Drivers for a Probabilistic Design Analysis", by E. Fox [13].

3.6.1 Random Variable Definition.

The words "random variable," in ordinary lay usage, connote that one does not know what value a variable will assume. However, for mathematicians this term has precise meaning: though we do not know this variable's value in any given case, we do know the values it can assume and the probabilities of these values. The result of a single trial associated with this random variable cannot be precisely predicted from these data, but we can reliably predict the result of a great number of trials. The more trials there are (larger sample), the more accurate the prediction. Thus, to define a random variable, we must indicate the values it can assume and the probabilities of these values.

Design variables exhibit differing variability according to the processes under which they are defined or the environment in which they are tested. Some variables have a large amount of data, such as those monitored by statistical process control (SPC), while other variables may have limited data available. Some variables are naturally skewed about a mean value, such as the maximum normal load factor at the aircraft center of gravity (n_z), while others may be symmetric about a mean value, such as a geometric tolerance.

The first delineation of random variables is whether the variable is continuous or discrete. A random variable is considered to be continuous if it can assume any value in a certain interval (a, b), whereas a random variable is called discrete if it can assume only a finite set of values in the interval.

3.6.2 Continuous Random Variables—The Probability Density Function (PDF) and Its Associated Cumulative Distribution Function (CDF).

If a random variable is defined in the interval (a, b), there may be an infinite number of possible values the variable can assume from a to b . Therefore the probability that the variable equals a certain value, say x , in the interval has no physical meaning and is zero. Physically meaningful would be the probability that the variable falls into a subinterval x to $x + \Delta x$. The probability density function (PDF) describes the distribution of such probabilities as a function of x . Commonly encountered examples of such PDFs are the normal, lognormal, Weibull, beta, and uniform; each of these will be discussed below. (The cumulative distribution function (CDF), the integral of the PDF from $-\infty$ to some finite value of the argument represents the probability that an arbitrarily selected value of the argument will be less than the value of the CDF for that argument.)

Because some distributions are unbounded on at least one side, they often specify expected frequency information in an extreme region where there is no observed data. Yet this extreme region largely influences the probability of failure; therefore these distributions should be used only if there is a large amount of data available (enough to obtain extreme values) or where experience has shown the distribution to be of a certain form. Examples of variables with potentially large amounts of data include SPC variables for a manufacturing process and accelerometer data for aircraft structure.

Continuous distributions which are bounded on both sides include beta and uniform distributions. The accuracy of these distributions depends primarily on determining the physical bounds. Smaller amounts of data are normally required because the data are used only to determine the most likely values between the bounds, i.e., there are no extreme values that need to be modeled in the tails of the distribution.

If it is impossible to define one value as being more likely than another, the uniform distribution is used. If some values have a greater chance of occurring than others, the beta distribution can be used. In addition to uniform and beta, continuous distributions such as normal, lognormal, and Weibull can be truncated at upper and/or lower limit values. The limits are determined by engineering judgment or physical limitations associated with the variable.

3.6.2.1 Normal Distribution.

The normal (Gaussian) distribution is the most widely known distribution. The equation shown in table 3-1 even appears on the German ten-mark bank beside the portrait of C.F. Gauss. The normal is a two-parameter distribution with mean and standard deviation, and as most engineers know, is symmetrical about its mean. Figure 3-2 shows the normal with the effect of different standard deviations. As σ decreases, the PDF gets squeezed toward the mean. The standard deviation is also the distance between the mean and the points of inflection of the PDF.

TABLE 3-1. PROBABILITY DISTRIBUTION DESCRIPTIONS

Type	Parameters	Probability Density Function (PDF)
Normal	Mean: μ ; Std. Dev: σ	$f(t; \mu, \sigma) = \frac{1}{\sigma\sqrt{2\pi}} e^{-\frac{1}{2}\left(\frac{t-\mu}{\sigma}\right)^2}$, where $-\infty < t < \infty$
Lognormal	Mean: μ ; Std. Dev: σ ; Location: t_0	$f(t; \mu, \sigma, t_0) = \frac{1}{\sigma(t-t_0)\sqrt{2\pi}} e^{-\frac{1}{2}\left(\frac{\ln(t-t_0)-\mu}{\sigma}\right)^2}$, $t > t_0$ 0, $t \leq t_0$
Weibull	Scale: θ ; Shape: β ; Location: t_0	$f(t; \theta, \beta, t_0) = \frac{\beta}{\theta} \left(\frac{t-t_0}{\theta}\right)^{\beta-1} e^{-\left(\frac{t-t_0}{\theta}\right)^\beta}$, $t > t_0$ 0, $t \leq t_0$
Beta	Shape parameters: ν, ω	$f(t; \nu, \omega) = \frac{t^{\nu-1}(1-t)^{\omega-1}}{B(\nu, \omega)}$, $0 \leq t \leq 1$ = 0 elsewhere ($B(\nu, \omega)$ is the Beta function)
Uniform	End points: a and b	$f(t; a, b) = \frac{1}{b-a}$, $a \leq t \leq b$ = 0 elsewhere
Poisson	Mean: λ	$f(t; \lambda) = \frac{\lambda^t \exp(-\lambda)}{t!}$, where $t = 0, 1, 2, 3, \dots$ and $\lambda > 0$
Binomial	# of trials, successes = n , t per trial prob. of success: p	$f(t; n, p) = \binom{n}{t} p^t (1-p)^{n-t}$, where $t = 0, 1, \dots, n$

Normal random variables are encountered in a wide variety of problems. From the central limit theorem we know that the sum of a large number of identical independent random variables is approximately normal. Actually this theorem even holds under much weaker conditions—the variables do not have to be identical and independent. It is this theorem that explains why normal random variables are so often encountered in nature. When we have an aggregate effect of a large number of small random factors, the resulting random variable is normal.

However, it must be recognized that everything is not normally distributed. The normal distribution, while oftentimes convenient to use in a probabilistic analysis with respect to complexity of calculations, is one of the least conservative distributions that can be used. This is

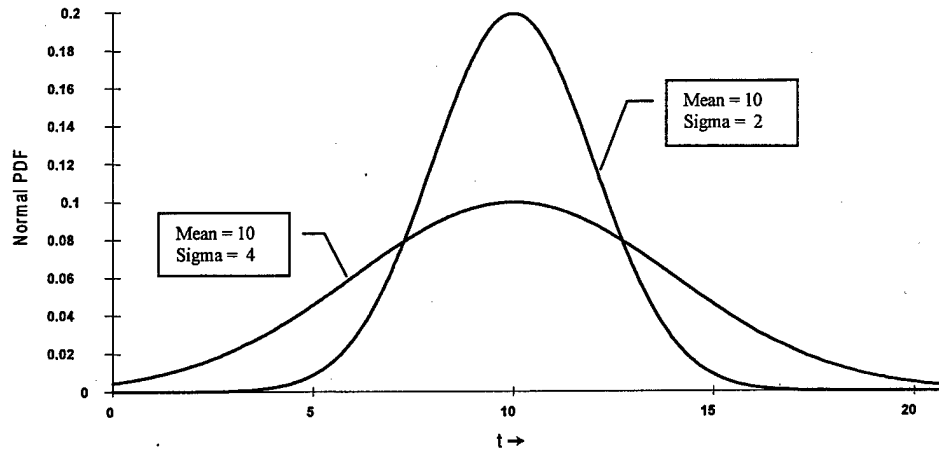


FIGURE 3-2. THE NORMAL DISTRIBUTION

because the function values drop off very quickly away from the mean, compared to the skewed tail of the lognormal or Weibull. What this translates to is a much smaller likelihood of obtaining extreme values from the distribution, which in turn translates to lower probability of failure.

3.6.2.2 Lognormal Distribution.

A random variable is lognormally distributed if the natural logarithm of the random variable is normally distributed. It starts at t_0 which is the location parameter (commonly set to zero). As seen in figure 3-3, the lognormal distribution is skewed to the right. The degree of skewness increases as the standard deviation increases for a given mean value. For the same standard deviation, the skewness also increases as the mean increases, as seen in figure 3-3. The mean and standard deviation of the lognormal distribution in terms of standard units (nonlogarithmic) are

$$\text{Mean} = e^{\mu + \frac{1}{2}\sigma^2} \quad \text{Standard Deviation} = \left[\left(e^{2\mu + \sigma^2} \right) \left(e^{\sigma^2} - 1 \right) \right]^{\frac{1}{2}}$$

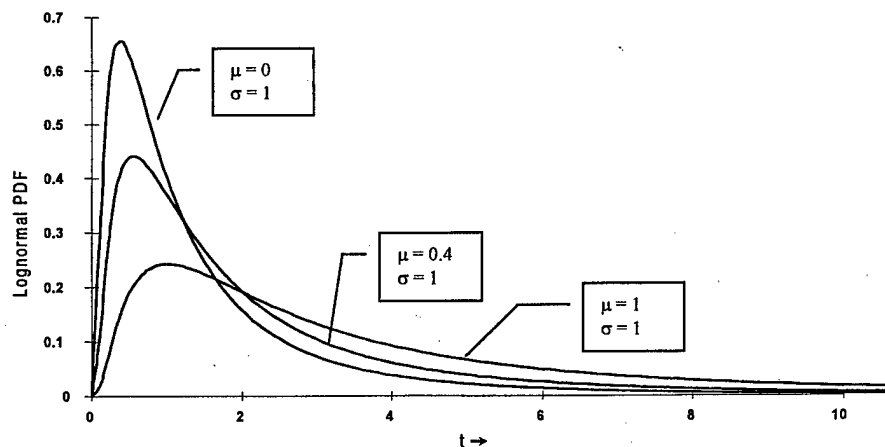


FIGURE 3-3. THE LOGNORMAL DISTRIBUTION

3.6.2.3 Weibull Distribution.

Waloddi Weibull delivered his now-famous paper [4] in 1951, claiming his distribution, or more specifically his family of distributions, applied to a wide range of problems. Initial reaction was mostly negative, but time has shown he was correct. Today it has many applications in different industries and in particular the aerospace industry. It can model unimodal distributions with shapes varying from highly skewed in either direction to symmetrical, as shown in figure 3-4. The Weibull distribution is widely used with brittle materials, such as carbon fibers and ceramics, as it is better able to cope with the large amount of scatter in the material properties of these types of materials [14, 15].

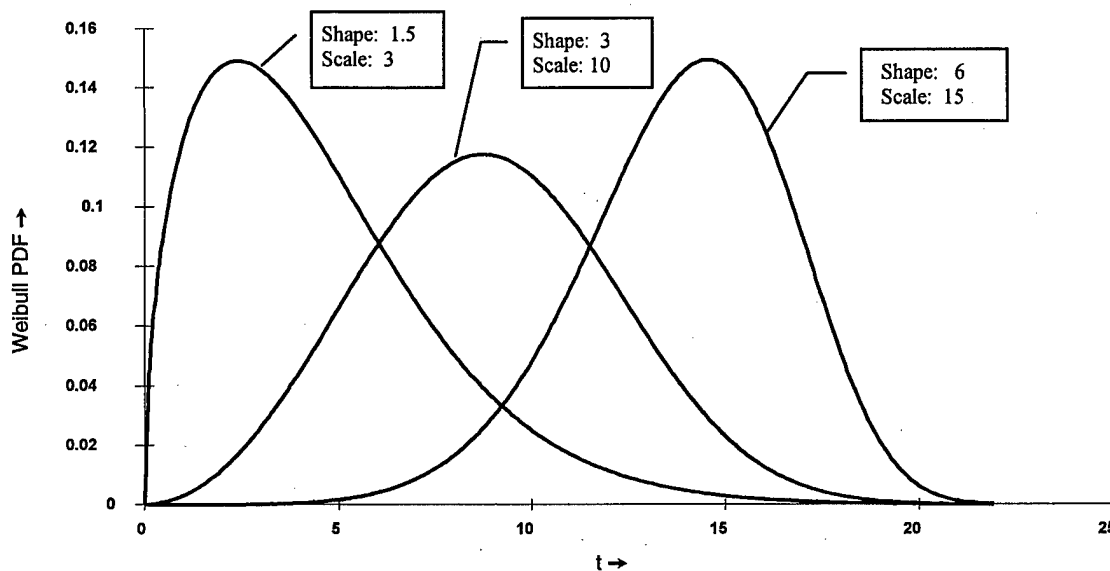


FIGURE 3-4. THE WEIBULL DISTRIBUTION

For the shape parameter (β) equal to 1, it becomes the two-parameter exponential distribution, while for $\beta > 1$, the function assumes the shapes shown in figure 3-4. For β values near 3, its coefficient of skewness approaches zero and the function is capable of approximating a normal distribution. A change in scale parameter (θ) has the same effect on the distribution as a change of the scale of the abscissa. If θ is increased while keeping the other two parameters constant, the distribution gets stretched out to the right and its height decreases. The area under the PDF from the location parameter (t_0) up to the scale parameter (θ) is 0.632. As its name implies, t_0 locates the distribution along the abscissa. When t_0 is zero, the distribution starts at the origin.

3.6.2.4 Beta Distribution.

This distribution is defined in a finite interval 0 to 1. As seen in figure 3-5, the distribution is capable of assuming a symmetric or skewed form. It is unclear why this is not seen often in examples of probabilistic methods; perhaps because of the unavailability of goodness-of-fit tests that apply to this distribution. Statistical capabilities in common computer software are rapidly enabling such goodness-of-fit tests (via optimization). Perhaps another reason for not using this

is the fact that its domain is bounded, and there may be concerns of being unconservative by choosing physical bounds.

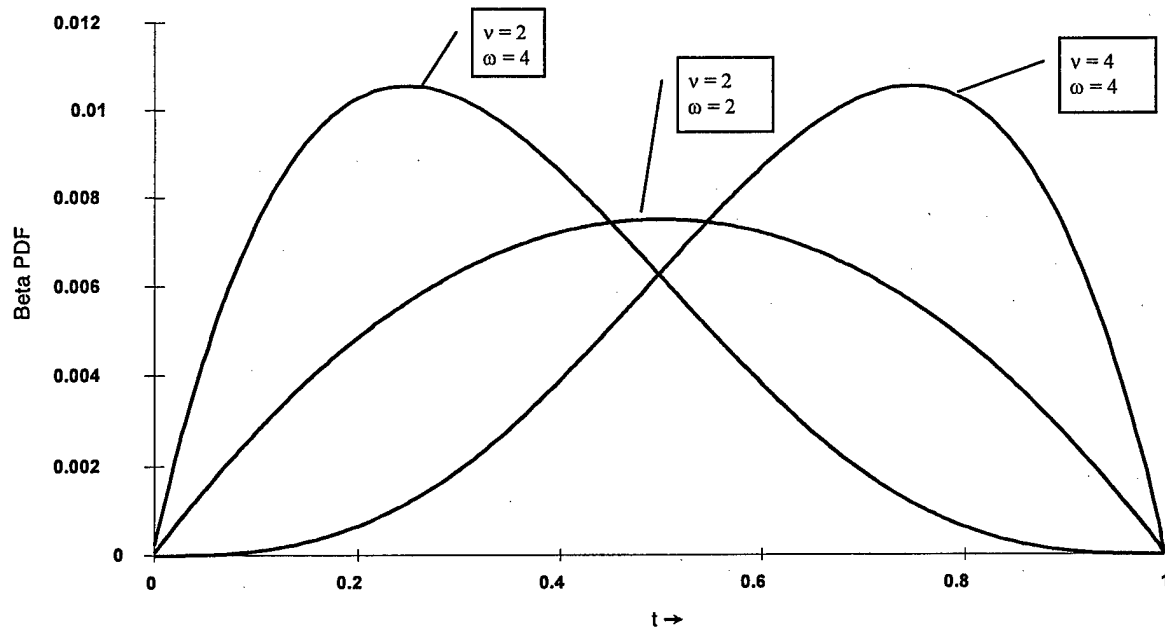


FIGURE 3-5. THE BETA DISTRIBUTION

3.6.2.5 Uniform Distribution.

As previously stated, the uniform distribution is used when no weight can be given to a specific value or interval within the bounded interval a to b . In figure 3-6, any value between 0 and 10 would have an equal chance of occurring.

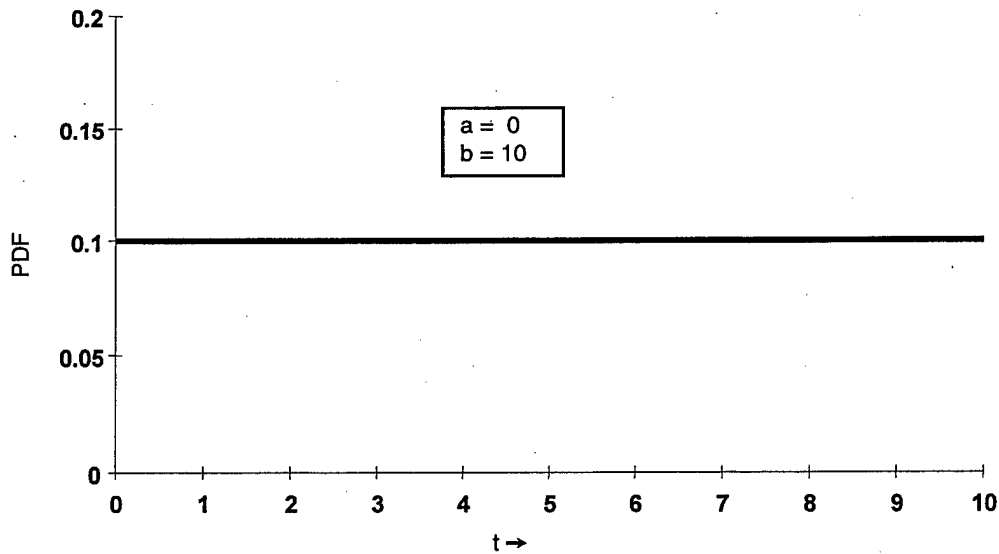


FIGURE 3-6. THE UNIFORM DISTRIBUTION

3.6.3 Discrete Random Variables and Poisson Distribution.

A discrete random variable can be defined by a table of (x_i, p_i) values, where x_i are the possible values of the variable and p_i the corresponding probabilities. The values x_i can be arbitrary, but the associated probabilities must be nonnegative and sum to 1. The table of probabilities may be predefined by the engineer or calculated from a discrete distribution such as the Poisson.

The Poisson distribution can be used to model the total number of occurrences of some phenomenon during a fixed time period or within a fixed region of space. The Northrop Grumman methodology (section 5) uses it to model the number of manufacturing defects in a structural component. The Poisson distribution may be obtained from the identity:

$$e^{-x} \sum_{n=0}^{\infty} \frac{x^n}{n!} = 1$$

This can also be written as:

$$e^{-x} \left(1 + \frac{x}{1!} + \frac{x^2}{2!} + \dots + \frac{x^n}{n!} + \dots \right) = 1$$

then

$$e^{-x} + \frac{x e^{-x}}{1} + \frac{x^2 e^{-x}}{2} + \dots + \frac{x^n e^{-x}}{n!} + \dots = 1$$

The interpretation of this distribution is as follows. Each term represents a probability. If x is defined as the expected, or average, number of occurrences of an event, then

e^{-x} = the probability that the event will not occur.

$x e^{-x}$ = the probability that the event will occur exactly once.

$\frac{x^2 e^{-x}}{2!}$ = the probability that the event will occur exactly twice, and so on

Let the manufacturing defect rate for a certain defect, based on defects per square foot, be defined as λ . Then for a structural component of area A , the number of expected defects would be $x = \lambda \cdot A$. The defect rate λ is always assumed to be constant. A Poisson PDF is shown in figure 3-7, with a mean or expected number (denoted x) of 2.

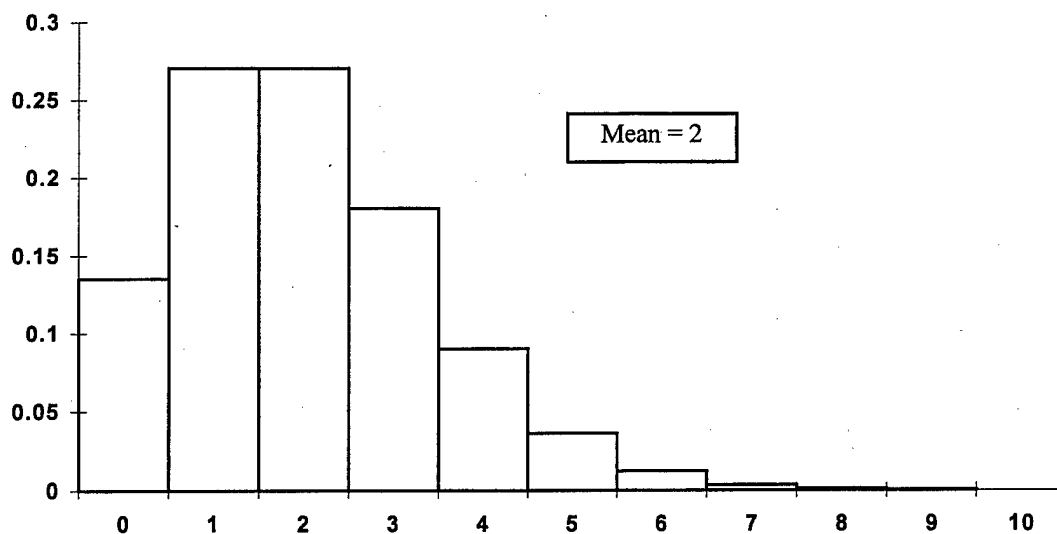


FIGURE 3-7. THE POISSON DISTRIBUTION

3.6.4 Considerations for Composite Material Properties and Sample Size for Material Testing.

The amount of scatter observed in composite material testing tends to be high relative to metals. Variability in composite material property data results from a number of sources, including variability in laying up the material, batch-to-batch variability of raw materials, and material testing methods. In addition, composite properties show higher (compared to metals) degradation due to environmental effects, which creates the need for testing at different temperatures and moisture absorption levels.

Because of the batch-to-batch variability, the data should not be indiscriminately pooled over batches, as pooling batches involves the implicit assumption that this (batch-to-batch) source of variability is negligible. Material property data should also be tested for outliers (values that statistically do not belong to the other data). Should one be identified, MIL-HDBK-17 suggests the physical cause for the suspicious value be investigated (e.g., testing or calibration error). If a cause cannot be found, the value should be kept.

The Weibull distribution has been shown to effectively model the behavior of brittle materials, including composites. MIL-HDBK-17 recommends the Weibull distribution be used, as a first choice, to model composite material failure behavior. As previously stated, one advantage of the Weibull is its ability to take on varying forms, from symmetric (approximately normal) to highly nonsymmetric distributions.

The purpose of taking a sample is to find out something about the population. The larger the sample, the less is the risk of distortion by extreme values, and the closer is the approximation between sample and population mean and standard deviation. For practical purposes, the sample standard deviation is sufficiently close to the population standard deviation when the sample size is at least 30.

At present, there is no criterion for determining the optimum sample size in material testing for application to probabilistic design. Obviously, the larger the sample sizes become, the narrower the confidence intervals of the estimates of the distribution parameters. One method has been suggested [16] to relate sample size to material cost as well as anticipated probability of failure. In this approach, the smaller the specified failure probability becomes, the larger the value of optimum sample size. The authors also relate optimum sample size to the type of distribution shown.

With composite materials, it is advantageous from a cost and schedule standpoint to test as few specimens as possible; therefore small sample sizes (usually considered to be less than 30) are often used to generate material strength values for design parameters. Another factor driving this is the many different required tests at different temperatures and moisture absorption levels, as mentioned above. For example, to qualify a composite material for a commercial application, the FAA requires property values for tension, compression, and shear tests subjected to the environmental conditions: hot-wet, cold-dry, and room temperature for three separate batches of material.

It has been suggested [17] that sample size is not an important issue with probabilistic design, because an initial estimate of the distribution parameters can be made with limited data, then probabilistic analysis runs made to determine the sensitivity of the material property in question. If the probability of failure is sensitive to the material property, then more testing would be prudent, and if not, additional testing would be a waste of time and money. This point is debated in section 7.

3.7 STEP 5—STRUCTURAL RELIABILITY ASSESSMENT.

This section begins with the basic mathematical formulation of the problem, along with simple examples for assessing structural reliability. Then more complex (real world) problems are formulated and four major solution approaches are described that have been developed by industry and academia. Sections 3.7.2 through 3.7.5 will give an example of each of the four solution approaches.

The basic problem for probabilistic analysis remains to formulate expressions defining the load (or stress) on the structure and the resistance to applied load (or strength) of the structure. For a typical design condition, both stress and strength can be plotted in the same horizontal axis as shown in figure 3-8. The mean strength, obviously, is greater than the mean applied stress. However, the overlap of PDFs suggests that it is possible for strength to be less than applied stress, which is the condition for failure. This illustration conveys the essence of probabilistic structural analysis: there is a possibility of failure, and it is defined in the small region of overlap between the PDFs.

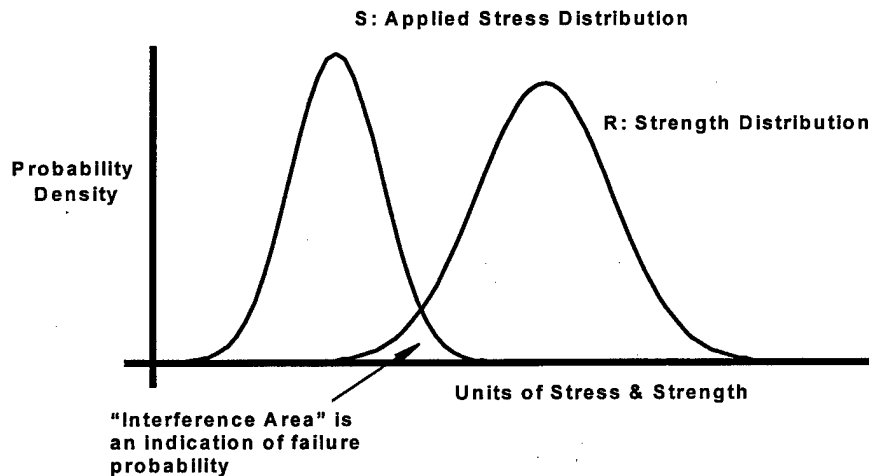


FIGURE 3-8. SIMPLIFIED (2-DIMENSIONAL) FORMULATION

A technically accurate description of the stress-strength curve overlap is shown in figure 3-9, showing the stress and strength along the horizontal and vertical axes, respectively. The line drawn represents the scenarios where stress = strength, or $g(R,S) = R - S = 0$. This is often referred to as the “limit state” that separates the failure region ($g < 0$) from the safe region ($g > 0$). The function $g(R,S)$ is commonly referred to as the performance function. The probability of failure is defined as the volume under the surface shown in the failure region where $g < 0$.

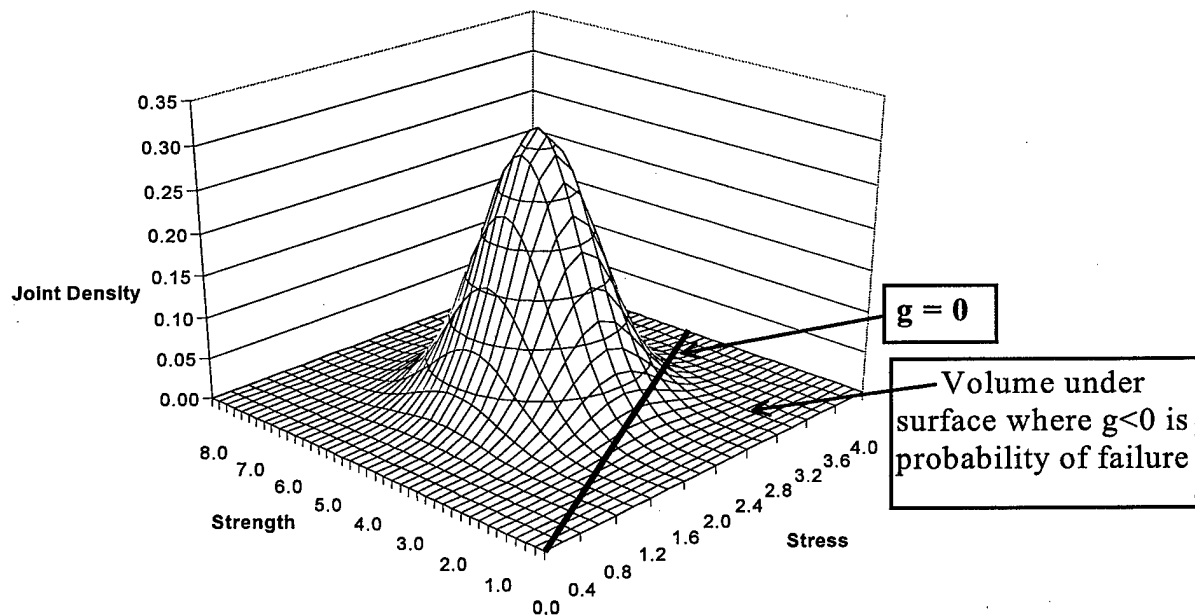


FIGURE 3-9. THREE-DIMENSIONAL REPRESENTATION OF PROBLEM

The probability of failure is defined as $PF = P[g(R,S) \leq 0]$. Aside from applied stress and material strength, there are numerous other R,S variates, listed in table 3-2, for which probabilistic analyses can be performed.

TABLE 3-2. LIMIT STATE FORMULATIONS USED IN AEROSPACE
STRUCTURE DESIGN

Failure Occurs if R	\leq S
Clearance	\leq Maximum displacement
Fracture toughness	\leq Stress intensity factor
Critical crack size	\leq Growing crack size
Critical material thickness	\leq Corrosion depth
Tolerable noise level	\leq Service noise level

The statistical variation of R and S are described by the probability density functions $f_R(r)$ and $f_S(s)$, respectively. The overlap region (volume) is quantitatively obtained from the following expression:

$$P_f = \iint_{\Omega} f_{R,S}(r,s) dr ds$$

where $f_{R,S}(r,s)$ is the joint density function and Ω is the failure set, i.e., the set of all values of R and S such that $g(R,S) \leq 0$. If the variables R and S are statistically independent (changing one has no effect on the other; they share no common variables), then the joint density function is expressed as the product of individual density functions as follows:

$$f_{R,S}(r,s) = f_R(r)f_S(s) \quad \text{and thus} \quad P_f = \iint_{\Omega} f_R(r)f_S(s) dr ds$$

We will now consider 3 scenarios producing different expressions for determining probability of failure: (1) one variable where probability of failure can be found using a statistics textbook and calculator; (2) two variables where probability can be found using standard numerical integration routines; and (3) more than two variables where alternative means must be used to determine the probability.

The example consists of a steel bar, with cross-sectional area A, subjected to uniaxial tensile load (denoted P), as shown in figure 3-10. The failure mode is yielding, i.e., the bar fails if the applied load exceeds the bar's yield strength (denoted F_y).

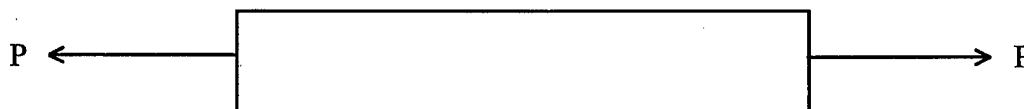


FIGURE 3-10. 17-7PH STEEL BAR LOADED IN TENSION

The three different cases will all use this example configuration, but each case will have a different number of parameters that will be considered random variables. The performance function for this example is written as $g = F_y \times A - P$, such that $g < 0$ indicates failure.

3.7.1 Single-Variable Failure Probability Determination.

The steel bar is being laboratory tested in a tensile machine. The load will be applied up to a certain level P , which is considered to be exactly (or very close to) known because the machine is calibrated. The dimensions of the bar were measured beforehand using high precision instruments, and its area was calculated to be 0.80 square inch. Thus the variation of parameters P and A is considered to be zero and the only probabilistic variable is yield strength. All parameters are assumed to be independent. This means that cross-sectional area and yield strength are both assumed to be unaffected by the applied loading.

The results from 17-7PH steel coupon testing were analyzed using a goodness-of-fit test, wherein it was determined that the data most closely fit a normal distribution with the following parameters:

$$\begin{aligned} F_y: \quad \text{Mean} &= 140,000 \text{ psi} \\ \text{Standard deviation} &= 10,000 \text{ psi} \end{aligned}$$

Problem: What is the probability of failure if the bar is subjected to a 100,000 lb. load?

Solution: The performance function is thus $g = F_y \times 0.80 - 100,000$. Failure occurs when $g \leq 0$, which translates to $F_y \leq 125,000$ psi as our definition of failure. Therefore we need to calculate the probability of a material with a published mean yield strength of 140,000 psi and standard deviation of 10,000 psi having been manufactured such that its yield strength is below 125,000 psi. This is depicted in figure 3-11.

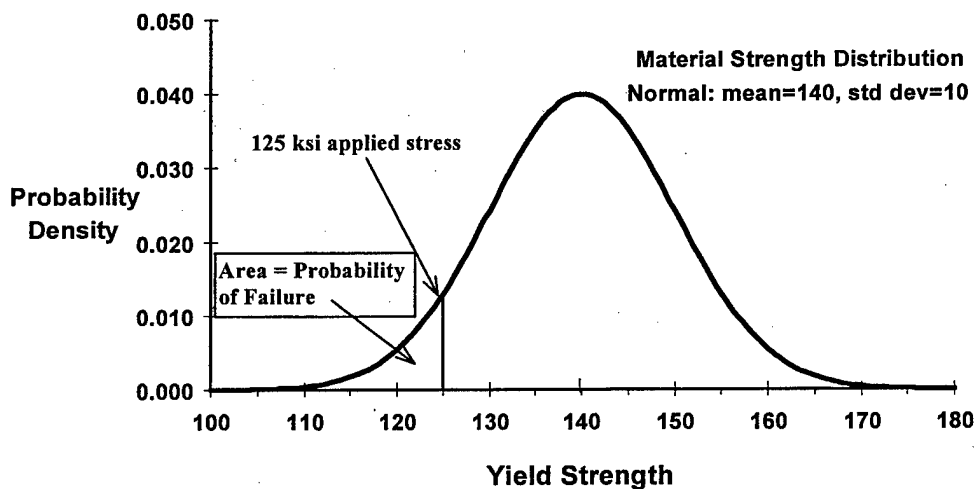


FIGURE 3-11. FAILURE PROBABILITY DETERMINATION: ONE VARIABLE

This probability can be found using a calculator and elementary statistics textbook. We first transform the stress values into a normal random variable z with a mean of zero and a standard deviation of 1. The distribution of a random variable with a mean of zero and a standard deviation of 1 is called a *standard normal distribution*, and a table of areas under this curve (or probabilities) is found in most statistics textbooks.

The transformation is accomplished by the following: $z = \frac{Value - \mu}{\sigma}$

The value 125,000 psi transforms into: $z = \frac{125,000 \text{ psi} - 140,000 \text{ psi}}{10,000 \text{ psi}} = -1.5$

Looking in a standard normal distribution table, we see that the area under the normal curve up to $z = -1.5$ is 0.0668. Therefore the probability of having a material strength less than 125,000 psi, knowing the material exhibits a mean value of 140,000 psi and a standard deviation of 10,000 psi, is approximately 0.067. Thus the probability of failure of the bar (region shown in figure 3-11) is 0.067.

3.7.2 Two-Variable Probability of Failure Determination.

In most cases, the probability of failure is determined via numerical integration when two PDFs are involved. This section begins by showing how to adjust the parameters of a PDF to account for an additional factor, which frequently arises in two-variable cases. An explanation is given next for normal-normal and lognormal-lognormal situations, circumventing the need to perform numerical integration. The section concludes with examples of normal-normal and lognormal-lognormal scenarios and an example (lognormal-normal) where numerical integration is required.

3.7.2.1 Adjustment of PDF Parameters.

Shifting (adding a factor) and scaling (multiplying by a factor) of design variables expressed in the performance function are commonly needed and are accomplished by changing the parameters of the PDFs. Very seldom will the performance function be of the form $g = x - y$, for the two-variable case. The more common case would be $g = C_1x - C_2y + C_3$. Yet the data which has been fit to a distribution are normally x and y . Therefore we need a PDF for the quantity $[C_1x]$ and a PDF for the quantity $[C_2y - C_3]$. The procedures for adjusting the parameters of the x, y PDFs to account for multiplicative and additive constants are shown in table 3-3.

For example, assume measurements were taken to define the yield strength variable, F_y . Assume a normal distribution was found to give the best fit, with mean (μ) of 100,000 psi and standard deviation (σ) of 10,000 psi. If the performance function is $g = 0.8 F_y - P$, then we are interested in using the mean and standard deviation of the quantity $0.8 \times F_y$.

So the new parameters (per table 3-3) are:

Mean: $0.8 \times 100,000 = 80,000$ and
Standard deviation: $0.8 \times 10,000 = 8,000$

TABLE 3-3. PROBABILITY DISTRIBUTION TRANSFORMATIONS

Distribution	Parameters	Transformation	New Parameters
Normal	μ, σ	Shift by C_3	$\mu + C_3, \sigma$
Lognormal	μ, σ, t_0	Shift by C_3	$\mu, \sigma, t_0 + C_3$
Weibull	θ, β, t_0	Shift by C_3	$\theta, \beta, t_0 + C_3$
Normal	μ, σ	Scale by $C_2 > 0$	$C_2 \mu, C_2 \sigma$
Lognormal	μ, σ, t_0	Scale by $C_2 > 0$	$\mu + \ln C_2, \sigma, C_2 t_0$
Weibull	θ, β, t_0	Scale by $C_2 > 0$	$C_2 \theta, \beta, C_2 t_0$

These adjusted parameters would then be used to assess the probability of failure.

3.7.2.2 First-Order Reliability Method.

Assuming the variables x and y are statistically independent and normally distributed, the variable (performance function) $g = x - y$ or $g = x + y$ is also normally distributed. That is, it can be shown [3-7] that the variable g , being a linear function of two Gaussian variables, is also Gaussian. Table 3-4 lists the mean and standard deviation associated with addition and subtraction of normal PDFs.

TABLE 3-4. COMBINING NORMAL DISTRIBUTIONS

Operation	Mean	Standard Deviation
$g = x + y$	$\mu_g = \mu_x + \mu_y$	$\sigma_g = (\sigma_x^2 + \sigma_y^2)^{1/2}$
$g = x - y$	$\mu_g = \mu_x - \mu_y$	$\sigma_g = (\sigma_x^2 + \sigma_y^2)^{1/2}$

If, for example, the performance function is $g = x - y$, then the mean and variance of g is determined by

$$\mu_g = \mu_x - \mu_y \quad \text{and} \quad \sigma_g = (\sigma_x^2 + \sigma_y^2)^{1/2}$$

The event of failure is $g < 0$. The probability of failure is now given in terms of g :

$$P(g < 0) = \int_{-\infty}^0 \frac{1}{\sigma_g \sqrt{2\pi}} e^{-\frac{1}{2} \left(\frac{g - \mu_g}{\sigma_g} \right)^2} dg$$

If we let $z = (g - \mu_g) / \sigma_g$, then $\sigma_g dz = dg$. When $g = 0$, the upper limit of z is given by

$$z = \frac{0 - \mu_g}{\sigma_g} = \frac{\mu_g}{\sigma_g} = -\frac{\mu_x - \mu_y}{\sqrt{\sigma_x^2 + \sigma_y^2}},$$

and when $g \rightarrow -\infty$, the lower limit of $z \rightarrow -\infty$.

The transformed integral becomes probability of failure = $\frac{1}{\sqrt{2\pi}} \int_{-\infty}^{\frac{\mu_x - \mu_y}{\sqrt{\sigma_x^2 + \sigma_y^2}}} e^{-z^2/2} dz$

The random variable z is the standard normal variable! Therefore the probability of failure can be found by looking in the standard normal table for the area under the curve from $-\infty$ to

$z = -\frac{\mu_x - \mu_y}{\sqrt{\sigma_x^2 + \sigma_y^2}}$. This approach was developed by Cornell [7] and is a part of the First-Order

Reliability Method (FORM) [19]. He named the ratio the “safety index” and denoted it as β .

That is $\beta = \frac{\mu_g}{\sigma_g} = \frac{\mu_x - \mu_y}{\sqrt{\sigma_x^2 + \sigma_y^2}}$ and $P_f = \Phi\{-\beta\}$ where Φ is the cumulative distribution function for

a standard normal variable (look-up tables are in most statistics textbooks). This equation makes calculation of probability of failure for the normal-normal case extremely simple and fast.

3.7.2.3 Lognormal-Lognormal Case.

The parameters μ and σ in the PDF equation shown in table 3-1 are the mean and standard deviation of the natural logarithms of the data. That is, if all the test data were converted to natural logarithms and then a mean and standard deviation of that data was calculated, those values would be μ and σ . As explained in section 3.6.2.2, the mean and standard deviation, in non-logarithmic units, are calculated by the following equation:

$$\text{Mean} = e^{\mu + \frac{1}{2}\sigma^2} \quad \text{Standard Deviation} = \left[\left(e^{2\mu + \sigma^2} \right) \left(e^{\sigma^2} - 1 \right) \right]^{\frac{1}{2}}$$

The equation used to calculate the probability of failure is identical to that used in the normal-normal case, but again, remember the above definition of μ and σ . The safety index is again

defined as $\beta = \frac{\mu_g}{\sigma_g} = \frac{\mu_x - \mu_y}{\sqrt{\sigma_x^2 + \sigma_y^2}}$ and $P_f = \Phi\{-\beta\}$ where Φ is the cumulative distribution function

for a standard normal variable (look-up tables are in most statistics textbooks). This makes calculation for the lognormal-lognormal case extremely simple and fast.

3.7.2.4 Other Two-Variable Cases.

Table 3-5 lists the expressions developed for the nine different combinations of normal, lognormal, and Weibull PDFs. For the combinations involving only lognormal and/or Weibull distributions, it is assumed that the starting point (s_0) of the stress distribution is less than the starting point (t_0) of the strength distribution. They can be solved with commercially available math software routines or a computer program can be written employing numerical integration techniques.

TABLE 3-5. PROBABILITY OF FAILURE EXPRESSIONS FOR PDF COMBINATIONS

Stress-Strength Distributions	Probability of Failure Expression
Normal - Normal (μ_s, σ_s) (μ_t, σ_t)	$\int_{-\infty}^{\infty} \frac{1}{\sqrt{2\pi}} \exp\left\{-\frac{1}{2} z^2\right\} \Phi\left[\frac{\sigma_s z + \mu_s - \mu_t}{\sigma_t}\right] dz$
Normal - Lognormal (μ_s, σ_s) (μ_t, σ_t, t_0)	$\int_{\frac{t_0 - \mu_s}{\sigma_s}}^{\infty} \frac{1}{\sqrt{2\pi}} \exp\left\{-\frac{1}{2} z^2\right\} \Phi\left[\frac{\ln(\sigma_s z + \mu_s - t_0) - \mu_t}{\sigma_t}\right] dz$
Normal - Weibull (μ_s, σ_s) (θ_t, β_t, t_0)	$\int_{\frac{t_0 - \mu_s}{\sigma_s}}^{\infty} \frac{1}{\sqrt{2\pi}} \exp\left\{-\frac{1}{2} z^2\right\} \left[1 - \exp\left\{-\left(\frac{\sigma_s z + \mu_s - t_0}{\theta_t}\right)^{\beta_t}\right\}\right] dz$
Lognormal - Normal (μ_s, σ_s, s_0) (μ_t, σ_t)	$\int_{-\infty}^{\infty} \frac{1}{\sqrt{2\pi}} \exp\left\{-\frac{1}{2} z^2\right\} \Phi\left[\frac{\exp(\sigma_s z + \mu_s) + s_0 - \mu_t}{\sigma_t}\right] dz$
Lognormal - Lognormal (μ_s, σ_s, s_0) (μ_t, σ_t, t_0)	$\int_{\frac{\ln(t_0 - s_0) - \mu_s}{\sigma_s}}^{\infty} \frac{1}{\sqrt{2\pi}} \exp\left\{-\frac{1}{2} z^2\right\} \Phi\left[\frac{\ln[\exp(\sigma_s z + \mu_s) + s_0 - t_0] - \mu_t}{\sigma_t}\right] dz$
Lognormal - Weibull (μ_s, σ_s, s_0) (θ_t, β_t, t_0)	$\int_{\frac{\ln(t_0 - s_0) - \mu_s}{\sigma_s}}^{\infty} \frac{1}{\sqrt{2\pi}} \exp\left\{-\frac{1}{2} z^2\right\} \left[1 - \exp\left\{-\left(\frac{\exp(\sigma_s z + \mu_s) + s_0 - t_0}{\theta_t}\right)^{\beta_t}\right\}\right] dz$
Weibull - Normal (θ_s, β_s, s_0) (μ_t, σ_t)	$\int_0^{\infty} \exp(-z) \Phi\left[\frac{\theta_s z^{1/\beta_s} + s_0 - \mu_t}{\sigma_t}\right] dz$
Weibull - Lognormal (θ_s, β_s, s_0) (μ_t, σ_t, t_0)	$\int_{\left(\frac{t_0 - s_0}{\theta_s}\right)^{\beta_s}}^{\infty} \exp(-z) \Phi\left[\frac{\ln(\theta_s z^{1/\beta_s} + s_0 - t_0) - \mu_t}{\sigma_t}\right] dz$
Weibull - Weibull (θ_s, β_s, s_0) (θ_t, β_t, t_0)	$\int_{\left(\frac{t_0 - s_0}{\theta_s}\right)^{\beta_s}}^{\infty} \exp(-z) \left[1 - \exp\left\{-\left(\frac{\theta_s z^{1/\beta_s} + s_0 - t_0}{\theta_t}\right)^{\beta_t}\right\}\right] dz$

3.7.2.5 Two-Variable Example Problems.

Consider the example of the steel bar in tension. The bar is put into service. It has been dimensionally checked beforehand, so the area (A) is a known constant. The bar is used as a link between two fittings and designed to fail in the interior region of the bar (as opposed to failing at the attachment). The applied loading, modeled as uniaxial tension, was measured on a similar application, wherein 50 applied load measurements were taken. Three cases will be discussed: (1) normal-normal; (2) lognormal-lognormal; and (3) lognormal-normal.

3.7.2.5.1 Scenario 1 (Normal-Normal Case).

The 50 measurements were statistically analyzed and it was determined through goodness-of-fit testing that the data best fit a normal distribution, with the following parameters:

$$\begin{aligned} P: \quad \text{Mean} &= 100,000 \text{ lb.} \\ \text{Standard deviation} &= 10,000 \text{ lb.} \end{aligned}$$

The results from the 17-7PH steel coupon testing were analyzed using a goodness-of-fit test as well, wherein it was determined that the data most closely fit a normal distribution with the following parameters:

$$\begin{aligned} F_y: \quad \text{Mean} &= 140,000 \text{ psi} \\ \text{Standard deviation} &= 10,000 \text{ psi} \end{aligned}$$

The bar's cross-sectional area was measured to be 0.80 square inch.

Problem: What is the probability of failure of the 17-7PH steel bar with a cross-sectional area of 0.80 in² in service?

Solution: The performance function becomes $g = F_y \times 0.80 - P$. We calculate the safety index as follows (remembering we must adjust the parameters μ_{F_y} and σ_{F_y} by the scale factor 0.8)

$$\beta = \frac{\mu_g}{\sigma_g} = \frac{0.8\mu_{F_y} - \mu_P}{\sqrt{0.8^2\sigma_{F_y}^2 + \sigma_P^2}} = \frac{12,000 \text{ lb.}}{12,806 \text{ lb.}} = 0.937$$

We know that $P_f = \Phi\{-\beta\} = \Phi\{-0.937\} = 0.1745$ from the standard normal probability table.

3.7.2.5.2 Scenario 2 (Lognormal-Lognormal Case).

The 50 load measurements appeared to be non-normal, being skewed to the right. These data were statistically analyzed and it was determined through goodness-of-fit testing that the data best fit a 2-parameter lognormal distribution with the following parameters:

$$\begin{aligned} P: \quad \mu &= 11.508 \\ \sigma &= 0.10 \end{aligned}$$

The results from the 17-7PH steel yield strength coupon testing were analyzed using a goodness-of-fit test as well, wherein it was determined that the data most closely fit a 2-parameter lognormal distribution with the following parameters:

$$\begin{aligned} F_y: \quad \mu &= 11.847 \\ \sigma &= 0.0713 \end{aligned}$$

The bar's cross-sectional area was measured to be 0.80 square inch.

Note: Values of μ and σ were chosen because they correspond (using the equations previously stated) to the means and standard deviations used in the previous normal-normal example. The corresponding means and standard deviations (for general information only—not used in the probability of failure calculation) of design variables F_y and P are:

F_y : Mean = 140,000 psi and P : Mean = 100,000 lb.
 Standard deviation = 10,000 psi Standard deviation = 10,000 lb.

Problem: What is the probability of failure of the 17-7PH steel bar with a cross-sectional area of 0.80 in² in service?

Solution: The performance function is $g = F_y \times 0.80 - P$. The parameter μ for the F_y distribution must be adjusted because the distribution that we must now deal with is $0.80 \times F_y$. Per table 3-3, only the lognormal parameter μ is affected (σ remains the same) by the scale factor 0.8. The adjusted parameter μ is

$$\mu = 11.847 + \ln(0.8) = 11.624. \quad \sigma = 0.0713 \text{ (unchanged).}$$

Now, the safety index can be determined by

$$\beta = \frac{\mu_g}{\sigma_g} = \frac{11.624 - 11.508}{\sqrt{.0713^2 + .100^2}} = 0.945$$

We know that $P_f = \Phi\{-\beta\} = \Phi\{-0.945\} = 0.1724$ from the standard normal probability table.

3.7.2.5.3 Scenario 3 (Lognormal-Normal Case).

The 50 load measurements appeared to be non-normal, being skewed to the right. These data were statistically analyzed and it was determined through goodness-of-fit testing that the data best fit a 2-parameter lognormal distribution with the following parameters:

P : $\mu_s = 11.508$
 $\sigma_s = 0.1000$

The results from the 17-7PH steel yield strength coupon testing were analyzed using a goodness-of-fit test as well, wherein it was determined that the data most closely fit a normal distribution with the following parameters:

F_y : $\mu = 140,000$ psi
 $\sigma = 10,000$ psi

The bar's cross-sectional area was measured to be 0.80 square inch.

Problem: What is the probability of failure of the 17-7PH steel bar with a cross-sectional area of 0.80 in^2 in service?

Solution: The performance function becomes $g = F_y \times 0.80 - P$. Remember that the parameter μ for the F_y distribution must be adjusted because the distribution that we must now deal with is $0.80 \times F_y$. Per table 3-3, both the mean and standard deviation of the normal distribution are scaled (multiplied) by 0.8. The adjusted parameters are:

$$\begin{aligned}\mu_t &= 140,000 \text{ psi} \times 0.8 = 112,000 \\ \sigma_t &= 10,000 \text{ psi} \times 0.8 = 8,000\end{aligned}$$

A computer program (FORTRAN) was written to solve the lognormal-normal integration equation given in table 3-5:

$$P_f = \int_{-\infty}^{\infty} \frac{1}{\sqrt{2\pi}} \exp\left(-\frac{1}{2}z^2\right) \Phi\left[\frac{\exp(\sigma_s z + \mu_s) + s_0 - \mu_t}{\sigma_t}\right] dz$$

or

$$P_f = \int_{-\infty}^{\infty} \frac{1}{\sqrt{2\pi}} \exp\left(-\frac{1}{2}z^2\right) \Phi\left[\frac{\exp(0.1z + 11.508) - 112,000}{8,000}\right] dz$$

The result from executing the program was 0.1734.

3.7.2.5.4 Two-Variable Example Problem Summary.

The same physical problem was used, with three different scenarios, showing the normal-normal, lognormal-lognormal solutions via the safety index shortcut method, then a lognormal-normal solution was obtained via numerical integration. The results are summarized in table 3-6.

TABLE 3-6. TWO-VARIABLE EXAMPLE SUMMARY (SIGNIFICANT OVERLAP)

Case	Stress Distribution	Strength Distribution	Probability of Failure
1	Normal $\mu = 100,000; \sigma = 10,000$	Normal $\mu = 112,000; \sigma = 8,000$	0.1745
2	Lognormal $\mu = 11.508; \sigma = 0.1; S_0 = 0$	Lognormal $\mu = 11.624; \sigma = 0.713; S_0 = 0$	0.1724
3	Lognormal $\mu = 11.508; \sigma = 0.1; S_0 = 0$	Normal $\mu = 112,000; \sigma = 8,000$	0.1734

One can conclude from this that the choice of distribution has negligible effect on the resulting probability of failure. While this is certainly the case for this set of scenarios wherein the distributions are close together and having a significant overlap, this cannot be extrapolated to cases where the distributions are far apart. To illustrate, consider the mean of the yield strength to be 200,000 psi, instead of 140,000 psi. This clearly will separate the distributions significantly. The resulting probabilities of failure are shown in table 3-7.

TABLE 3-7. TWO-VARIABLE SUMMARY ILLUSTRATING TAIL SENSITIVITY

Case	Stress Distribution	Strength Distribution	Probability of Failure
1	Normal $\mu = 100,000; \sigma = 10,000$	Normal $\mu = 160,000; \sigma = 8,000$	1.4×10^{-6}
2	Lognormal $\mu = 11.508; \sigma = 0.1; S_0 = 0$	Lognormal $\mu = 11.982; \sigma = 0.05; S_0 = 0$	1.1×10^{-5}
3	Lognormal $\mu = 11.508; \sigma = 0.1; S_0 = 0$	Normal $\mu = 160,000; \sigma = 8,000$	1.4×10^{-5}

The results from table 3-7 exemplify the tail sensitivity frequently mentioned in probabilistic literature. This issue is discussed further in section 7.

3.7.2.6 Probability of Failure With More Than Two Variables.

In many real world design and analysis situations, particularly with aerospace structures, the performance function is not even a definable entity. Even if it is, there will most likely be more than two random variables involved, and the resulting multiple integral is in general very difficult to evaluate. This section will discuss methods that have been developed to accommodate these situations.

The Monte Carlo simulation technique, in its simplest form, is presented first. Refinements to the technique to speed up the simulation will be briefly mentioned. This will be followed by a detailed discussion of the response surface method and finally a high-level explanation of limit state approximation methods which have been the focus of most of the published probabilistic methods research in the past 15 years.

3.7.3 Monte Carlo Simulation.

The general idea of this method is to solve mathematical problems by the simulation of random variables. In 1949, an article [20] entitled "The Monte Carlo Method" appeared. The name "Monte Carlo" is derived from that city in the Principality of Monaco famous for its casinos. One of the simplest mechanical devices for generating random variables is the roulette wheel, thus the association. The theoretical foundation of this method had been known long before this 1949 article was published, and certain problems were solved by means of random sampling [21]. However, because simulation of random variables by hand is a laborious process, use of the Monte Carlo method as a universal numerical technique became practical only with the advent of computers.

To understand what kinds of problems are solvable by this method, it is important to note that the method enables simulation of any process whose development is influenced by random factors. Monte Carlo simulation is a widely used technique for probabilistic structural analysis, serving two main purposes: (1) validating analytical methods and (2) solving large, complex systems when analytical approximations are not feasible.

The second case results when the performance function $[g(X)]$ is a function of many variables or when it cannot be expressed in terms of the random variables X_i . In this case, $g(X)$ can only be evaluated numerically through a structural analysis such as the finite element method for sets of input variables. That is, Monte Carlo simulation can provide input to perform multiple finite element analyses of the system (one analysis/result per unique set of input variables) and then calculate the number of times failure and success are predicted.

In order to evaluate the failure probability corresponding to a known performance function, $g(X)$, the Monte Carlo simulation method would consist of the following steps:

1. Given the predefined PDFs of the random variables in the performance function, generate a single value of each variable.
2. Assess the performance function: if $g(X) < 0 \Rightarrow$ system failure.
3. Repeat steps 1 and 2 N times.
4. Estimate the probability of failure by $P_f = N_f / N$, where N_f is the number of failures.

In order to evaluate the failure probability corresponding to an unknown performance function, the Monte Carlo simulation method would consist of the following steps:

1. Given the predefined PDFs of the random variables involved in the deterministic structural analysis (e.g., FEM), generate a single value of each random variable.
2. Perform the deterministic analysis, and record if failure is predicted.
3. Repeat steps 1 and 2 N times.
4. Estimate the probability of failure by $P_f = N_f / N$, where N_f is the number of failures.

3.7.3.1 Accuracy and Number of Required Trials.

Remember that this P_f value is an estimate of the true P_f . Actually it is a mean value of the failure probability. The accuracy of this estimate depends on the sample size, i.e., number of simulations. As N approaches infinity, the estimated P_f will stabilize (if the random number generator is good) to the true value. Of course, the true value itself is an estimate of the actual P_f due to the inaccuracies in the PDFs, analysis models, etc. One key issue to resolve is determination of the number of simulations required.

The error of calculations is, as a rule, proportional to the square root of the quantity $(1/N)$, where N is the number of trials. Hence it is clear that to decrease the error by a factor of 10, it is necessary to increase N by a factor of 100 [21]. To address the question of how many simulations are required for an estimated probability of failure, Shooman [22] derived the

following formula relating the number of simulations N and the percentage error:

$\% \text{ error} = 200 \sqrt{\frac{1 - P_f}{N P_f}}$. This equation was developed using a 95% confidence level. Therefore,

there is a 95% chance that the error in the estimated probability will be less than the error generated by this equation. For example, if 10,000 simulations were performed and the estimated probability was 0.01, then this equation yields 20% error. That is, we are 95% sure the actual probability of failure will lie between 0.01 ± 0.002 .

3.7.3.2 Generating Random Numbers From PDFs.

Values of each input variable should be chosen such that the total group chosen is representative of the probability characteristics of that variable. The basic building block is the ability to generate random numbers from a uniform distribution between zero and 1, denoted $U(0,1)$. Every value in the interval has equal likelihood of being chosen. Random number generators are common features of computer software. Once a random number is picked from $U(0,1)$, it is used to generate a random value of the PDF of interest. If the CDF of the random variable X is denoted $F_X(x)$ and u is the random number generated, then the corresponding value of the variable (X) is $x = F_X^{-1}(u)$. The procedure is illustrated in figure 3-12.

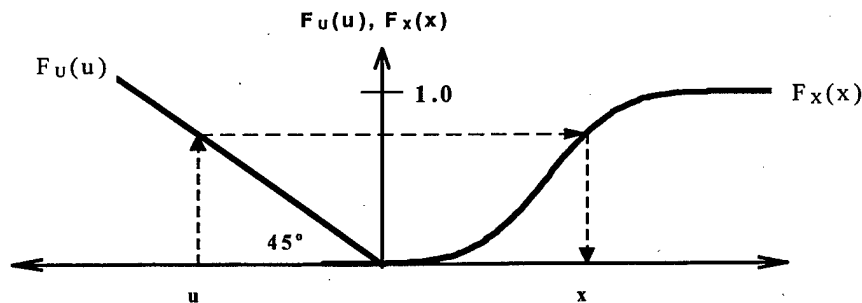


FIGURE 3-12. TRANSFORMING A $U(0,1)$ PICK TO RANDOM VARIABLE

This shows the CDF of the random variable X on the right side and the CDF of U on the left side. Since U is a pick from a uniform $(0,1)$ distribution, the CDF value at U is also U ! That is, the uniform PDF is $f_X(x) = \frac{1}{b-a}$, and its CDF is $F_X(x) = \frac{x-a}{b-a}$. Since $a = 0$ and $b = 1$ for the $U(0,1)$ distribution, we see that the CDF value of U is indeed U .

Now, per figure 3-12, we take the CDF value (U) and find the value of the random variable X that has that particular cumulative probability. This cumulative probability can be found by commercially available statistical computer software as well as most spreadsheet software. That is, the value U is passed in, and knowing the variable's distribution parameters, a cumulative probability is returned.

3.7.3.3 Correlated Random Variables.

If some or all variables are correlated (a change in one has an effect on another), then it is erroneous to sample from each PDF as if they were independent. In general, it is difficult to generate correlated variables. There are procedures [23, 24] for transforming correlated variables into uncorrelated variables, but the explanation and associated mathematics are beyond the scope of this document.

3.7.3.4 Simulation Efficiency Improvement Approaches.

A straightforward Monte Carlo method, while very useful for a number of applications, becomes extremely time-consuming to be practical for large finite element models. Each finite element run may take several hours, and with the probability of structural failure (hopefully) being very small, direct Monte Carlo analysis is often unfeasible. To overcome this, research efforts have addressed ways to increase simulation efficiency. The main techniques will be briefly explained; details will be left to the interested reader.

Importance Sampling [23]: This technique concentrates sampling points in the region which mainly contributes to the failure probability, instead of spreading them out evenly across the whole range of possible values of each random variable. Instead of generating a huge amount of successful (in the sense that the performance function $g(X) > 0$) simulations, this technique seeks to generate only a few simulations, most of which lead to failure. This is done by modifying each variable's PDF to generate these important samples; the modifications are taken into account while computing failure probability. Recently, adaptive importance sampling techniques have been developed [25], which also focus sampling in the probability-critical regions to increase efficiency.

Stratified Sampling [23]: After the number of simulations (N) is calculated, based on the expected failure probability, the domain of the random variables (assumed independent) is divided into regions of equal probability, such that the sum of regions adds up to N . Then one random sample is generated from each region, and the g -function is evaluated for each sample, from which failure probability is estimated from the ratio of the number of failures to the total number of simulations. A similar approach is called Latin Hypercube Sampling. Both of these methods are useful in representing the structural behavior accurately over a large domain, which is quite different from importance sampling techniques. Representing structural behavior over a large domain becomes important when utilizing response surface techniques, which will be described in section 3.7.4.

3.7.3.5 Summary and General Discussion.

Monte Carlo simulation has a major advantage over all other methods because it does not restrict the way in which the analysis must be structured. Monte Carlo is generally the baseline against which other methods are compared. In fact, in many papers, the result of the particular approach is stated as percentage error from the Monte Carlo result. The reason for this is that, given sufficient simulations, the Monte Carlo answer will always converge to the same result. As discussed before, this resulting probability of failure, although it has converged, is still an estimate of the true failure probability.

3.7.3.6 Monte Carlo Example Problem.

This example consists of a 17-7PH steel bar, with cross-sectional area A and yield strength F_y , subjected to uniaxial tensile load P , as shown in figure 3-13. For like-manufactured bars, the yield strength F_y is normally distributed with mean 140,000 psi and standard deviation 10,000 psi, while the area A is uniformly distributed between 0.7 and 0.9 square inch. The applied load P follows a lognormal distribution with location parameter $\mu = 11.508$ and shape parameter $\sigma = 0.1$, meaning that $\log(P)$ follows a normal distribution with mean 11.508 and standard deviation 0.1. (The mean of this lognormal distribution is approximately 100,000 psi and the standard deviation is about 10,000 psi.)



FIGURE 3-13. 17-7PH STEEL BAR LOADED IN TENSION

Problem: What is the probability of failure, i.e., the probability that the applied load will exceed the yield capability of the bar?

Solution: The performance function for this example is written as $g = F_y \times A - P$, where F_y , A , and P are the random variables described above, and failure is defined as any combination of F_y , A , and P values which produce $g < 0$. Although the probability distribution for each random variable is known, the resulting distribution for g is difficult to quantify (a lognormal subtracted from a product of a normal and uniform distribution). Could the distribution of g be quantified, then the probability of failure would simply be the cumulative distribution function value at 0. However, in this example the Monte Carlo method is used to determine the probability of failure.

During each Monte Carlo trial, a value from each probability distribution is randomly sampled (independently of the other two), and the resulting performance function value g is calculated. Numerous trials are repeated and the resulting proportion of trials in which g is less than zero is an estimate of the probability of failure. As the number of trials approaches infinity, this estimate naturally approaches the true probability of failure. Figure 3-14 shows the spreadsheet used to perform the Monte Carlo simulation for 100 trials. Table 3-8 summarizes the estimated probability of failure for various number of simulations.

TABLE 3-8. MONTE CARLO SIMULATION RESULTS

Number of Simulations	Probability of Failure
100	0.240
1,000	0.226
5,000	0.208
10,000	0.214
50,000	0.218
100,000	0.217

Monte Carlo	Random	Yield Strength: F_y	Random	Area: A	Random	Applied Load: P	g function	Failure
trial	draw	~ Normal	draw	~ Uniform	draw	~ Lognormal	$g = F_y A - P$	if $g < 0$
	from	Parameters	from	Parameters	from	Parameters		
	U (0,1)	140000 10000	U (0,1)	0.700 0.900	U (0,1)	11.508 0.100		1: failure 0: no failure
1	0.1673	130352	0.5884	0.818	0.8242	109225	-2639	1
2	0.1583	129984	0.5636	0.813	0.7764	107367	-1725	1
3	0.1737	130602	0.6644	0.833	0.4411	98044	10732	0
4	0.7903	148076	0.0431	0.709	0.9024	113268	-8338	1
5	0.3319	135654	0.0604	0.712	0.0507	84472	12123	0
6	0.0402	122512	0.6516	0.830	0.4092	97250	4474	0
7	0.0514	123682	0.5770	0.815	0.9050	113443	-12593	1
8	0.1729	130571	0.8982	0.880	0.7669	107031	7825	0
9	0.1604	130070	0.1046	0.721	0.2749	93731	39	0
10	0.7289	146094	0.4067	0.781	0.5544	100880	13270	0
11	0.2377	132863	0.8092	0.862	0.2791	93851	20656	0
12	0.7407	146456	0.0777	0.716	0.5247	100127	4669	0
13	0.3369	135792	0.3491	0.770	0.6915	104611	-76	1
14	0.2182	132216	0.9454	0.889	0.5013	99540	18009	0
15	0.1175	128124	0.0799	0.716	0.9078	113632	-21898	1
16	0.5821	142073	0.3171	0.763	0.9144	114101	-5638	1
17	0.6285	143279	0.8526	0.871	0.9008	113164	11564	0
18	0.6181	143005	0.6654	0.833	0.8335	109622	9512	0
19	0.6119	142844	0.1382	0.728	0.9327	115570	-11630	1
20	0.4098	137718	0.4418	0.788	0.8182	108973	-402	1
21	0.8848	151992	0.5364	0.807	0.4462	98172	24529	0
22	0.3195	135309	0.9708	0.894	0.1178	88379	32608	0
23	0.9307	154812	0.9041	0.881	0.8298	109464	26899	0
24	0.0743	125554	0.7019	0.840	0.7970	108131	-2618	1
25	0.7281	146070	0.4832	0.797	0.9841	123330	-6964	1
26	0.7697	147379	0.7000	0.840	0.9042	113391	10407	0
27	0.6047	142656	0.2667	0.753	0.5445	100626	6843	0
28	0.3753	136822	0.3023	0.760	0.0876	86891	17157	0
29	0.1061	127526	0.4658	0.793	0.4974	99443	1705	0
30	0.8455	150172	0.6893	0.838	0.8010	108284	17540	0
31	0.5341	140855	0.3613	0.772	0.8793	111875	-3098	1
32	0.6344	143436	0.7464	0.849	0.8213	109101	12717	0
33	0.1156	128026	0.1835	0.737	0.9303	115357	-21041	1
34	0.4341	138341	0.6903	0.838	0.5804	101549	14389	0
35	0.5151	140379	0.1641	0.733	0.6301	102870	2	0
36	0.6410	143611	0.2850	0.757	0.9751	121080	-12367	1
37	0.8980	152703	0.5414	0.808	0.8387	109852	13573	0
38	0.6133	142880	0.8088	0.862	0.7822	107578	15552	0
39	0.2792	134147	0.1016	0.720	0.2107	91822	4807	0
40	0.8259	149379	0.9852	0.897	0.6452	103284	30714	0
41	0.7839	147855	0.2084	0.742	0.8482	110291	-629	1
42	0.3570	136335	0.4005	0.780	0.4802	99016	7339	0
43	0.2996	134744	0.5774	0.815	0.6223	102659	7222	0
44	0.2301	132616	0.4992	0.800	0.6081	102276	3795	0
45	0.0396	122444	0.9131	0.883	0.4850	99136	8935	0
46	0.7764	147602	0.4700	0.794	0.5627	101092	16105	0
47	0.8402	149955	0.2263	0.745	0.1144	88224	23532	0
48	0.3512	136180	0.5749	0.815	0.0817	86563	24420	0
49	0.6167	142968	0.7085	0.842	0.8223	109144	11193	0
50	0.1848	131026	0.6635	0.833	0.4522	98321	10784	0
51	0.3489	136118	0.1588	0.732	0.6828	104356	-4750	1
52	0.1943	131379	0.5613	0.812	0.3124	94760	11953	0
53	0.5086	140216	0.4789	0.796	0.9411	116358	-4775	1
54	0.9342	155080	0.1502	0.730	0.6314	102904	10311	0
55	0.0412	122631	0.8799	0.876	0.1703	90463	16961	0
56	0.4812	139530	0.5067	0.801	0.0725	86014	25796	0
57	0.3082	134992	0.4570	0.791	0.6580	103641	3192	0
58	0.1067	127556	0.7957	0.859	0.1227	88596	20993	0
59	0.2991	134730	0.5478	0.810	0.8221	109136	-65	1
60	0.2231	132363	0.3520	0.770	0.1262	88746	13242	0
61	0.2779	134108	0.2283	0.746	0.6922	104631	-4631	1
62	0.8310	149581	0.3778	0.776	0.4773	98943	17065	0
63	0.5940	142378	0.6433	0.829	0.6977	104797	13184	0
64	0.4524	138805	0.5261	0.805	0.1538	89858	21911	0
65	0.0220	119852	0.9286	0.886	0.7698	107133	-978	1
66	0.7485	146698	0.3370	0.767	0.1377	89228	23349	0
67	0.9856	161874	0.2055	0.741	0.1186	88413	31550	0
68	0.6115	142833	0.0523	0.710	0.4077	97212	4264	0

FIGURE 3-14. MONTE CARLO SIMULATION FOR EXAMPLE PROBLEM
(Trials 1 through 68)

Monte Carlo trial	Random draw from U (0,1)	Yield Strength: F_y ~ Normal Parameters	Random draw from U (0,1)	Area: A ~ Uniform Parameters	Random draw from U (0,1)	Applied Load: P ~ Lognormal Parameters	g function $g = F_y \cdot A - P$	Failure if $g < 0$
		140000 10000		0.700 0.900		11.508 0.100		1: failure 0: no failure
69	0.0745	125568	0.7070	0.841	0.0213	81246	24408	0
70	0.3818	136992	0.8046	0.861	0.2752	93740	24199	0
71	0.9369	155293	0.5073	0.801	0.1885	91094	33366	0
72	0.1647	130246	0.5647	0.813	0.1826	90893	14989	0
73	0.2412	132975	0.9907	0.898	0.4728	98832	20598	0
74	0.4743	139355	0.1364	0.727	0.1667	90335	11016	0
75	0.7135	145638	0.9253	0.885	0.7997	108234	20664	0
76	0.0200	119458	0.4036	0.781	0.1314	88968	4295	0
77	0.0411	122621	0.0169	0.703	0.9044	113400	-27151	1
78	0.8623	150905	0.5004	0.800	0.9966	130406	-9668	1
79	0.5768	141938	0.3233	0.765	0.2240	92239	16295	0
80	0.5703	141771	0.0950	0.719	0.0965	87364	14569	0
81	0.1694	130434	0.6188	0.824	0.1430	89438	18007	0
82	0.5735	141853	0.7247	0.845	0.8992	113065	6794	0
83	0.5482	141212	0.4820	0.796	0.7923	107951	4510	0
84	0.0759	125671	0.0539	0.711	0.0298	82424	6902	0
85	0.9043	153064	0.2909	0.758	0.8226	109157	6892	0
86	0.3335	135698	0.8957	0.879	0.2138	91918	27381	0
87	0.5158	140397	0.1215	0.724	0.6837	104381	-2691	1
88	0.8147	148954	0.5718	0.814	0.6572	103620	17682	0
89	0.6217	143099	0.7544	0.851	0.8227	109162	12597	0
90	0.3105	135055	0.3717	0.774	0.6447	103269	1309	0
91	0.4650	139121	0.7581	0.852	0.6772	104192	14287	0
92	0.0693	125193	0.2231	0.745	0.2154	91969	1252	0
93	0.4847	139616	0.2294	0.746	0.5198	100003	4134	0
94	0.8902	152276	0.9535	0.891	0.9425	116493	19141	0
95	0.1851	131039	0.0424	0.708	0.2077	91725	1112	0
96	0.8552	150591	0.4652	0.793	0.0103	78940	40485	0
97	0.2762	134058	0.6126	0.823	0.1796	90790	19474	0
98	0.8945	152510	0.3946	0.779	0.2104	91810	26982	0
99	0.0757	125653	0.4947	0.799	0.8442	110105	-9715	1
100	0.1145	127969	0.4198	0.784	0.0707	85897	14425	0
							No. of Failures=	24
							Estimate of PF=	0.24

FIGURE 3-14. MONTE CARLO SIMULATION FOR EXAMPLE PROBLEM
(Trials 69 through 100) (Continued)

3.7.4 Response Surface Approximation Method.

For complex structures, the performance function is not available as an explicit function of the random design variables. The performance (or response) of the structure can only be evaluated numerically at the end of a (often time-consuming) structural analysis procedure such as the finite element method. The goal of the response surface methodology (RSM) is to find a predictive equation relating a response such as stress or deflection to a number of input variables. Once we accomplish this, the equation can be used to determine the response, given values of input variables, instead of having to repeatedly run the time-consuming deterministic structural analysis.

The response surface thus represents the result (or output) of the structural analysis encompassing (in theory) every reasonable combination of all input variables. From this, we can create (via simulation) thousands of combinations of all design variables, and perform a pseudo structural analysis for each variable set, by simply looking up (via interpolation) the corresponding surface value. Each approximation of structural analysis output is thus generated in a matter of milliseconds. The end result is the creation of a stress or strength PDF. This is the

bottom line. Once the stress and strength PDFs are defined, other methods (numerical integration, Monte Carlo, limit state approximation) can be used to determine the probability of failure. The general steps, shown graphically in figure 3-15, to use the RSM are as follows:

1. Perform the deterministic analysis (e.g., FEM) at strategically predetermined values of the random variables.
2. Using the results of step 1, construct an approximate closed-form expression for the response variable (could be stress or strength) in terms of the design variables, using regression techniques.
3. Create a response (e.g., applied stress) PDF from simulation of the design variables using the regression equation.
4. Find the probability of failure from the response PDFs using numerical integration, Monte Carlo simulation (section 3.7.3), or approximation methods (section 3.7.5).

3.7.4.1 Step 1—Analyze Structure at Chosen Values.

The challenge is to define representative combinations of the design variables to produce a representative output (response). Statistical design-of-experiments techniques can be used to select these representative combinations and systematically simulate the structural analysis. This is analogous to Monte Carlo simulation, but by using experimental design methods, strategic combinations of design variable values are employed to attempt to create an envelope containing all possible (within engineering reason) output values.

There are several experimental design plans commonly used (not necessarily for probabilistic analyses), including full and partial factorial. References for further study are in references 26-28. One approach mentioned in literature with a proven application (section 4.9) is the Box-Behnken method [29]. Box-Behnken designs require that all design variables be run at three levels (as depicted in figure 3-15): low, nominal, and high. If there are three design variables, then a total of 13 tests (runs of the structural finite element model) are required. Specifically the 13 tests would be performed as shown in table 3-9.

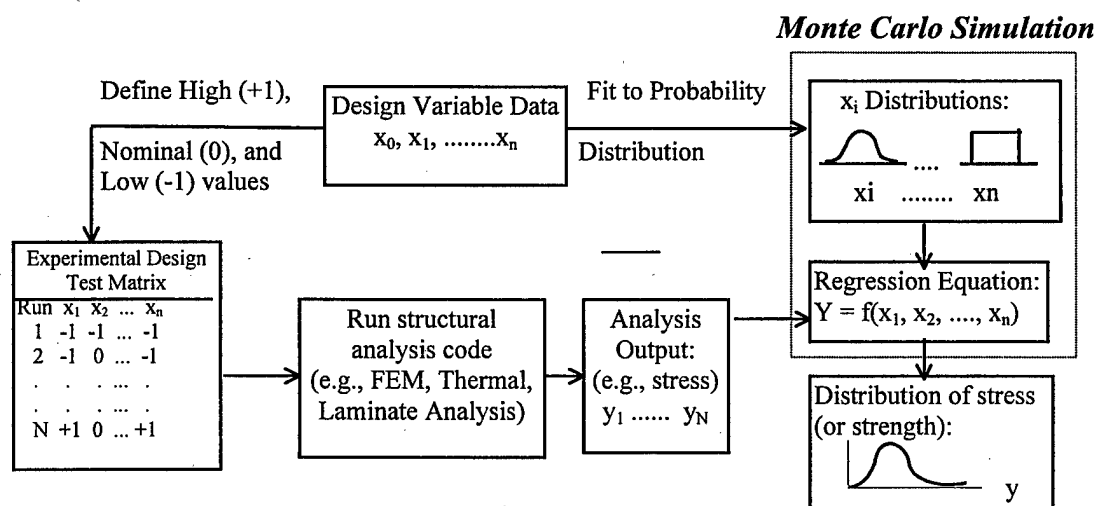


FIGURE 3-15. RSM PROCEDURE USING THREE LEVELS OF DESIGN VARIABLES

TABLE 3-9. BOX-BEHNKEN EXPERIMENTAL DESIGN MATRIX

Test Run No.	Variable 1	Variable 2	Variable 3
1	Low	Low	Nominal
2	Low	High	Nominal
3	High	Low	Nominal
4	High	High	Nominal
5	Low	Nominal	Low
6	Low	Nominal	High
7	High	Nominal	Low
8	High	Nominal	High
9	Nominal	Low	Low
10	Nominal	Low	High
11	Nominal	High	Low
12	Nominal	High	High
13	Nominal	Nominal	Nominal

3.7.4.2 Step 2—Develop Regression Equation.

Once all 13 structural FEM runs have been executed, a linear regression equation relating the design variable, Y , to the variables x_1, \dots, x_n can be obtained. The Box-Behnken design was developed for fitting second-order response surfaces, and the regression equation that can be estimated is of the form

$$Y = \beta_0 + \sum_{i=1}^N \beta_i x_i + \sum_{i=1}^N \beta_{ii} x_i^2 + \sum_{ii < j}^N \beta_{ij} x_{ij}$$

It is assumed that the regression equation will produce accurate estimates for the variable Y as long as the values for all the design variables are somewhere between their low and high values. That is, the regression model should not be extrapolated. One goal in regression analysis is to not have excessive terms in the equation, as the model is being forced to twist and turn through too many data points, thereby misrepresenting the nature of the response surface. To obtain the best small model, the first step is to eliminate those terms which do not make physical sense. That is, there may be physically meaningless combinations of variables (interactions). Next a stepwise regression procedure can be employed to ensure all variables (and combinations thereof) are contributing significantly to the model. Reference 30 provides a good discussion of regression theory.

3.7.4.3 Step 3—Develop Response Variable PDF.

Once the regression equation using all the design variables is developed, Monte Carlo simulation is used to generate a distribution for the response variable. A random draw is made from each design variable probability distribution, as shown in figure 3-15, and then a single response value associated with the set of chosen design variable values is calculated via interpolation. The result is a series of response values which can then be fit to a probability distribution or used to create a discrete distribution if a continuous distribution does not provide an adequate fit.

3.7.4.4 Step 4—Evaluate Probability of Failure.

Assuming (1) RSM generates both stress and strength distributions or (2) if only one is generated, the other is obtained by some other means, then the probability of failure can be calculated by integration, Monte Carlo methods, or limit state approximation methods.

Several important notes regarding the response surface methodology:

- Probability distributions for the input variables must be accurate.
- Regression equations must fit analysis results well and since they are only quadratic in nature, should only be used in situations where there are no abrupt changes in the response for moderate changes of input variables.
- Monte Carlo simulation must be run enough times to get an accurate depiction of the response variable's probability distribution.

3.7.4.5 Response Surface Method Example Problem.

An example of the response surface method is taken from reference 31. The hoop stress (response variable) in a gas turbine disk is influenced by the following six life drivers (input variables): radial temperature, modulus of elasticity, rotor speed, radial load, density, and coefficient of thermal expansion. Probability distributions for these input variables are given in table 3-10. FEM is used to determine hoop stress for combinations of these six input variables.

TABLE 3-10. PROBABILITY DISTRIBUTION DEFINITION FOR HOOP STRESS DETERMINATION

Design Variable	Probability Distribution
1. Temperature (°F)	Uniform (80, 220)
2. Modulus of Elasticity (psi, a function of temperature)	Uniform (-2σ , $+2\sigma$), where -2σ and $+2\sigma$ represent the lower and upper bounds of the modulus versus temperature curves.
3. Rotor Speed (rpm)	Normal (Base, 1.5% Base)
4. Radial Load (lb)	Normal (2.9×10^6 lb, 0.145×10^6 lb)
5. Density (lbm/in)	Normal (0.286, 0.0015)
6. Coefficient of Thermal Expansion (in/in/°F, a function of temperature)	Uniform (-2σ , $+2\sigma$), where -2σ and $+2\sigma$ represent the lower and upper bounds, respectively, of the CTA versus temperature curves.

Problem: What is the probability distribution for hoop stress in the gas turbine disk?

Solution: The input variables and their levels (coded as -1, 0, and +1 for low, nominal, and high, respectively) are given in table 3-11. In this methodology, low and high levels are selected to represent moderately extreme values. Rather than conduct a finite element analysis for each of

TABLE 3-11. LOW, NOMINAL, AND HIGH DEFINITIONS FOR VARIABLES

Input Variable	-1	0	1
F ₁ : Temperature (°F)	80	150	220
F ₂ : Modulus of Elasticity (psi)	-2σ	Nominal curve	+2σ
F ₃ : Rotor Speed (rpm)	Base - 3%	Base	Base +3%
F ₄ : Radial Load (lb)	2,610,000	2,900,000	3,190,000
F ₅ : Density (lbm/in.)	0.283	0.286	0.289
F ₆ : CTA (in/in/°F)	-2σ curve	Nominal curve	+2σ curve

the 729 combinations of the six input variable levels, the Box-Behnken method is implemented. Table 3-12 shows which combinations of input variables are analyzed.

TABLE 3-12. THREE-LEVEL BOX-BEHNKEN DESIGN TEST MATRIX

F ₁	F ₂	F ₃	F ₄	F ₅	F ₆
±1	±1	0	±1	0	0
0	±1	±1	0	±1	0
0	0	±1	±1	0	±1
±1	0	0	±1	±1	0
0	±1	0	0	±1	±1
±1	0	±1	0	0	±1
0	0	0	0	0	0

Since the designation ±1 represents two levels of the corresponding input variable, each of the first six rows corresponds to eight FEM runs. With the final row pertaining to the FEM run where all input variables are at nominal level, there are a total of 49 FEM runs required for this matrix. Results of these runs are shown in table 3-13.

TABLE 3-13. RESULTS OF FEM FOR GIVEN INPUT VARIABLE LEVELS

Run No.	F ₁	F ₂	F ₃	F ₄	F ₅	F ₆	Response
1	-1	-1	0	-1	0	0	138.80
2	-1	-1	0	+1	0	0	147.00
•	•	•	•	•	•	•	•
•	•	•	•	•	•	•	•
•	•	•	•	•	•	•	•
49	0	0	0	0	0	0	151.90

Stepwise regression is used to determine an equation which expresses the response, σ_{hoop} , in terms of the six input variables:

$$\sigma_{hoop} = 151.8 + 8.77F_1 + 0.41F_2 + 8.1F_3 + 4.14F_4 + 0.97F_5 + 0.79F_6 + 0.11F_3^2 + 0.2F_1F_2 + 0.37F_1F_5 + 0.25F_3F_4$$

This equation is then used to predict (very quickly) the hoop stress for different values of the input variables. To determine the hoop stress probability distribution, Monte Carlo simulation is used to generate values of the input variables from their respective distributions, and the regression equation is used to calculate the hoop stress value. The result of numerous simulations is a probability distribution for hoop stress.

3.7.5 Limit State Approximation.

These approximation methods have been the main thrust of probabilistic research over the past 15 years, and thus are the subject (either development or application) of numerous probabilistic analysis technical papers and reports. The premise is that the probability of failure as defined by the equation:

$$PF = \int_{..D..} \int f(x_1, \dots, x_n) dx_1 \dots dx_n$$

cannot be evaluated in closed form except for a limited set of design driver distributions. Monte Carlo simulation for complex structural analysis codes is impractical from an execution time standpoint, especially for low failure probabilities. Applying a technique such as the response surface method or importance sampling, to reduce the amount of structural analyses (e.g., FEM) required, is one way of approaching the problem. Another approach to solving the multivariable integral is to employ limit state approximation methods. These are also referred to as point expansion methods in the literature and can be divided into two groups: (1) mean value and (2) most probable point.

The first group, consisting of the Mean Value First Order (MVFO) and Mean Value First-Order Second-Moment methods, while being fairly easy to implement, have been shown to be potentially inaccurate for high reliability (low probability of failure $\sim 10^{-5}$ or below) calculations, as well as for highly nonlinear performance functions [17]. Since this document is dealing with aerostructures, we are definitely in the high-reliability region, and thus these approaches will not be addressed.

3.7.5.1 Most Probable Point Methods.

There are several methods in this group, the main ones being First-Order Reliability Method (FORM) and Second-Order Reliability Method (SORM). These methods are the most complex, both mathematically and conceptually, among all probabilistic analysis methods and will therefore not be described in excruciating detail here. The main steps to performing these analyses will be given and references given for the interested reader.

In the first- and second-order reliability methods (FORM/SORM), the approach is to transform the integral above to an approximately equal integral that can be efficiently evaluated. This is done by the following steps:

1. Transform the design variable distributions into standard normal distributions. That is, transform $g(x) = 0$ into $g(u) = 0$ where u is a vector of standardized, independent Gaussian variables (see figure 3-16).

2. Identify the *most probable point (MPP)*, or *design point*. For a given limit state function, the main contribution to failure probability comes from the region where g is closest to the origin in the transformed design variable space (u -space). The MPP is defined as the closest point to the origin in the transformed space.
3. Develop a polynomial approximation to the performance function (g -function) around the MPP. Thus the g -function is approximated by a simply defined (quadratic) surface through that point (MPP). Compute probability of failure using the newly defined g -function and the transformed variables.

This technique is graphically depicted in figure 3-16. Note that this is a three-dimensional depiction of the problem. For n -dimensional problems, there is a hypersurface $g(u) = 0$, which is the boundary between failure and success, known as the limit state surface.

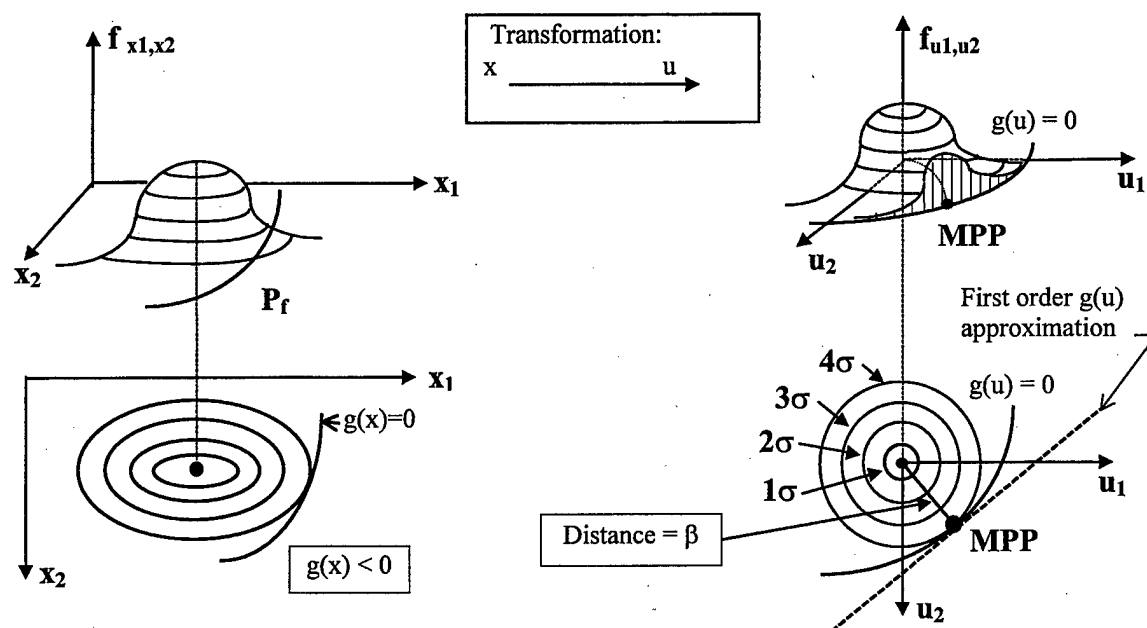


FIGURE 3-16. TRANSFORMATION TO STANDARD NORMAL SPACE

3.7.5.1.1 Step 1—Transform Variables.

FORM and SORM reliability approximations are carried out in the space of a set of standard, uncorrelated normal variates Y , obtained by transforming the basic variables. This transformation is dependent on the form of the probability distribution of each variable. The advantage of doing this probability transformation is to be able to exploit the superior properties of standard normal space. Specifically, the probability density in this space is symmetric (see figure 3-16) and it decays exponentially with the square of the distance from the origin. The transformation can be made in several ways. The most accepted method is the Nataf model [32] to transform a set of correlated, non-normal variables $X = (X_1, \dots, X_n)$ to the space of

uncorrelated standard normal variables $U = U_1, \dots, U_n$). A paper [33] by E. Nikolaidis et al. compares two commonly used methods.

Other attempts to improve on the fit between the transformed normal and original distribution are in the probabilistic literature [17, 23]. The well-known the Numerical Evaluation of Stochastic Structures Under Stress (NESSUS) probabilistic software uses a 3-parameter normal distribution, with the third parameter adjusting the distribution to better fit in the tail region, which influences the probability of failure [34].

The specific details of the different methods for transformation are mathematically complex and lengthy and will not be given here. References 17 and 23 give exhaustive details on this transformation.

3.7.5.1.2 Step 2—Identify Most Probable Point.

The MPP is the point on the limit state with the highest joint density, as can be seen in figure 3-16. That is, the point is most probable because it has the maximum joint probability density or largest contribution to failure. The MPP can be found by using an optimization algorithm or other iteration algorithms [23]. The optimization begins by guessing that the MPP lies at the set of mean values of each variable involved. Then the distance from the origin to the limit state surface (or hypersurface) is minimized subject to the constraint that the point (MPP) lies on the limit state.

The details of the optimization procedures are beyond the scope of this report; further details can be found in references 17 and 23. Determining the MPP is at the heart of these approximate reliability methods, and many issues are involved such as dealing with correlated variables, the type of search methods used in the optimization routines, and convergence criteria.

3.7.5.1.3 Step 3—Develop g-Function and Determine Failure Probability.

The function $g(u)$ is approximated by a polynomial in the vicinity of the MPP. The first-order reliability method (FORM) estimate is

$$P_f = P(g \leq 0) \approx \Phi(-\beta)$$

where β represents the minimum distance to the limit state. Gradients of the polynomial function are used to find the minimum distance.

Several second-order (SORM) approximations are available to improve accuracy. These higher-order approaches take into account the curvature of the limit state around the minimum distance point. The simplest of the SORM approximations, based on a paraboloid fitting, is from Breitung [35]:

$$P_f = P(g \leq 0) \approx \Phi(-\beta) \prod_{i=1}^{n-1} (1 + \beta k_i)^{-1/2}$$

where k_i denotes the i^{th} main curvature of the limit state at the minimum distance point. For practical problems which usually have a large β value, the quadratic form of the limit state

equation is a very good approximation of the actual probability. There have been many derivatives of the second-order approach to improve upon the accuracy of the approximation as well as decrease the number of evaluation of the failure function. These can be found in reference 23.

3.7.6 General Discussion of Limit State Approximation Methods.

The FORM approach is not accurate for limit state functions with large curvature at the MPP. SORM approaches are more accurate than FORM, but are more complex mathematically and require more failure function calculations, which may be costly. The accuracy of these methods depends on how well the approximate g-function represents the exact g-function. Perhaps the most important feature of these methods is they can be used to perform sensitivity calculations. Sensitivity factors can be calculated for each variable to determine the dominant variables, with respect to probability of failure.

Only a high-level overview of these methods was given in this section. The mathematical details of these methods are, in general, very difficult for most industry engineers to comprehend. There are three published documents that contain highly detailed explanations of these methods along with other facets of probabilistic analysis.

- Integration of Probabilistic Methods into the Design Process (SAE) [17]
- Modern Structural Reliability Methods (NASA) [23]
- Engineering Probabilistic Methods (SAE) [36]

3.7.7 Limit State Approximation Example Problem.

The stress applied to the bar depicted in figure 3-17 is denoted by S and is determined by dividing the load P by the cross-sectional area, A (considered to be constant). The resistive strength is denoted by R .

Statistics of the design variables are as follows:

- $R \sim \text{Normal: } \mu = 60; \sigma = 6$
- $P \sim \text{Normal: } \mu = 100; \sigma = 10$
- $A = 2.5$ (deterministic)

Note that normal distributions for R and Q are assumed. These distributions may actually be Gaussian or may result from a non-normal distribution being transformed to a normal via the approaches discussed in section 3.7.5.1.1. The transformation of the original distribution to an equivalent normal is a critical step in the limit state approximation approach.

The stress (load/area) distribution is formulated as

- Mean: $100/2.5 = 40$
- Standard Dev: $10/2.5 = 4$

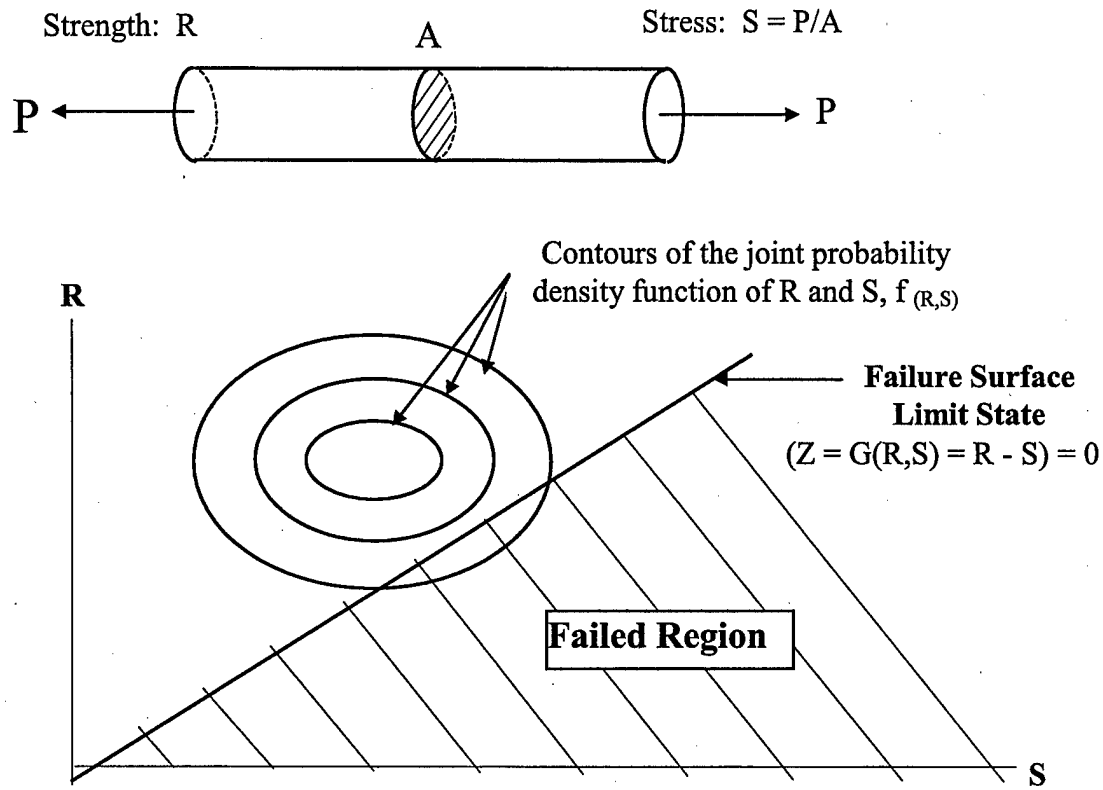


FIGURE 3-17. ORIGINAL PARAMETER SPACE WITH VARIABLES R AND S

The limit state is formulated as

$$z = R - S = 0.$$

The reduced variables are defined as

$$r = \frac{R - \mu_R}{\sigma_R} \quad s = \frac{S - \mu_S}{\sigma_S}$$

Substituting for R and S in these limit state equation yields

$$z = r\sigma_R + \mu_R - (s\sigma_S + \mu_S) = 0,$$

or

$$z = \sigma_R r - \sigma_S s + (\mu_R - \mu_S) = 0.$$

This limit state equation can be seen in figure 3-18. There is a theorem that states *The distance between the line $L: Ax + By + C = 0$ and the origin is given by*

$$d(0, L) = \frac{|C|}{\sqrt{A^2 + B^2}}. \text{ Applying this theorem to the limit state equation yields the following}$$

$$\text{value for the distance: } d = \frac{|\mu_R - \mu_S|}{\sqrt{\sigma_R^2 + \sigma_S^2}} = \beta. \text{ We have thus derived the formula for the}$$

distance from the origin to MPP (for linear limit state equation) in the reduced coordinate space, shown in figure 3-18.

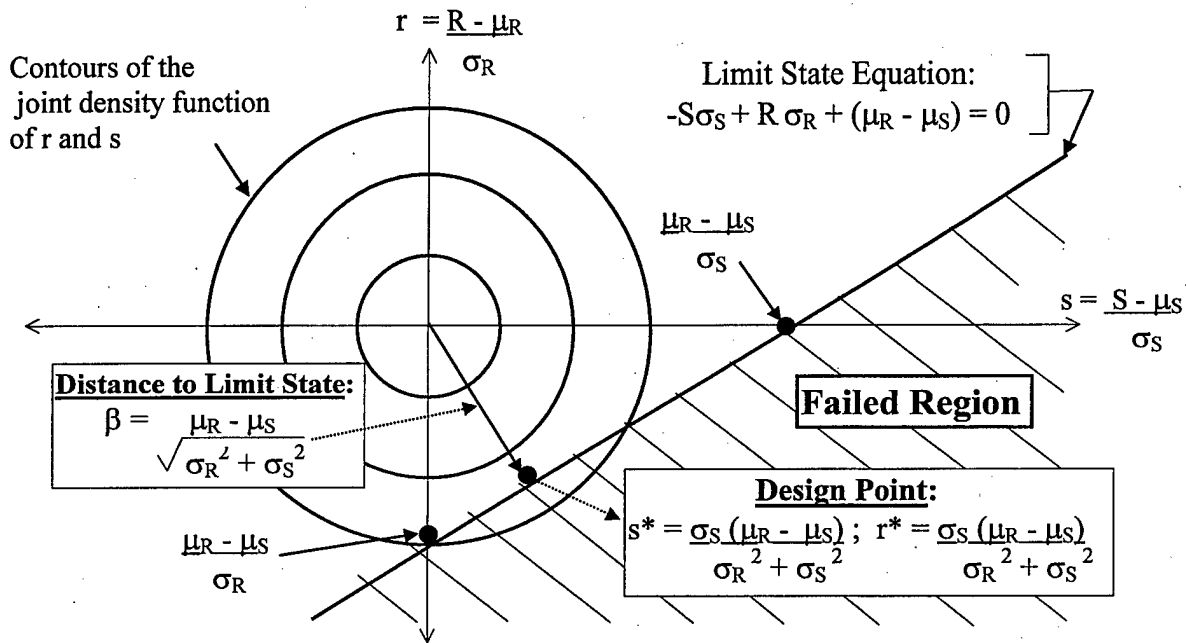


FIGURE 3-18. REDUCED COORDINATES PARAMETER SPACE WITH VARIABLES R AND S

Plugging in the values for the example, the limit state equation is $z = 6r - 4s + (60 - 40) = 0$. The distance from the origin to this limit state is thus $d = 20 / (6^2 + 4^2) = 2.77 = \beta$.

The design point, as shown in figure 3-19, is thus

$$s^* = 4(20)/(6^2 + 4^2) = 1.54$$

$$r^* = -6(20)/(6^2 + 4^2) = -2.31$$

The design point in the original parameter space is

$$R^* = 60 - (2.31)(6) = 46.14$$

$$P^* = 100 + (1.54)(10) = 115.40$$

The resulting probability of failure is then estimated as $P = \Phi(-\beta) = \Phi(-2.77) = 0.0028$. The accuracy of this estimate is a function of how well the normal distributions model stress and strength behavior.

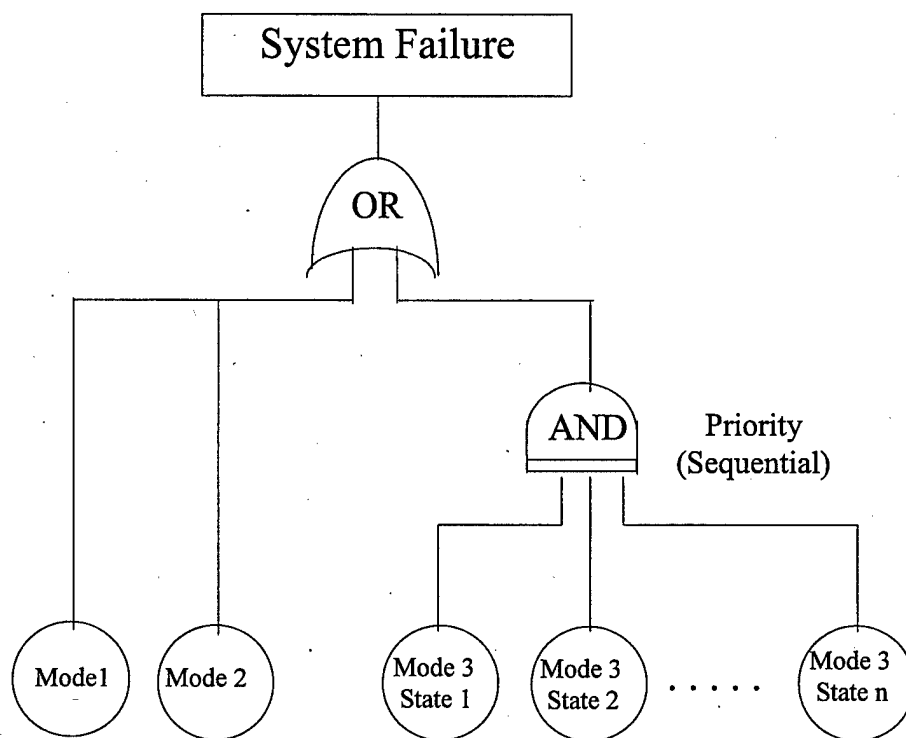


FIGURE 3-19. PROBABILISTIC FAULT TREE ANALYSIS METHODOLOGY

3.8 STEP 6—DETERMINE SYSTEM PROBABILITY OF FAILURE.

Once failure probabilities of individual locations have been calculated, the last step is to determine an overall probability of failure for the structural component or entire air vehicle. If all the N locations are independent, then the system probability of failure is calculated as

$$P_{f, system} = 1 - \prod_{i=1}^N (1 - P_{f, i})$$

In general, two structural locations are independent if the stress (or strength) of one has no influence on (and cannot be used to predict) the stress (or strength) of the other. This is somewhat intuitive for material strength. If, for example, a shear bay has a given material strength, it says nothing about the material strength of the adjacent shear bay. Only the material variability determined through testing could be used to sample the strength. So while the same strength distribution might apply to each shear bay, the random sampling is what makes the actual strength of one independent of the other. Actually, the shear strength of each is deterministic—a single value—but is unknown, so we use statistics to address the uncertainty in our prediction.

If an aircraft structure were subjected to only one load condition and the stresses throughout determined through analysis or testing, then the stresses would be totally dependent. In fact, the stress at one location could be used to predict the stress at any and all other locations. However, we know that aircraft structure is subjected to a variety of load conditions. Assuming these conditions are not simple linear multipliers of each other, the relationship between stress at any two locations is not correlated over the totality of load cases. In fact, they are so varied, that from a statistical standpoint they can be considered completely uncorrelated. This is how one can justify the independence of locations from a stress standpoint.

For example, within a shear bay, the stresses are correlated (that is, regardless of load condition, if we know the stress at one point, we know it everywhere in the bay), hence dependent. Between shear bays, however, knowing the stresses in one is of no help in predicting the stresses in the other, hence they are independent.

Fault tree analysis provides an organized means of identifying sources of structural system failure and their interactions which lead to one of more failure paths. Fault tree analysis theory will not be addressed here; further information can be found in reference 37. When dependency exists, the probability of a fault tree becomes very difficult to calculate by analytical approaches, and simulation approaches are more suitable. But simulation may require excessive time.

To address this need for efficient means for performing fault tree analysis with dependence, probabilistic fault tree methods were developed in the early 1990s. One methodology [38] has been integrated into the Southwest Research Institute's NESSUS software. The basic steps involved are:

- Develop a fault tree to represent the structural system.
- Construct an approximate performance function for each failure event based on most probable point (section 3.7.5).
- Determine sampling sequence.
- Calculate systems reliability using efficient Monte Carlo simulation (adaptive importance sampling).

Figure 3-19 shows how failure modes and sequential failure can be modeled using a fault tree. Sequential failures can be modeled using the PRIORITY AND gate. A sequence of limit state functions corresponding to a sequence of updated structural configurations with load redistribution must be generated during the analysis.

One advantage to using this approach is the ability of the analysis to provide a probabilistic ranking of the failure modes as well as problem variables.

4. SUMMARY OF INDUSTRY EFFORTS: 1980 THROUGH 1996.

Tables 4-1 and 4-2 list academia, industry, and government efforts in developing and applying the probabilistic methodology. Table 4-1 shows universities that have published research pertaining to probabilistic methods.

TABLE 4-1. PROBABILISTIC METHODS PUBLICATIONS—ACADEMIA

University	Subjects Applicable to Aerospace
University of Arizona	Probabilistic/Statistical Methods Development
Cleveland State University	Probabilistic Composite Mechanics
Massachusetts Institute of Technology	Probabilistic Calculation of Laminate Properties
State University of New York	Probabilistic Composite Mechanics
Tennessee State University	Probabilistic Methods Curriculum
University of Osaka	Composites Design Optimization
University of Texas at San Antonio	Probabilistic Material Strength Degradation
University of California, Berkeley	Probabilistic Finite Element Method
University of California, Los Angeles	Reliability-Based Structural Optimization
Vanderbilt University	Probabilistic/Statistical Methods Development
Virginia Polytechnic Institute and State University	Reliability-Based Structural Optimization
Wright State University	Reliability-Based Structural Optimization

Table 4-2 shows industry and government efforts, listing the approximate year the effort was started along with the subjects addressed and aircraft or aerospace components on which the method was applied. The approximate year started column is the year of the earliest publication found. This information was obtained from literature searches and subsequent research into nearly 100 published technical papers and reports on the subject.

4.1 DISCUSSION AND EXPLANATION OF INDUSTRY EFFORTS.

Fifteen industry efforts into probabilistic analysis development and application will be summarized in the following sections. Each summary will include the type of problem being solved and the basic theory of the probabilistic method. In addition, references will be provided for further study.

4.2 AIR FORCE.

One of the first, if not the first, efforts employing probabilistic methods in the aerospace industry, by J.W. Lincoln [39, 40], was to assess the risk of structural failure due to unstable cracking in older aircraft. One risk assessment addressed cracking due to static overload on the F-16 aircraft, while another assessed risk on the T-38 aircraft from fatigue cracking due to repeated loads. Probability of failure is determined from numerically integrating the applied stress and component strength PDFs.

TABLE 4-2. AEROSPACE COMPANIES WITH PUBLISHED PROBABILISTIC METHODS ARTICLES

Company	Approximate Year Started	Aerospace Subjects Addressed	Published Aerospace Applications	Material
Air Force	1980	Probabilistic/Statistical Methods Development Acceptable Risk Levels Aging Aircraft Risk Assessment	Risk Analysis: F-16 Wing, T-38 Wing	Metallic
NASA Lewis	1984	Probabilistic/Statistical Methods Development Probabilistic Composite Mechanics Probabilistic Design for Composites Probabilistic Fracture Mechanics Defect/Damage Modeling Probabilistic Thermal-Mechanical Fatigue Probabilistic Fault Tree Analysis	Space Propulsion Components Space Cantilevered Truss Generic Composite Laminate Panel Stiffened Composite Cylindrical Shell Generic Composite wing	Metallic Composite
Southwest Research Institute (SwRI)	1984	Probabilistic/Statistical Methods Development Probabilistic Finite Element Modeling Probabilistic Fracture Mechanics Probabilistic Fault Tree Analysis Reliability-Based Optimization	Space Propulsion Components Generic Truss Structure	Metallic
Jet Propulsion Laboratory	1985	Probabilistic Certification Probabilistic Fracture Mechanics	Space Propulsion Components	Metallic
Rockwell	1987	Probabilistic/Statistical Methods Development Probabilistic Finite Element Modeling	Space Propulsion Components Orbiter Docking Frame Structure	
NYMA (formerly Sverdrup Co.)	1988	Probabilistic/Statistical Methods Development Probabilistic Composite Mechanics Probabilistic Design for Composites Probabilistic Fault Tree Analysis Probabilistic Thermal-Mechanical Fatigue	Space Propulsion Components Generic Composite Laminate Panel Stiffened Composite Cylindrical Shell Generic Composite Wing	Metallic Composite
Northrop Grumman	1988	Probabilistic Design for Composites Defect/Damage Modeling	Risk Analysis: B-2 Wing Section, A-6 Wing, AV-8b Wing, Lear Fan Wing	Composite

TABLE 4-2. AEROSPACE COMPANIES WITH PUBLISHED PROBABILISTIC METHODS ARTICLES (Continued)

Company	Approximate Year Started	Aerospace Subjects Addressed	Published Aerospace Applications	Material
Aerospatiale (France)	1989	Inspection Interval Determination Probabilistic Certification Damage Modeling	ATR72, Airbus 330, 340	Metallic Composite
Pratt & Whitney	1989	Probabilistic Fracture Mechanics	Turbofan Engine Components	Metallic
General Electric	1990	Acceptable Risk levels Probabilistic Fracture Mechanics	Turbofan Engine Components	Metallic
NASA Marshall	1991	Probabilistic/Statistical Methods Development Probabilistic Structural Dynamic Analysis	Generic Beam Structure	
Thiokol Corporation	1991	Probabilistic Design for Composites	Solid Rocket Motor	Composite
NASA Langley Research Center	1992	Reliability-Based Structural Optimization Probabilistic Fatigue Analysis	Generic Truss Structure	
TsAGI (Russia)	1993	Probabilistic Design for Composites Defect/Damage Modeling	Lear Fan Risk Analysis	Composite
Grumman Aerospace	1993	Probabilistic Design for Composites	Validation Test of IPACS Composite Material Analysis Program	Composite
Nanchang Aircraft Company (China)	1994	Probabilistic/Statistical Methods Development	Generic Wing Structure	
Alpha STAR Corporation	1996	Probabilistic Design for Composites	Unknown	Composite

Lincoln defines cumulative probability of failure as $P(X > x)$, which is different than the typical statistics textbook definition, $P(X < x)$. Given an expected number of exceedances for a given stress level during one flight hour, E , the probability that stress is exceeded during a single-flight hour is calculated by:

$$E \geq 1 \Rightarrow P = 1$$

$$E < 1 \Rightarrow P = E$$

Essentially, the method equates expectation with probability, which significantly loses accuracy for expectations greater than ~ 0.1 . For example, just because 20 ksi is exceeded on average 1 time per flight hour (FH) does not mean that it will be exceeded every FH. However, the approximation is good for $E \rightarrow 0$, which is the critical part in his probabilistic analysis.

Extrapolation of the stress exceedance curve is critical to the calculation of failure probability. A fit of this probability function was done using Weibull plotting techniques [41], whereby the shape and scale parameters were found. The function was then extrapolated beyond measured data. The total wing probability of failure takes all locations into account statistically by assuming independence and uses a series reliability calculation. This failure probability is time dependent since the crack length is time dependent; therefore, the analysis must be rerun to assess the single-flight failure probability after different accumulated flight times.

Lincoln's method has a "restoration" feature, wherein repair of a crack is simulated. The strength of the component can be restored to its original strength. Probability of crack detection (called wing inspection reliability) is used in the analysis, hence inspection intervals can be studied and optimized. This method thus provides a means to assess the impact of different inspection intervals on failure probability.

4.2.1 F-16 Risk Assessment.

In this assessment, the risk due to cracking from static overload was analyzed. The method uses numerical integration to determine the joint probability of an applied stress and material strength distribution. The general procedure was as follows:

1. Establish an allowable failure rate.
2. Determine PDF for applied stress from load exceedance as described above.
3. Determine PDF for material strength from wing skin measurements, yield strength test measurements, and MIL-HDBK-5 mechanical property data.
4. Calculate failure probability using numerical integration.

This analysis provided a measure of single-flight probability of failure for the most severe load profile. This was a static strength analysis, focusing on finite stresses rather than crack-like singularities. No crack growth was modeled.

4.2.2 T-38 Risk Assessment.

T-38 service flight loads data showed that a mission change made the load environment considerably more severe than used in its initial damage tolerance assessment. A subsequent deterministic assessment showed that the inspection frequency should be increased by a factor of 3. A risk assessment was performed to determine if this increased inspection was essential to safety. Unlike the F-16 analysis, the risk T-38 analysis was based on crack growth models. Probability of failure of a particular location on the wing was based on the joint probability of exceeding a given stress level and attaining a critical crack length. Also factored into the method is the probability of crack detection. The general procedure was as follows:

1. Determine the PDF for applied loads based on flight loads exceedance functions normalized using expected exceedances per flight, then fit using a 2-parameter Weibull distribution. This is the same procedure used in the F-16 analysis.
2. Define the crack population based on tear-down data from 19 aircraft. Normalize the data to an average flight time using traditional fracture analysis (some cracks were artificially grown while others on high-time aircraft had to be decreased).
3. Fit a cumulative distribution function to the crack data at the average flight time.
4. From structural analysis methods, determine critical crack length versus applied stress at the analysis locations.
5. Using fracture mechanics theory, develop crack growth curves (crack length versus flight hours) at the analysis locations.
6. Develop a crack length versus probability of detection curve.
7. Calculate failure probability using numerical integration to determine the joint probability of exceeding an applied stress and attaining a critical crack length.

4.3 NASA LEWIS.

C. Chamis, of NASA Lewis, has been instrumental in the development of probabilistic design methods and analysis, particularly for space propulsion (turbine engine) components and more recently for composite structure. The early work, begun in the mid-1980s, was funded via the Probabilistic Structural Analysis Methods (PSAM) project. This was in response to a need for quantifying component reliability on the space shuttle program, in light of the Challenger accident. Southwest Research Institute was NASA Lewis' primary contractor for development of probabilistic structural analysis methods.

The PSAM project's goals were to develop a comprehensive structural analysis system capable of modeling uncertainty in loading, geometry, material behavior, and boundary conditions. The target application was space propulsion components. From this came the Numerical Evaluation of Stochastic Structures Under Stress (NESSUS) probabilistic finite element computer program. NYMA Inc. participated in applying the NESSUS program and in subsequent development efforts in composite probabilistic methods.

The analytical procedures used in NESSUS are discussed in section 3.7.5. The development and description of the probabilistic finite element software NESSUS will be discussed in the section describing the work done at Southwest Research Institute. Discussion of applications of the NESSUS software will appear in several subsequent sections, as several aerospace companies have NESSUS applications.

4.3.1 Integrate Probabilistic Analysis of Composite Structures (IPACS).

Chamis led the NASA Lewis effort to develop a probabilistic design methodology for composites. NYMA Inc. was subcontracted to perform most of the development work, the result being the IPACS methodology [42, 43] which combines composite micromechanics theory, structural mechanics, system concepts, and manufacturing considerations. Figure 4-1 shows a schematic of the program. The methodology starts with fiber mechanical and physical properties, resin properties and fiber placement techniques, and then applies a micromechanics approach to produce a laminate theory. This is followed by a probabilistic finite element analysis utilizing the structural analysis. IPACS does not require extensive specimen testing which is cited by many as adding to the cost of composite applications.

PICAN, structural response simulator, and FPI (an extension of the first- and second-order limit state approximation method) have been integrated into the computer code IPACS for a comprehensive probabilistic assessment of composite structural response. As depicted in figure 4-1, IPACS consists of two computer modules: (1) PICAN, for simulating probabilistic composite mechanics and (2) NESSUS, for simulating probabilistic structural responses using the information obtained from PICAN. These two modules can simulate uncertainties, from constituent materials to the composite structure including its boundary loading conditions, and environmental effects [44].

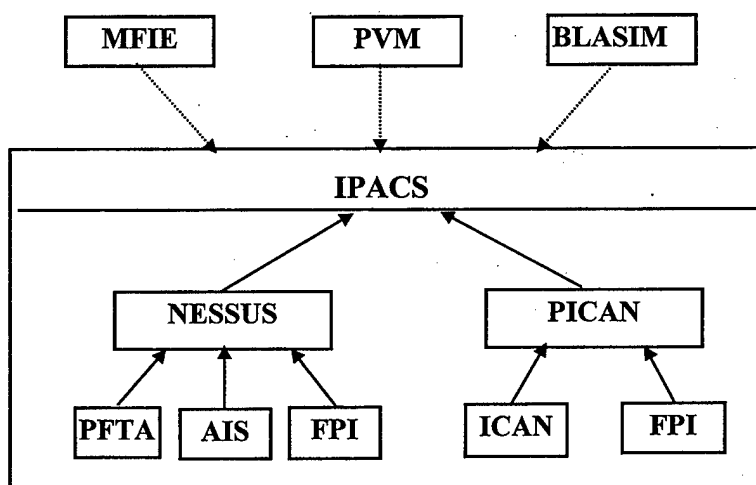


FIGURE 4-1. INTEGRATED PROBABILISTIC ANALYSIS OF COMPOSITE STRUCTURES (IPACS)

Figure 4-2 shows the physics which forms the basis for the IPACS code. The assessment starts with the identification of primitive variables at the micro and macro composite scales including

the fabrication process. These variables are selectively perturbed several times in order to create a database for the determination of the relationships between the desired material behavior and structural response and primitive variables. Composite micromechanics is used to carry over the scatter in primitive variables to the ply and laminate scales (steps A and B in figure 4-2).

Laminate theory (via ICAN) is then used to determine the scatter in the material behavior at the laminate scale (step C). This leads to the perturbed resultant force, moment-strain, and curvature relationships used in the structural analysis. Next, the finite element analysis is performed to determine the perturbed structural responses corresponding to the selectively perturbed primitive variables (step D). This completes the description of the hierarchical composite material and structure synthesis shown on the left side of figure 4-2.

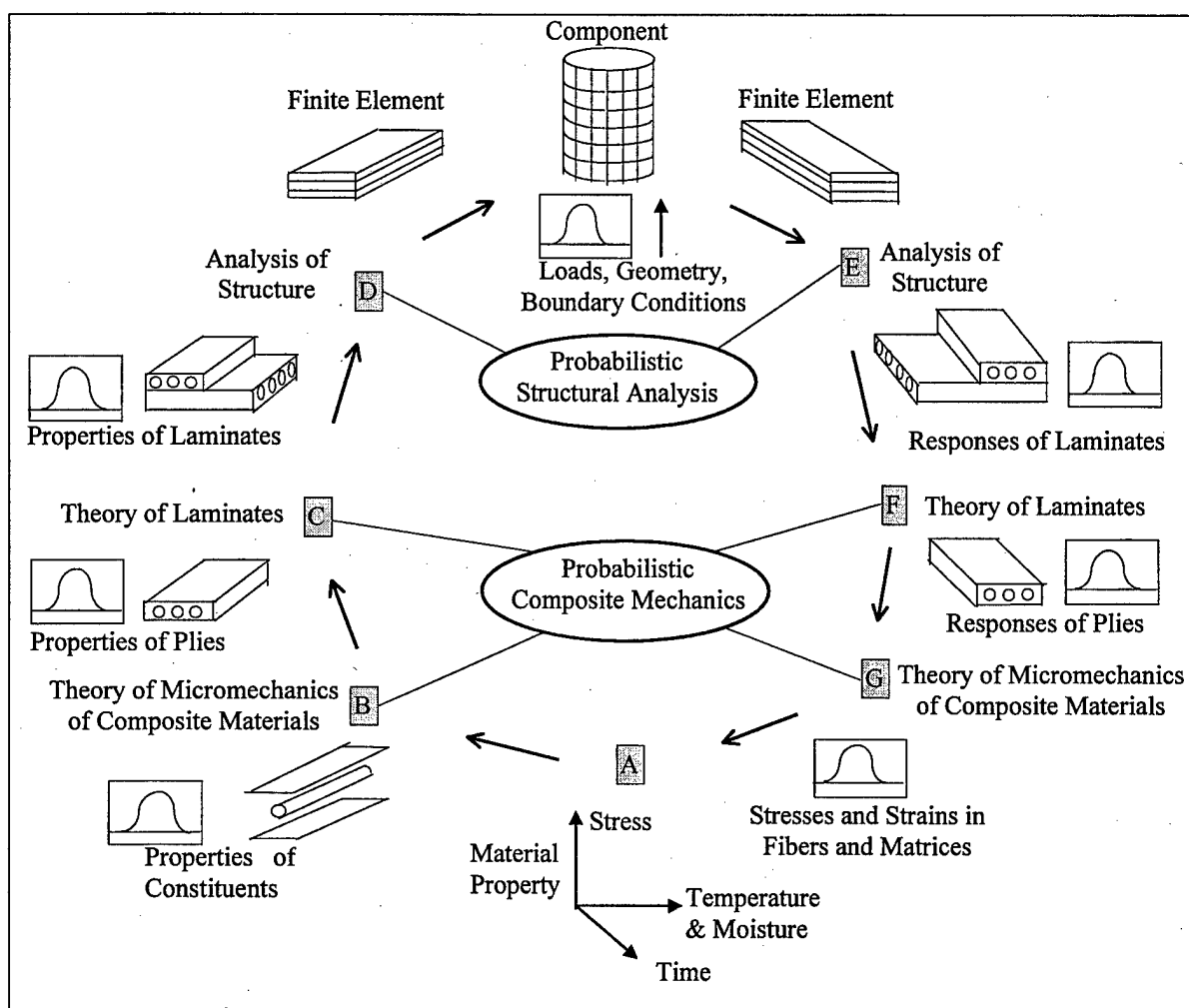


FIGURE 4-2. NASA LEWIS COMPOSITES PROBABILISTIC ANALYSIS

Steps E through G show the progressive decomposition of the structural response to the laminate (E), ply (F), and fiber and matrix (G) constituent scales. After the decomposition, the perturbed fiber, matrix, and ply stresses can be determined. Fast probability integration (FPI) [25] is used to determine the functional relationship between the response (e.g., compressive strength) and

primitive variables. The CDF of the response is then calculated using this functional relationship.

4.3.2 Integrated Composite Analyzer (ICAN).

ICAN simulates composite material behavior starting from the lowest composite scale (fiber and matrix constituents) to higher scale (ply, laminate). Micromechanics and laminate analysis based on linear elastic theory are used to compute constituent, ply, and laminate level properties required for the global structural analysis. ICAN also decomposes the global structural response to laminate, ply, and constituent response levels (stress and strains) which helps the user to evaluate failure, as shown in figure 4-2. Failure analysis is performed based on different failure criteria such as first-ply failure criteria, fiber break criteria, modified distortion energy criterion, and Hoffman's criteria [45].

4.3.3 Probabilistic Integrated Composite Analyzer (PICAN).

ICAN has been integrated with FPI, leading to PICAN for the probabilistic assessment of composite mechanics. PICAN starts with defining uncertainties in material properties and fabrication variables at the most fundamental scale. Then the uncertainties are progressively propagated to higher scales. Probability density and cumulative distribution functions can be obtained at the various composite scales for all material properties and fabrication variables. Sensitivity of various design variables to composite material properties is also obtained [46].

4.3.4 Adaptive Importance Sampling (AIS).

AIS is different from traditional Monte Carlo importance sampling methods for its ability to automatically adjust, and thereby minimize, the sampling space. AIS is embedded in NESSUS. There are two features of this method: (1) the sampling region is focused on the most important region where it has the highest possibility of failure, and (2) the sampling region is gradually increased by deforming the sampling boundary until the sampling region covers the failure region sufficiently. More details can be found in references 17 and 23.

4.3.5 Probabilistic Fault Tree Analysis (PFTA).

With traditional Fault Tree Analysis, probabilities for basic events are determined which are assumed to be independent. However, when dependency exists between basic events, Monte Carlo simulation is one method that can offer accuracy. PFTA, which is embedded into the NESSUS software, can also address this dependency as well as calculate system reliability. PFTA can also deal with a structural system having multiple failure paths due to multiple components or multidesign criteria. More details can be found in section 3.8 of this document and references 23 and 35.

4.3.6 Multifactor Interaction Equation (MFIE or TMFIE).

To account for the degradation or aging of material properties due to cyclic loads, the MFIE model was developed at NASA Lewis. MFIE has been used to simulate long-term behavior of

polymer matrix composites and is planned for application to the high-speed civil transport (HSCT) design.

MFIE evaluates the magnitude of degradation and properties of constituent materials at every time step, which in turn is used for micromechanics and laminate analysis at each step. Sensitivity evaluations of response variables to the random variables at every time step are also performed to compute the respective scatter in response variables. More details can be found in references 47 and 48.

4.3.7 Parallel Virtual Machine (PVM).

The PVM is an integrated framework for heterogeneous network computing, allowing scientists to exploit a series of networked machines when carrying out complex scientific computations. With the use of a message sent over the network, multiple tasks of an application can be incorporated to solve a problem in parallel.

PVM is conducted within the IPACS software. Information needed for individual perturbation finite element analysis is sent to an available workstation by PVM message passing routines. Individual finite element analysis is then carried out at each workstation. Once perturbation analysis is complete, structural responses are sent back to the control workstation. After all results are returned to the control station, limit state approximation methods to compute probability of failure are performed. More details can be found in reference 49.

4.3.8 Blade Assessment for Ice Impact (BLASIM).

BLASIM is a specialized code for turbofan engine compressor blades subjected to ice impact, simulating local and far-field damage in many different blade-type structures. Capabilities include static, dynamic, resonance margin, and supersonic flutter simulation. Various types of loading including pressure, temperature, and centrifugal can be applied. A coarse finite element mesh consisting of triangular plate finite elements can be generated with minimal execution time [50].

4.3.9 Recent Work by NASA Lewis.

A technical paper [51] was published in 1996 describing computational methods to probabilistically simulate fracture in bolted composite structures. An approach that is independent of stress intensity factors and fracture toughness was used to simulate progressive fracture. A fast probability integrator assessed the scatter in the composite structure response before and after damage. These methods were demonstrated for a bolted joint of a polymer matrix composite panel under edge loads.

4.4 SOUTHWEST RESEARCH INSTITUTE (SwRI).

Nearly 40 technical papers on probabilistic analysis from SwRI authors have been presented since 1986. The work was funded from the NASA Probabilistic Structural Analysis Methods (PSAM) project, which was (what ended up to be) a 12-year research and development program, which SwRI was the prime contractor. Rockwell Corporation and several universities were

subcontractors for this effort. The project was funded in 2 phases: (1) probabilistic structural response analyses of the space shuttle main engine components (1984-1989) and (2) structural system risk assessment, qualification, certification, and health monitoring (1990-1995). The objective of the program was to develop probabilistic structural analysis methods for critical space shuttle main engine (SSME) metallic components such as turbine blades, transfer ducts, piping systems, and liquid oxygen posts.

A major accomplishment of the PSAM program was the development of the NESSUS computer program, which integrates limit state approximation and efficient Monte Carlo methods with general structural analysis capabilities. This can be classified as a probabilistic finite element tool. Rockwell Corporation has applied NESSUS to critical SSME components; this is discussed in section 4.6.1. The NESSUS program has also been used in geomechanics, nuclear waste, and rotordynamics research [52-54].

NESSUS numerically simulates structural mechanics and design variable uncertainties using limit state approximation methods integrated with finite element and boundary element methods. The output provides (1) probability of failure calculations and probability distribution analysis (e.g., generating a stress distribution) and (2) probabilistic sensitivity analysis to identify critical failure modes and random variables. Figure 4-3 show NESSUS capabilities. It appears to be a very impressive probabilistic analysis tool.

Random Variables

Loads

- Forces
- Pressures
- Temperatures
- Vibrations

Material Properties

- Moduli
- Poisson's ratio
- Yield stress
- Hardening parameters
- Material orientation

Geometry

User-defined

Probabilistic Methods

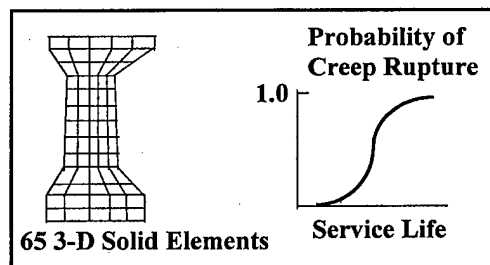
Fast Probability Analysis

- Advanced mean value
- First and second order
- Fast convolution

Sampling

- Standard Monte Carlo
- Latin Hypercube
- Adaptive importance

Probabilistic Fault Tree



Probabilistic Analysis

- Full probability distribution
- Component reliability
- System/multifailure modes
- Probabilistic sensitivities
- Probability-based risk/cost

Performance Functions

- Structural response: stress, strain, displacement
- Fatigue and fracture life
- Creep rupture life
- User-defined subroutines

NESSUS/FEM

- 1,2,3D elements
- Static
- Transient dynamics
- Buckling
- Vibrations
- Nonlinearities

Interfaces

- ABAQUS
- ANSYS
- DYNA
- NASTRAN
- PATRAN
- PRONTO
- User-defined

Hardware

- Mainframes
- Workstations
- PC, Macintosh

FIGURE 4-3. NESSUS FEATURES AND CAPABILITIES

4.4.1 Probabilistic Methods in NESSUS.

Figure 4-3 lists Fast Probability Analysis under the heading Probabilistic Methods. This method, developed by teams headed by Y.-T. Wu of SwRI, contains first- and second-order reliability methods (FORM/SORM), convolution, advanced first order, conventional Monte Carlo, and Monte Carlo with efficient sampling. Wu led pioneering efforts in extending FORM/SORM techniques to develop the Advanced Mean Value First-Order (denoted AMV+) method to better account for nonlinear performance functions.

In addition, he led development of a fast convolution method, which used the convolution theorem and the fast Fourier transform (FFT) technique to compute the probability of failure when the approximate linear or quadratic g-functions involve independent, non-normal random variables. This fast convolution method can calculate the exact probability of failure for a linearized performance function. Therefore, once the function is linearized, this procedure can be applied to compute accurate probability of failure results.

From 1990 to 1994, much of the method development focused on Adaptive Importance Sampling (AIS) Monte Carlo to compute reliability and design parameter sensitivities. In this approach, sampling is focused around the failure domain, thereby minimizing over-sampling in the safe region. Significant efficiency can be gained relative to conventional Monte Carlo simulation. This is discussed in section 3.7.3.4.

4.4.2 Performance Functions in NESSUS.

In addition to stress, strain, and displacement analyses, the scope of the code was expanded in 1992 to include probabilistic life and fatigue prediction of structures. In 1994, NESSUS could handle problems governed by linear elastic fracture mechanics where the crack path, weight function, Green's function, i.e., or influence function, was known. The stress intensity factors are determined using the stress along the crack path of the uncracked body. The stress along the crack is determined by finite element analysis of the uncracked structure. Figure 4-4 depicts the NESSUS probabilistic fatigue crack growth algorithm.

What dictates failure in real structures will usually be a sequence or interaction of individual failure modes. To address this, a probabilistic fault tree analysis methodology was embedded into NESSUS. As discussed in section 3.8, a fault tree provides a systematic way to deal with multiple failure paths composed of multiple components and/or multiple failure modes.

In traditional fault tree analysis, probabilities are assigned to the bottom events, and propagated through gates (AND, OR, etc.). For typical structural reliability analysis problems, however, the failure events will often times be correlated due to sharing common variables. To account for this dependency, it is necessary that the limit state functions, rather than simply the probabilities, be used to define the bottom events.

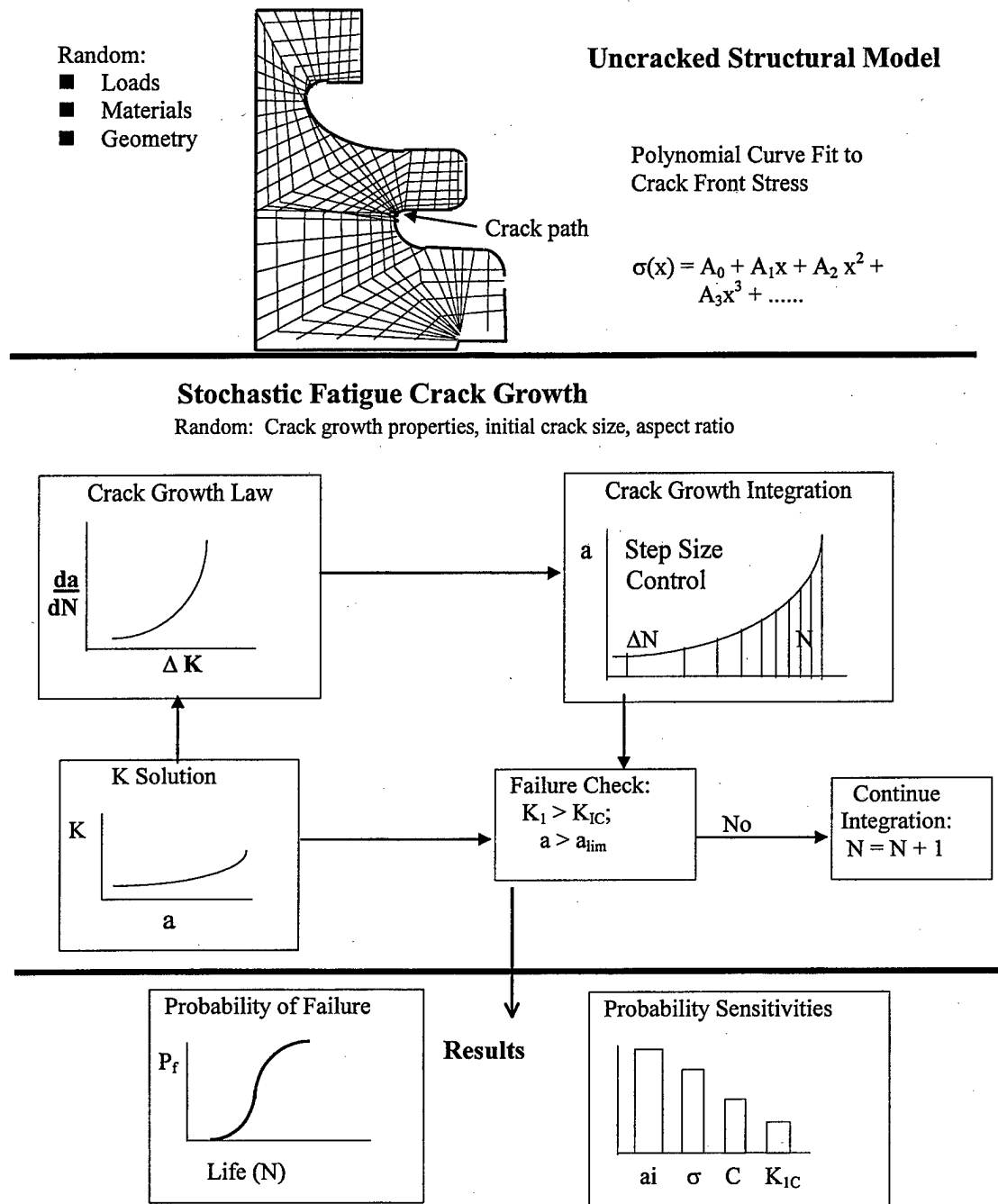


FIGURE 4-4. NESSUS PROBABILISTIC FATIGUE CRACK GROWTH ALGORITHM

4.4.3 Recent Work.

SwRI is involved in (as of 1997) development of a damage tolerance design code to augment the safe-life approach. The goals are to produce a probabilistic design code capable of being interfaced with external finite element and fracture mechanics codes, providing risk sensitivities that identify the relative importance of input parameters. The project targeted engine rotor design and analysis [55].

4.5 JET PROPULSION LABORATORY (JPL).

In 1985, the JPL Engine Certification Project was initiated to develop an improved methodology for quantitatively evaluating and establishing flight readiness (certification). The program was entitled Probabilistic Failure Analysis (PFA). The *Challenger* accident (1986) impacted the development of this technology in several ways. First, Professor Richard Feynman, during the failure investigation, determined that design engineers believed the risk of engine failure to be about 1 in 200; higher management understood the risk to be 1 in 100,000 [56]. Somewhere between design and certification, the real information was being lost. NASA began to examine different approaches for identifying risk, perhaps at the design level. Risk could then be elevated to certification in a quantitative procedure, rather than qualitatively implied from the safety factor.

The second influence of the *Challenger* accident was that a significant amount of money was appropriated for the advancement of safety and risk technology. In addition to the JPL Engine Certification project, the Probabilistic Structural Analysis Methodology (PSAM), described in section 4.3, received large sums of funding.

In 1988, an effort was initiated with the Marshall Space Flight Center to begin technology transfer of the JPL probabilistic methods. From 1988 through 1990, little progress was made. The PFA technology (described below) as defined, documented, and presented was extremely difficult for the reviewers to penetrate and understand. Because of this, coupled with the fact that it was not being applied, the PFA program was cancelled by the Shuttle Program Office. Later, it was reinstated with limited funding through 1992, during which time a new Marshall team was formed, and together with JPL members, were tasked to (1) gain a thorough understanding of the PFA method, (2) assess the utility of the method along with supporting software tools, and (3) develop a plan for the technology transfer of the method to NASA Marshall.

4.5.1 PFA Methodology [57].

Figure 4-5 depicts the PFA methodology. For each critical failure mode, information comes from two sources: operating experience and engineering analyses. Operating experience may consist of success/failure data, development testing, flight operations, and certification testing, etc. Engineering analyses characterize the conditions under which specific failure mode may occur, such as pressure, accumulated time in service, etc. Within the engineering analyses, parameter uncertainties and failure mode models are merged with the quantitative model of the failure phenomenon.

PFA utilizes a FEM to develop a response surface equation, which is based on a design of experiments approach (described in section 3.7.4). After a closed-form relationship is defined between the input and output parameters, direct Monte Carlo simulation is applied to establish the failure model. After finishing the engineering analyses, the prior failure probability, which is called prior distribution, can be estimated. Then, a Bayesian statistical algorithm is used to update this prior distribution to reflect available success/failure data. The system failure risk estimate for service life is performed with one or more relevant failure modes using their probability distributions from the Bayesian analysis to arrive at the probability of a failure

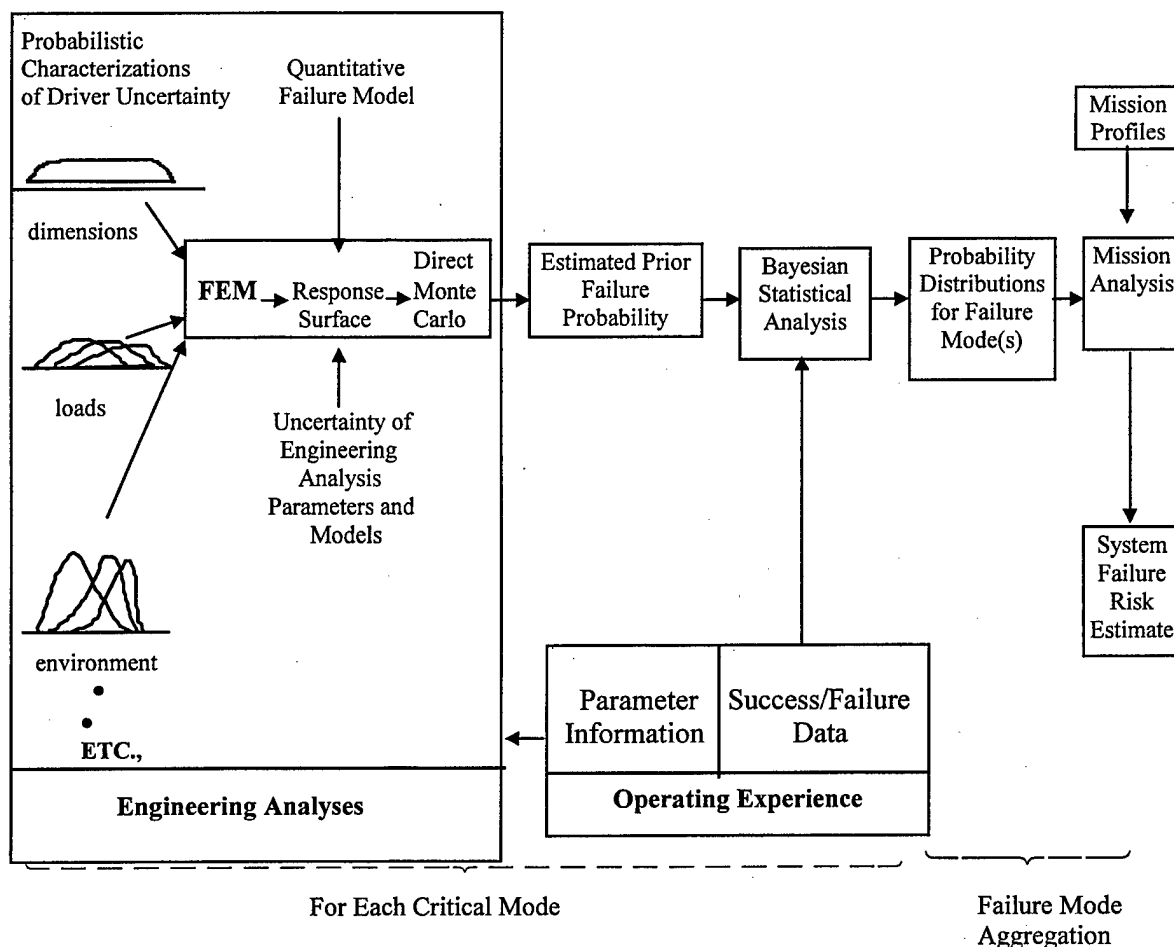


FIGURE 4-5. PROBABILISTIC FAILURE ASSESSMENT METHODOLOGY

occurring during a mission or set of missions. By conducting sensitivity analyses, the responsible drivers can be identified and subsequent corrective action can be taken.

The PFA methodology has been applied to high-cycle [58] and low-cycle fatigue [59] failure analysis, as well as flaw propagation [60].

4.5.2 NASA Marshall Conclusions and Recommendations [56].

After evaluating the PFA method and software for 18 months, the MSFC task group said that while recognizing the ground breaking efforts of the JPL team, that succeeded in introducing and advancing the probabilistic approach within NASA, the PFA approach could not be easily understood and practically applied and therefore should not be adopted for probabilistic structural analysis at NASA. The team also reviewed the NESSUS procedures and methods and said it had potential to become a standard design tool for probabilistic analysis in NASA applications. The specific criticism of the JPL approach stemmed from the reports documenting the approach being difficult to comprehend, the Bayesian updating concept appeared unnecessary (and complex), and the methodology was very application specific (software must be restructured for different applications).

4.6 ROCKWELL INTERNATIONAL CORPORATION.

The Rocketdyne Division of Rockwell International, having design and manufacturing responsibility of the space shuttle's main engine, was obviously an integral part of the development and application of NASA Lewis' Probabilistic Structural Analysis Methods program. One particular application of the NESSUS code was the high-pressure fuel turbopump (HPFTP) turbine blade on the main engine.

4.6.1 SSME Turbopump Blade Application.

This example became well known and was the subject of numerous technical papers [61 through 64] and presentations at technical conferences. The example describes a method of obtaining probabilistic (dependent) pressure, temperature, and centrifugal steady-state load descriptions of the second-stage turbine blade from the top of the airfoil to the intersection with the "fir tree" (the fir tree-shaped attachment region at the inner end of the blade).

Rocketdyne applied NESSUS to determine the structural response of the turbopump blade shown in figure 4-6. The finite element model shown has about 6,000 degrees of freedom. Random design variables for the blade consisted of nine manufacturing variables and nine loading variables. Manufacturing variables include three rigid-body orientations of the airfoil (associated with the process of machining used on the blade root), three orientations of the cubic single crystal being evaluated, and three material properties for the single crystal. The nine loading variables concerned operating conditions for the turbopump, each of which had some predictable effect on rotor speed, blade temperature, and pressure loading conditions for steady-state operation.

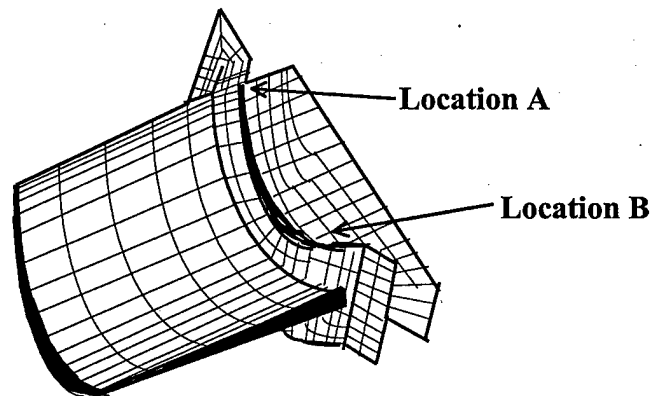


FIGURE 4-6. SSME HPFTP SECOND STAGE TURBINE BLADE FE MODEL

Engine simulation was used to define the effect of each design (operating condition) variable on the three loading conditions. Results of the NESSUS analysis are plotted in figure 4-7. The two parts of the figure correspond to the two limiting locations identified on the finite element model. The plots depict the CDF of effective stress at both locations. Of most importance in the design study were the probabilistic sensitivity or importance factors shown. At location A, the dominant factor was hot-gas seal leakage, resulting in the highest blade stress. At location B, two single crystal orientations were among the most dominant factors.

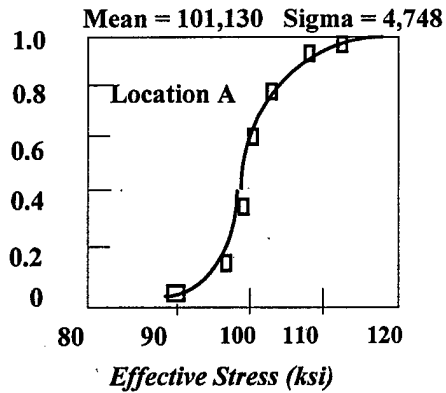
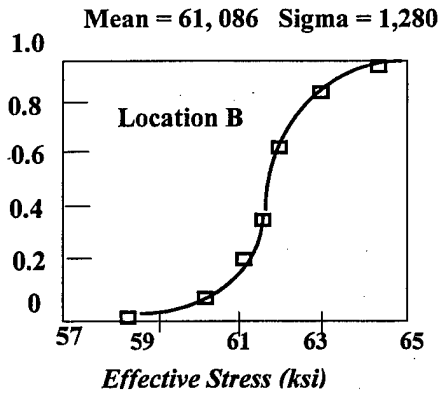


FIGURE 4-7. NESSUS CDF RESULTS FOR LOCATIONS A AND B

4.6.2 Probabilistic Analysis Methodology Development Efforts.

Around 1990, a multiyear research project began at Rockwell to develop a finite element-based first-order reliability analysis method. The objective was to develop probabilistic methods and algorithms that could be integrated with finite element structural analysis. The result was a computer program named Finite Element-Based Reliability (FEBREL). The probabilistic methods in FEBREL provide a means of modeling uncertainties, computing probabilities, and performing sensitivity analyses [66].

M. R. Khalessi led development of a Most Probable Point Locus (MPPL) procedure, which is incorporated into FEBREL. This procedure applies to limit state approximation methods. The procedure examines the performance (g) function along a most probable point locus in search of the most probable point(s) on the limit state surface and identifies unusual conditions, such as multiple most probable points. This addressed a published criticism that limit state approximation methods may not converge or there may exist multiple minimum points (values of beta).

An interface program was developed to enable data transfer between FEBREL and MacNeil-Schwendler Corporation's MSC/NASTRAN finite element software. Demonstration examples of both static and dynamic problems are given in reference 67. Figure 4-8 shows the FEBREL-MSC/NASTRAN structure. FEBREL was also interfaced to the LS DYNA-3D finite element package and applied to perform a probabilistic transient dynamic impact analysis of a horizontal 7-ft free fall of a U.S. Army munitions container onto a rigid surface [68].

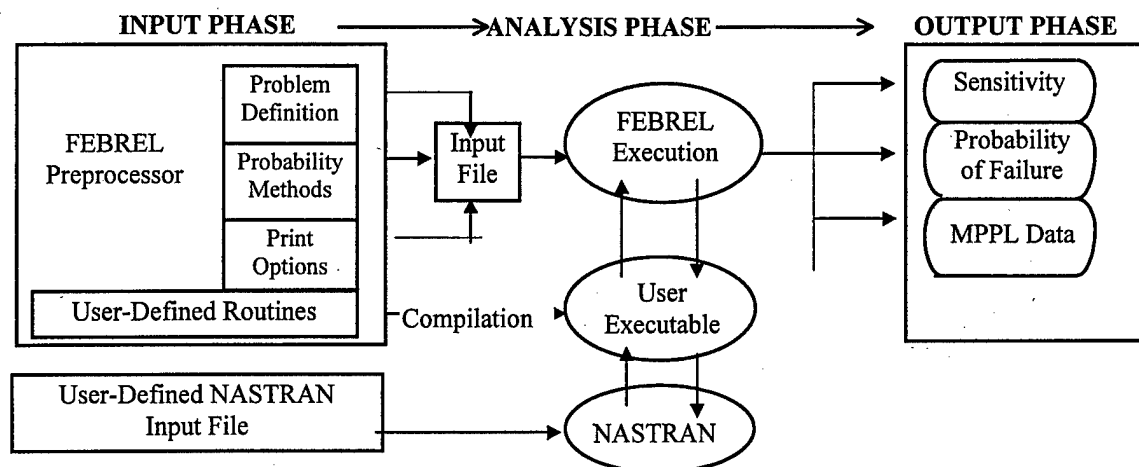


FIGURE 4-8. FEBREL-MSC/NASTRAN CODE STRUCTURE

4.7 NYMA, INC.

Formerly called Sverdrup Technology, NYMA has been a subcontractor to NASA Lewis Research Center, primarily in development of probabilistic analysis methods associated with composites. NYMA led the development of the Integrated Probabilistic Assessment of Composite Structures (IPACS) software which is described in section 4.3.

For long term behavior prediction of composites, the ICAN computer code was modified to implement time dependent multifactor interaction equations (MFIE) and perform sensitivity evaluation for random variables [47, 48]. A discussion of MFIE can be found in section 4.3.6. MFIE was expanded to include time-dependent degradation effects of composite material behavior due to environmental, fabrication and load effects. The result was a module to NESSUS called TMFIE.

A methodology to compute probabilistic fatigue life of polymeric laminated composites was the subject of a 1995 technical paper. Matrix degradation effects due to long term environmental exposure and mechanical and thermal cyclic loads are accounted for via simulation. Several test cases were run using graphite/epoxy laminates.

In addition, NYMA led the effort to incorporate a parallel processing capability into the IPACS software. This capability (denoted PVM) is discussed in section 4.3.7. Recent work includes probabilistic simulation of progressive fracture in composite laminated bolted joints [69].

4.8 AEROSPATIALE.

The work of Rouchon et al. in composite probabilistic analysis [70] primarily deals with probabilistic inspection. This issue is related to damage tolerance in connection with accidental service induced damage. Accidental damage is addressed through a scheduled inspection program based on the proportion of flight time variable. The proportion of flight time is defined as follows:

Proportion of flight time = probability of failure per flight hour \times avg. time in failed condition, where the average time in failed condition is assumed to equal 50% of the interval of time between inspections.

The methodology requires a comprehensive database on the probability of impact damage on structures, allowing for the components involved, aircraft operating conditions, damage location, etc.

Probabilistic analysis was used to determine inspection intervals such that the probability of failure was no greater than 1.0×10^{-9} /flight hour. The expression for PF is

$$PF = \int P(at) Pr(at) [1-Pd(at)] d(at)$$

where

$P(at)$ is the probability of occurrence of damage size "at,"

$Pr(at)$ is the probability of load exceeding the residual strength for damage size "at," and

$Pd(at)$ is the probability of detecting damage of size "at."

It is not stated if these functions are PDFs or CDFs, but $P(at)$ should be a PDF, while $Pr(at)$ and $Pd(at)$ should be CDFs. The integration is over possible damage sizes "at." For a specific "at," they multiply its incremental probability $[P(at \text{ all})]$ by (1) the probability that the load is greater than $r(at)$, which is the residual strength at the value "at" (note that as "at" increases, this probability approaches 1, thus is a cumulative probability) and (2) 1 minus the probability that the defect "at" is detected (note also that as "at" increases, this probability approaches 1, thus is a cumulative probability also). Then the integration over all values of "at" of this three-factor product yields the PF.

This methodology makes the following assumptions about requirements on probabilistic and conditional probabilistic measures:

- Acceptable probability of structural failure is $\leq 1 \times 10^{-9}$ per flight hour.
- Probability of occurrence of a defined damage size is $\leq 1 \times 10^{-5}$ per flight hour.
- Probability of experiencing limit load and gust is $\leq 2 \times 10^{-5}$ per flight hour.
- Probability of experiencing ultimate load is $\leq 1 \times 10^{-8}$ per flight hour.

Relationships between various impact energies and damage sizes due to events such as tool drops are used to define $P(at)$. The paper does not show the function $Pr(at)$. A mean and standard deviation for the probability of occurrence of a given load level per flight is obtained from the probability of exceeding limit load and exceeding ultimate load per flight hour due to gust.

There is no description of the residual strength vs. damage size relationship, only that it can be defined. The paper does not show the function $Pd(at)$, but it does give a mean value and "A" value for indentation damage size for three inspection methods: visual, external detailed visual, and internal detailed visual.

Rouchon recommended that the inspection program require a probabilistic approach for its determination [71]. The probabilistic inspection concept is a new approach to certification which allows for inclusion of the maintenance philosophy at the design stage. The concept depends on a random sample size of aircraft to be chosen from the fleet for inspection. The next inspection time is defined based on findings from current inspection. Total probability of failure includes not only the probability of structural failure but also the probability of failure due to structural damage which was undetected by the inspection program. Optimum definition of time between inspections and optimum life-cycle cost may be achieved by using this approach.

Rouchon illustrated the approach on inspection scheduling for the ATR72 aircraft [72]. The inspection interval is determined such that larger impact damage, where residual strength after impact is between limit and ultimate, corresponds to a calculation of the stress-strength failure probability which is less than 10^{-9} per flight hour. Low-level impact damage, which does not reduce strength below ultimate, is covered by demonstration of no growth for the life of the aircraft. Figure 4-9 shows all inspection decisions as a function of residual strength after impact damage, length of inspection interval, and the corresponding probability of failure.

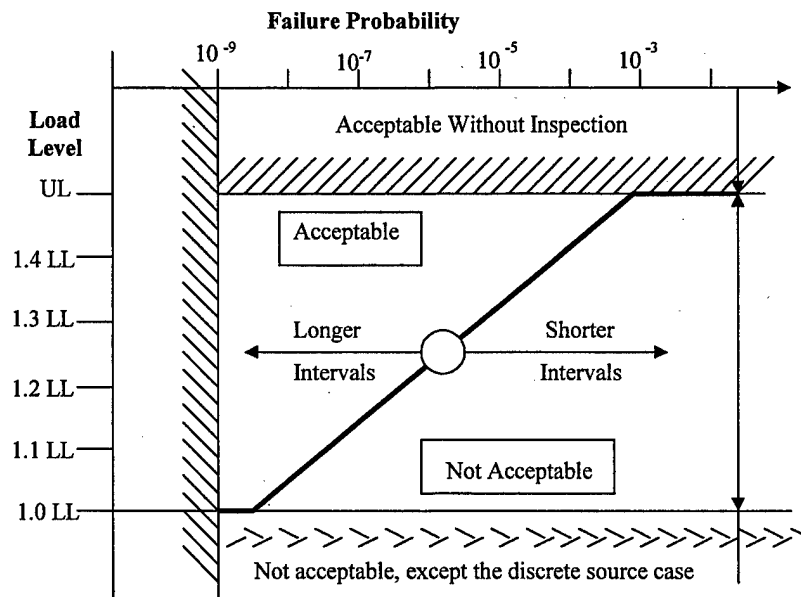


FIGURE 4-9. INSPECTION CRITERIA AND PROBABILITY LEVELS

4.9 PRATT & WHITNEY.

Pratt & Whitney is developing a general Probabilistic Design System (PDS) for gas turbine disks under a 5-year contract of the sponsorship of the Air Force Material Command-Wright Laboratory [73]. The Air Force sponsored program is comprised of six phases:

Phase I	Data Acquisition	Phase IV	Application
Phase II	Method Development	Phase V	Application Test
Phase III	Validation Test	Phase VI	Method Extension

Phases I and II were completed in early 1994. Comparison of the design system to field experience and subscale disk testing was conducted in Phase III. The benefits of the statistical approach to rotor design will be evaluated in Phase IV. The turbine rotor, to be designed by probabilistic methods, will be tested in Phase V. Suggestions for modifying the United States Air Force Engine Structural Integrity Program (ENSIP) by using probabilistic design will be made in Phase VI.

The goal of the PDS program is to reduce engine component weight by integrating deterministic design methods and tools with probabilistic design methods. A key to achieving this goal is to develop a probabilistic analysis system that would be used by designers in the mainstream design process. To accomplish this, there are four criteria addressed in reference 74: (1) probabilistic design must be based on existing tools used in deterministic design; (2) probabilistic design must require only a small amount of additional time over that required for current deterministic design; (3) results must be quantifiably accurate; and (4) the software and method must be user-friendly.

Anticipated payoffs from using probabilistic methods in gas turbine engine design include rotor weight reduction, increased design life and rotor speed, risk quantification, and availability.

4.9.1 Methodology.

In the referenced papers [74, 75], the term design variable (e.g., stress, LCF life, plastic growth) refers to what is normally called a response or output variable, and life driver (e.g., temperature, modulus) refers to an input variable. The method entails selecting representative combinations of the input variables to produce representative values of the response variable. The philosophy is that achieving an extreme response is more likely due to all input variables being at moderately extreme values than due to one being at an extreme value while the others are near nominal. The approach is depicted in figure 4-10 and the general steps taken are:

1. Find the driver factors and distributions associated with these factors. To obtain these distributions for the design variables, it is necessary to describe the basic life drivers with appropriate statistical probability distributions. A Box-Behnken experimental design is utilized to select representative combinations of life drivers. More details can be found in references 25 and 27.
2. Create statistical distributions of the output variables due to uncertainties which were specified for the input variables. Take the results from the Box-Behnken matrix and fit a second-order response surface regression equation using stepwise regression.
3. Evaluate the response surface equation. Two steps to achieve this are (1) to run a stepwise regression model which will select the variables from a large list of candidate variables which do the best job at explaining the variability in the response variables of interest and (2) to determine whether this resulting response surface model adequately approximates the design code. Additional details about assessing goodness of response surface in this methodology can be found in reference 76.

4. Calculate the probability of failure. Use Monte Carlo simulation to obtain the distributions of output variables, since it is very easy to evaluate a response surface equation by simulation.

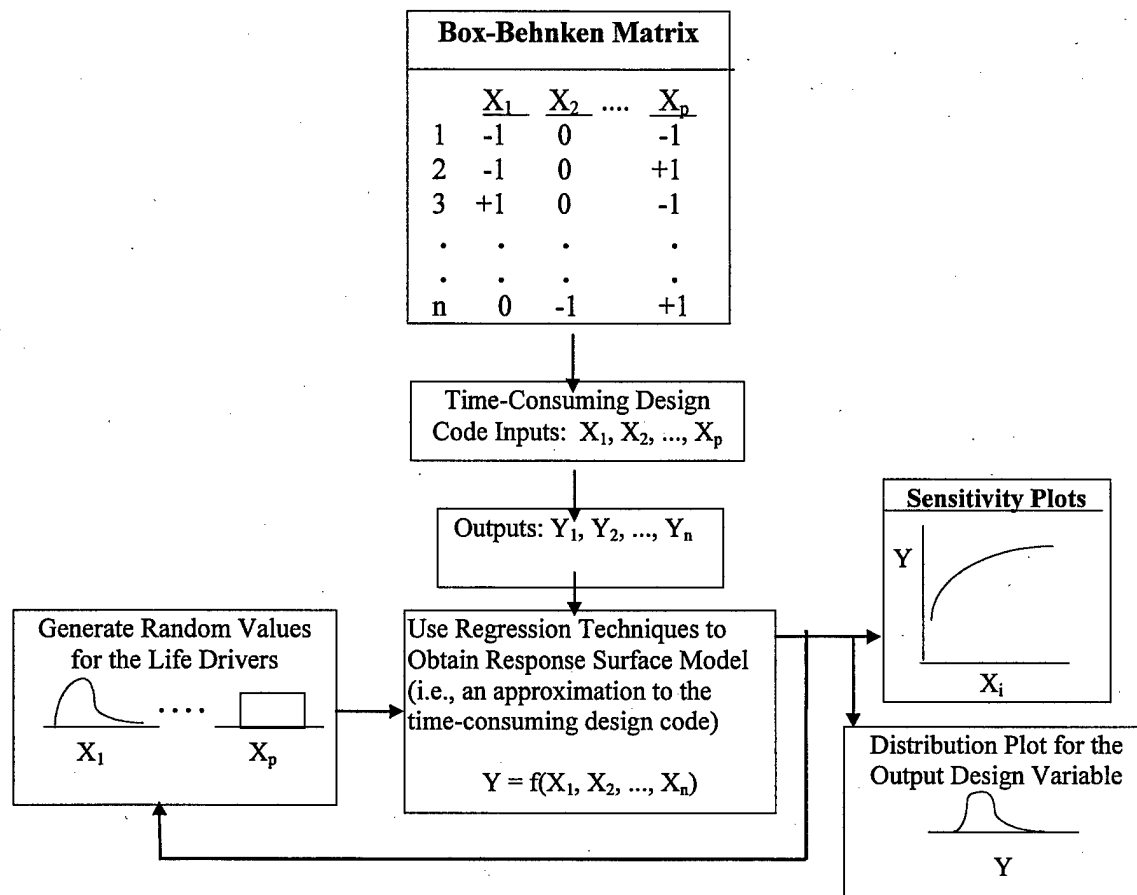


FIGURE 4-10. STRUCTURE OF PRATT & WHITNEY PROBABILISTIC DESIGN SYSTEM

4.9.2 Box-Behnken Experimental Design Procedure.

The following is an explanation for the case of three input variables in the Box-Behnken approach. Imagine a cube whose volume represents all possible combinations of three continuous input variables. The center of this cube would correspond to the input variables at their nominal values. The corner points represent the eight possible combinations of the three input variables at their extreme values: (Low, Low, Low), (Low, Low, High),... (High, High, High).

The Box-Behnken Matrix method does not evaluate the response variable for the eight corner points of this cube. Instead, it considers those 12 points where two of the input variables are at extreme values and the other is at nominal, corresponding to the midpoints of the 12 edges comprising the cube. It also considers the center point of the cube, thus bringing the total number of deterministic evaluations to 13.

The regression equation consisting of an intercept term, linear terms, and quadratic terms (including interaction terms) is then fit to the 13 data points: $(x_1, x_2, x_3, y)_i$, $i=1$ to 13. For the three input variable case, the equation consists of 10 parameters (b_i):

$$y = b_0 + b_1x_1 + b_2x_2 + b_3x_3 + b_4x_1^2 + b_5x_2^2 + b_6x_3^2 + b_7x_1x_2 + b_8x_2x_3 + b_9x_1x_3$$

where y is the response and x_1 , x_2 , and x_3 are the input variables.

The number of parameters in the regression ($= \frac{1}{2}[n+2][n+1]$, where n is the number of input variables) and the number of Box and Behnken evaluations are shown in table 4-3. Monte Carlo simulation is used to sample from the input variables' PDFs, and the response is calculated using the regression equation. The response PDF is then formed from the numerous responses generated.

TABLE 4-3. BOX-BEHNKEN DESIGN OF EXPERIMENTS PARAMETERS

n	Parameters	Number of B&B Evaluations
3	10	13
4	15	25
5	21	41
6	28	49

4.9.3 Summary and Discussion of Pratt & Whitney Method.

Two things must happen if this method is to work: (1) the input variable PDFs must be accurate, and of greater concern (2) the regression routine must be reasonable. For example, in the three input variable case, only 13 points are used to determine a best fit equation with 10 parameters! However smart the regression routine is in eliminating terms of little significance, the user should note what terms are left and see if they make sense, especially the interaction terms $x_i x_j$.

The authors claim that the regression equation should do an excellent job of predicting the response, as long as low values and high values for the input variables are selected in the moderately extreme region. For the example given in the paper, it did just that. There were six input variables, thus 49 deterministic evaluations. The regression routine managed to do a best fit with 11 parameters out of the possible 28, through elimination of insignificant terms. Examples were given of how small deviation existed between the regression equation's predictive value and the actual value. Naturally, this comparison could only be made at the 49 points deterministically evaluated. Hopefully, the true response and the regression-predicted response at points away from the 49 are in agreement (i.e., there are no cliffs in the response within the moderately extreme values of the input variables).

Sensitivities can be determined in two ways: (1) plot the data obtained from the Box-Behnken matrix by selecting one output and one input variable and (2) use the response surface equation and differentiate the response surface variable with respect to the input variable for which a sensitivity is desired.

In summary, Pratt & Whitney does a thorough and believable job in defining the stress PDF, but does not address the strength PDF. The response surface approach can be a good alternative to Monte Carlo simulation, taking significantly less computer run time. As a word of caution, the author notes that response surface methods sometimes lose accuracy when the g-function is highly nonlinear.

4.10 GENERAL ELECTRIC (GE).

GE's development of a probabilistic design tool is a part of the Air Force's drive to meet the Integrated High Performance Turbine Engine Technology (IHPTET) goal to develop and demonstrate technologies by the turn of the century that will double the 1985 level of turbopropulsion capability [77]. To point out the over-conservatism of the present deterministic design approach, it is noted that certain engine components had been retired at the end of their deterministically calculated lives, but then reissued if found to be fit for reissue (typically 95% of turbine engine disks). Probabilistic analysis of an existing design showed that failure rates were 0.71 in 1000. With a target failure rate of 1 in 1000, weight savings (18 lb. per disk) could be achieved while at the same time increasing the calculated PF to this value.

GE's system involves the direct integration approach, along with fast probability integration (this term is not defined). There is discussion of carefully seeding test specimens and model disks with known imperfections to verify the life and failure mode as predicted by the PDS, but not enough detail is given to determine its validity.

Another technical paper [78] describes the use of a Taguchi Experimental Matrix to investigate the effect of [modulus x proportion limit], thermal coefficient of expansion, Poisson's ratio, and creep parameter on two response variables. These four parameters are the major drivers for mechanical fatigue life. The stochastic nature of the four effects is what justifies the use of probabilistic analysis. Thus, response variable sensitivity can be studied.

4.11 NASA MARSHALL FLIGHT CENTER (MSFC).

The role of NASA Marshall has been primarily to educate the industry on the subject of probabilistic methods. As discussed in section 4.5, a MSFC task force was formed in 1991 to review the JPL method. This led to an evaluation of the state of the art in probabilistic methods. Their dissemination of knowledge gained was impressive, as the MSFC task force produced a well-written 60-page technical report in 1993 [56] containing a thorough review of the JPL method, as well as an explanation and review of other probabilistic approaches for application in aerospace structural design.

4.11.1 Probabilistic Methods Documentation.

In 1994, NASA Marshall published a comprehensive 200-page report entitled "Modern Structural Reliability Methods" [23], which details the approaches involved. This is an excellent source for detailed mathematics involved with Monte Carlo, response surface, and limit state approximation methods. Much of the information in section 3 of this document was obtained from this reference.

Among the recommendations of the MSFC task force was to suggest the goal should be to supplement current safety factor deterministic approaches with probabilistic methods. To this end, several technical papers were written by V. Verderaiame [79 through 81], explaining the First-Order Reliability Method (FORM) and relating it to the safety factor approach. There was a twist, however, as the explanation of the First-Order Reliability Method was not the same as it appeared in other literature.

4.11.2 Proposed First-Order Method.

In the papers by Verderaiame, the normal distribution was exclusively used in all parameter modeling, in conjunction with normal distribution combining techniques (see section 3.7.2.2), to combine multiple normal distributions into a single normal distribution for both the applied stress and component strength.

The reasoning behind this is quoted [79]: "Normal distributions are overwhelmingly observed in structural data and are justified by the central limit theorem. The normal distribution assumption allows the statistical characterization of random variables to be completely and expediently determined by the mean and standard deviation. Normal distribution techniques are the best developed and easiest to learn and apply. To employ other distributions for small sample sizes is to prematurely consider unnecessary and burdensome statistical information. Note that only the worst-case sides of the two distributions are involved in the failure concept. Hence, when a phenomenon is known to be non-normal, the distribution may be split, with the mode (peak frequency point) representing the mean.... This normalization of skewed distributions amounts to trading a little eloquence for reduced labor and lead time."

This method assumes a closed form solution to the problem exists, which for aerospace structures is usually not the case (e.g., finite element methods are normally used for defining stress PDF). As Fox [13] points out in his 1992 paper entitled *Statistical Characterization of Life Drivers for a Probabilistic Design Analysis*, "Everything in the world is not normally distributed.... It should be noted that the normal distribution is perhaps one of the least conservative distributions that can be used." So while all-normal approach may be a good academic exercise to get engineers up the learning curve, its practicality is highly questionable.

4.11.3 Recent Work at NASA Marshall.

In 1995, a paper [82] was published addressing probabilistic dynamic synthesis. This is described as a new methodology for performing analysis of structures composed of substructures whose dynamic characteristics can be statistically identified. The method uses the substructure eigenvalues, eigenvectors, and residual flexibility as random vectors for determining the response value by combining new probabilistic analysis techniques with the residual flexibility method of component mode synthesis. Future work was proposed and a test case performed on a spring-mass system model.

4.12 THIOKOL CORPORATION.

A probabilistic design approach [83] was developed in 1991 by Thiokol entitled Statistical Approach for Engineering Reliability (SAFER). It is believed only one paper was published on

this, but it appears as though significant effort was put forth. Probabilistic analysis was applied to a new solid rocket motor case design. The analysis ultimately determines the probability that stress exceeds strength. More specifically, the hoop stress PDF is referred to as the performance distribution, while the hoop strength PDF is called the capability distribution.

The general process of SAFER is as follows:

- Identify initial system and component requirements. These are usually obtained from the system loading and environmental conditions defined in the mission profile.
- Given the preliminary design, identify the driving failure mode(s).
- Perform structural reliability analysis. Experimental design methods are used along with a regression equation to model stress in terms of design variables that are input to classical laminated plate theory. Stress and strength equations are generated by randomly varying design variables over their naturally occurring range using Monte Carlo simulation. This is basically the same as the response surface method as explained in section 3.7.4. Probability of failure is calculated by combining distributions of stress and strength via stress-strength integration methods.

In the application, the performance equation (for hoop stress) is a function of eight performance variables, six of which are described by normal PDFs and two of which are described by uniform PDFs. The capability equation (for hoop strength) is a function of three capability variables, two of which are described by normal PDFs and the other by a uniform PDF. Monte Carlo simulation is used to sample from the performance and capability variables, then regression equations are used to determine the value of hoop stress and hoop strength. (It is stated that this regression equation was developed from experimental design methods and classical laminated plate theory, but no more details are given.) After numerous MC trials, the mean and standard deviation of hoop stress and strength are applied to normal distributions and the probability of failure is calculated.

The validity of this analysis rides on the regression fit for hoop stress; it is unknown if extreme or moderately extreme values of the performance variables were considered. It is also unknown how many sets of performance variable values were used in developing the regression fit.

4.13 NASA LANGLEY.

In a paper published in 1992 [84], two examples are given for the reliability of graphite/epoxy stiffened panels:

- *Effect of bow-type initial imperfection on reliability.* Three PDFs for bow size are initially considered: maximum extreme value, normal, and minimum extreme value, each with a mean of zero and standard deviation of 0.02 inch. Reliability versus fraction of (deterministic) design load is plotted. Then assuming quality control procedures would eliminate panels with bow sizes larger than 0.04 inch, the three PDFs were truncated at

± 0.04 in., and the analysis was repeated. Results were then compared to the original analysis.

- *Effect of allowable strains on reliability.* Two random variables considered in this analysis are the percentage of failed plies (PFP) and the coefficient of variation (COV) of the allowable strains. Fixing $COV=5\%$, reliability versus applied load was plotted for various PFP values. Then fixing $PFP = 20\%$, reliability versus applied load was plotted for various COV values. Although very clearly written, this paper describes an oversimplified model. It does, however, convey very simply what probabilistic analysis is all about. Also, it addresses the impact of having a good quality control program in place. Optimized structural design should include the costs and benefits of various levels of quality control. It concludes with the obvious requirement of having an excellent math model and low variability of important parameters in predicting the failure load for a structure.

The first studies the effect of an overall bow in the panel (stress) and the second studies the effect of allowable strain (strength). Each problem studies the effect of only one random variable at a time.

Reference 85 contains an interesting approach to comparing deterministic and probabilistic designs. A 10-bar truss is evaluated in terms of dynamic performance and is not destroyed if failure occurs. Failure is defined as a damping ratio for any of several vibration modes being below a specified value. A deterministically optimized design is defined as one in which the margin against failure is maximized under the constraints that utilized resources do not exceed allocated resources. This is not the same as the typical deterministic design approach used for aircraft structure, where the constraint is margin of safety ≥ 0 at ultimate load, while the objective function to be minimized is weight, cost, etc. A probabilistically optimized design is one in which the probability of failure is minimized under these constraints.

The following issues for reliability-based design are offered:

- Modeling uncertainties associated with the assumptions and simplifications in the analysis is a key task.
- A tail sensitivity problem exists, i.e., determining the shape of the stress PDF's right tail and the strength PDF's left tail.
- The calculated probability of failure, as a result of the aforementioned issues, should be used only as a subjective measure of safety, making important the question of whether the resulting designs are still better than their deterministic counterparts.

The extended interior penalty function technique incorporated in the code NEWSUMT-A was used for performing optimization in both cases. The end result was that the probabilistic optimum was considerably safer than the deterministic optimum. The reasons given for this were (1) the probabilistic approach accounted for the uncertainties in a rational way, and (2) the

probabilistic approach accounted for the sensitivity of the cost and performance of the system with respect to the uncertainties.

4.14 GRUMMAN AEROSPACE.

As part of a contract with NASA Lewis under the Advanced Composites Technology (ACT) program, Grumman was involved in applying and assessing the Integrated Probabilistic Assessment of Composite Structures (IPACS) computer program, developed by NYMA Inc. under contract with NASA Lewis and described in section 4.3.1. Since IPACS was in an evolving state at the time, many suggestions were documented [86]. A comparison was made between IPACS' predicted material response distributions and Grumman's test results for the unnotched specimens. Specifically, IPACS was used to predict tensile modulus and strength distributions for longitudinally loaded test specimens tested at room temperature.

Strength predictions were obtained from two failure criteria, one based on Chamis' combined stress criterion and the other on the maximum uniaxial stress criterion. Analyses were performed using three NESSUS analysis options: (1) FORM (a limit state approximation method), (2) SORM, and (3) Monte Carlo simulation.

Good correlation was found in a comparison of predicted and measured longitudinal modulus distributions for the unnotched unidirectional, cross-ply, and quasi-isotropic laminates. Correlation of strength distributions for the unnotched laminates were judged good for the unidirectional laminate and fair for the cross-ply laminate. Strength correlation for the quasi-isotropic laminate was not good because IPACS (at the time) did not have a progressive failure capability. For the cross-ply and quasi-isotropic laminates, the linear response surface (FORM analysis) was accurate for the prediction of modulus distributions but inaccurate for the prediction of tension strength distributions because of nonlinearity with the random variables.

4.15 THE CENTRAL AERO-HYDRODYNAMIC INSTITUTE (TsAGI).

The Central Aero-Hydrodynamic Institute (TsAGI), from the Russian Federation, developed a methodology for probabilistic analysis of composite aircraft structure named Probabilistic Design of Damage Tolerant Composite Aircraft Structures (ProDeCompoS) [87]. It includes databases and a library of application programs. The analysis uses a large amount of information:

- Mechanical characteristics of composite materials
- Manufacturing processes
- Results of nondestructive inspection during manufacture, testing, and service.
- Data from experimental investigations

4.15.1 General Input Requirements to the Software.

The following inputs are depicted in figure 4-11:

- Types of manufacturing flaws and their statistical distribution with respect to dimensions

- Types of in-service damage and their statistical distribution with respect to dimensions
- Dimensions of damages which occur after typical mechanical impacts
- Estimates of effects of manufacturing flaws and damages on the residual strength and endurance
- Parameters of statistical distribution functions for the residual strength and endurance
- Design conditions, values of applied loads, environmental factors, and their statistical characteristics
- Inspection and repair schedules
- Failure probability estimation methods

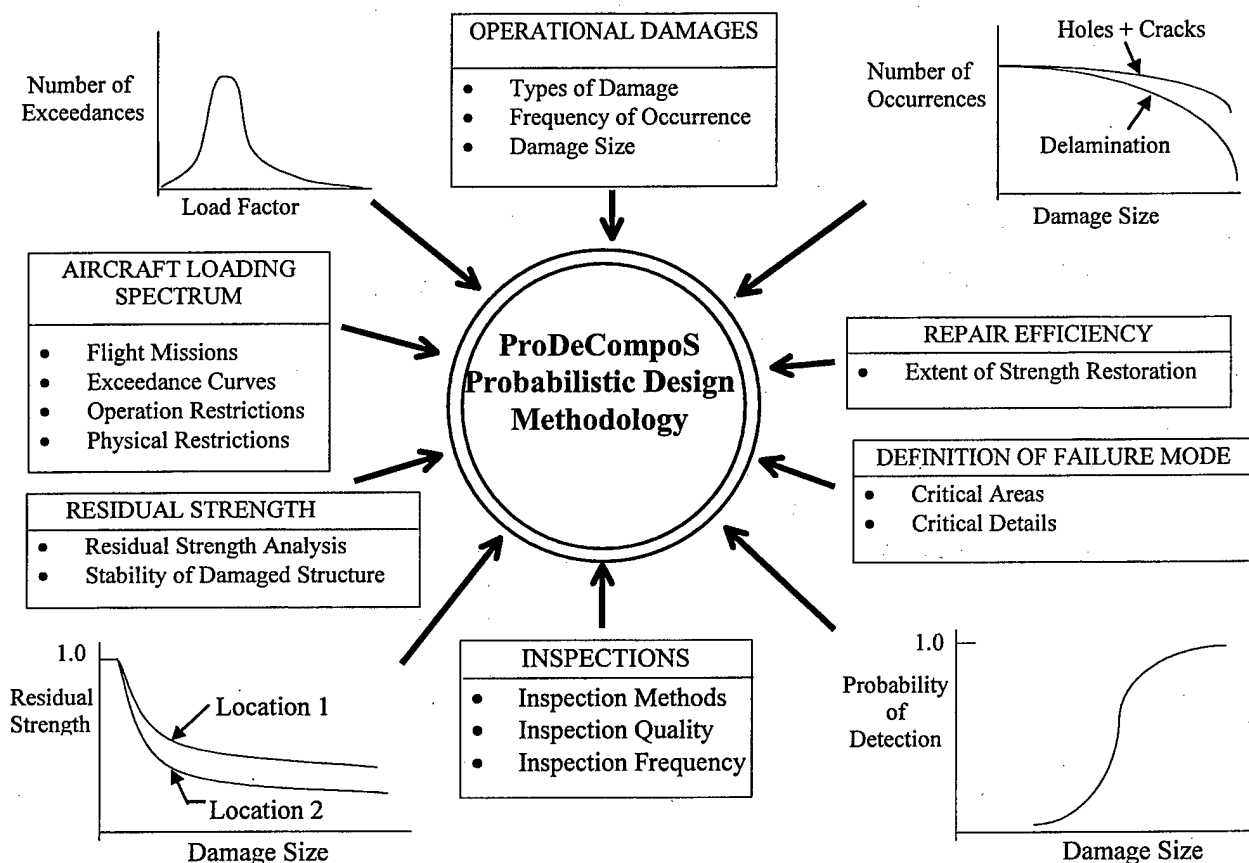


FIGURE 4-11. TsAGI PROBABILISTIC METHODOLOGY

4.15.2 ProDeCompos Methodology.

The ProDeCompos methodology is formulated as flight-by-flight numerical simulation of the combined stress-strain state of the structure, taking into account diverse random sources of loads.

In each time instant (interval), the stress state is compared to the strength state, which is simulated depending on the initial strength state and its random variation during operation. The structural loads should be modeled in a probabilistic manner to allow determination of the maximum expected value of load for any time of operation. The comparison of stress level vs. strength level determines local structural failure. When N load histories and residual strength histories are simulated and M failures are observed, the probability of failure is evaluated as $\beta = M/N$. The total structural failure probability for time "t" from the beginning of operation is calculated by

$$\beta = 1 - \prod_{i=1}^N (1 - \beta_i)$$

where β_i is the failure probability of a piece of structure for the i^{th} loading case. The time chosen is usually the service life, and therefore it gives the probability that component failure will occur during the aircraft lifetime. Attempting to back out a single-flight probability of failure (which is done in application examples) from this is not intuitive.

This method calculates probability of failure differently for the scenario of damaged vs. undamaged structure. That is, if during the simulation of an aircraft lifetime no damage occurs to the structure, the component strength is not degraded and the probability of failure is calculated from the well-known formula

$$\beta = \int_0^{\infty} f_{l_{\max_i}}(x) F_{p_i}(x) dx$$

where $F_{p_i}(x)$ is the cumulative distribution function for the load-bearing capacity of the structural location for the i^{th} design case, and $f_{l_{\max_i}}$ is the probability density function of maximum load for time t . The expected number of defects during the aircraft's service life is modeled via Poisson distribution. If the expected number of damages exceeds one, Monte Carlo simulation is used to determine probability of failure for that location. If the expected number of damages during the service life is less than one, an approximate composite method is applied, which is an equation for conditional probability of failure. Applications include Lear Fan 2100 and SU-29 wing analyses.

4.16 NANCHANG AIRCRAFT MANUFACTURING GROUP.

One technical paper was found from this company dealing with the development of a new Sequential Response Surface Method together with Monte Carlo Importance Sampling. This technique is based on Bucher's g-function approximation method [88] together with FEM methods to calculate response parameters and approximation techniques of structural optimization. The goal is to develop a response surface. This method was tested using a 3-bar truss structure and a multiweb wing structure model. The sequential response surface method was shown to be efficient and accurate. Results of both cases were compared to the probabilistic analyses obtained using a probabilistic finite element method (program named PFEM1—no reference given) and Monte Carlo simulation. More development efforts were identified and recommended.

4.17 ALPHA STAR CORPORATION.

Under sponsorship from NASA, Alpha STAR developed the computational structural and material analysis and design tool GENOA [89]. This software is dedicated to parallel and high-speed analysis to perform probabilistic evaluation of high-temperature composite response of aerospace systems. The technique is specifically designed to exploit the availability of processors to perform computationally intense probabilistic analysis to assess uncertainties in structural analysis and composite micromechanics.

The objectives achieved were (1) utilization of the power of parallel processing and static and dynamic balancing optimization to make the complex simulation of structure, material, and processing of high temperature composites affordable and (2) computational integration of probabilistic mathematics, structural mechanics, and parallel computing.

5. NORTHROP GRUMMAN METHODOLOGY THEORY.

This section gives a detailed explanation of one industry method. The Northrop Grumman Commercial Aircraft Division (NGCAD) methodology uses numerical integration (discussed in section 3.7.2) along with Monte Carlo simulation (section 3.7.3) to determine probability of failure.

Section 5.1 gives a historical overview of development of the NGCAD probabilistic design methodology. A high-level overview of the procedure in flow chart form and description of the main components is given in section 5.2. Section 5.3 shows a detailed flowchart of the process; each subcomponent of the procedure is then described in detail. Section 5.4 shows additional probability calculations, and section 5.5 describes the program output. An example problem illustrating the method is given in section 5.6.

5.1 HISTORICAL OVERVIEW.

Development of the NGCAD probabilistic design methodology for composites began in 1988 as a study to determine the degree of conservatism in composite design allowables. It was later expanded to perform a risk assessment of the USAF B-2 bomber. In 1989, the risk analysis was refined and development of a probabilistic design process was funded as Independent Research and Development. The methodology was subsequently used to analyze structural risk (probability of structural failure) on several different aircraft wings. Up through 1997, the program was funded under contract from the FAA. A PC-based program has been developed and is available from the FAA.

5.2 NGCAD PROBABILISTIC DESIGN METHODOLOGY OVERVIEW.

The Northrop Grumman probabilistic design methodology employs numerical integration with Monte Carlo simulation to determine probability of failure of a structural component and/or system of structural components. The approach is to perform detailed probabilistic analyses at representative locations yielding individual probabilities of failure which are then statistically combined to produce a system probability of failure.

The maximum operating stress (σ_{\max}) per flight probability density function (PDF) is determined from the maximum vertical load factor ($n_{z\max}$) per flight PDF (a program input) and the linear relationship between n_z and stress (also based upon program inputs). The baseline material strength PDF is a program input as well. The program accommodates normal, lognormal, and Weibull PDF types. The equations for these PDF types are shown and explained in section 3.3.

The equation for probability of failure is $PF = \int_{\Omega_f} f(s)G(s)ds$, where $f(s)$ is the σ_{\max} per flight

PDF, $G(s)$ is the material strength cumulative distribution function (CDF), and Ω_f is the domain of $f(s)$. (The CDF is known for any of three PDF types and contains the same parameters.) The sole purpose of Monte Carlo simulation is to position the σ_{\max} per flight and material strength PDFs relative to each other accounting for gust, environment, and defects. In each Monte Carlo trial, the PDFs are modified to account for these effects through use of shift values and scale

factors. Shifting the PDF means incrementing its domain values by a constant, C_1 , thus the cumulative probability once associated with s becomes associated with $s+C_1$. Scaling involves multiplying the domain values by a scalar, $C_2 > 0$, thus the cumulative probability once associated with s becomes associated with sC_2 . Note that shifting preserves the standard deviation of the distribution, while scaling preserves the coefficient of variation (ratio of standard deviation to mean).

Shifting and scaling are accomplished by changing the parameters of the PDF (described in table 3-1), as described in table 5-1. Once the PDFs are positioned by various shift values and scale factors, a single numerical integration is performed to determine the PF for that Monte Carlo trial. Results from numerous Monte Carlo trials are averaged arithmetically to determine the component PF.

TABLE 5-1. PROBABILITY DISTRIBUTION TRANSFORMATIONS

Distribution	Parameters	Transformation	New Parameters
Normal	μ, σ	Shift by C_1	$\mu + C_1, \sigma$
Lognormal	μ, σ, t_0	Shift by C_1	$\mu, \sigma, t_0 + C_1$
Weibull	θ, β, t_0	Shift by C_1	$\theta, \beta, t_0 + C_1$
Normal	μ, σ	Scale by $C_2 > 0$	$C_2 \mu, C_2 \sigma$
Lognormal	μ, σ, t_0	Scale by $C_2 > 0$	$\mu + \ln C_2, \sigma, C_2 t_0$
Weibull	θ, β, t_0	Scale by $C_2 > 0$	$C_2 \theta, \beta, C_2 t_0$

Figure 5-1 gives a high-level depiction of the methodology with the design process, material production, manufacturing process, and operations comprising the model. For each Monte Carlo

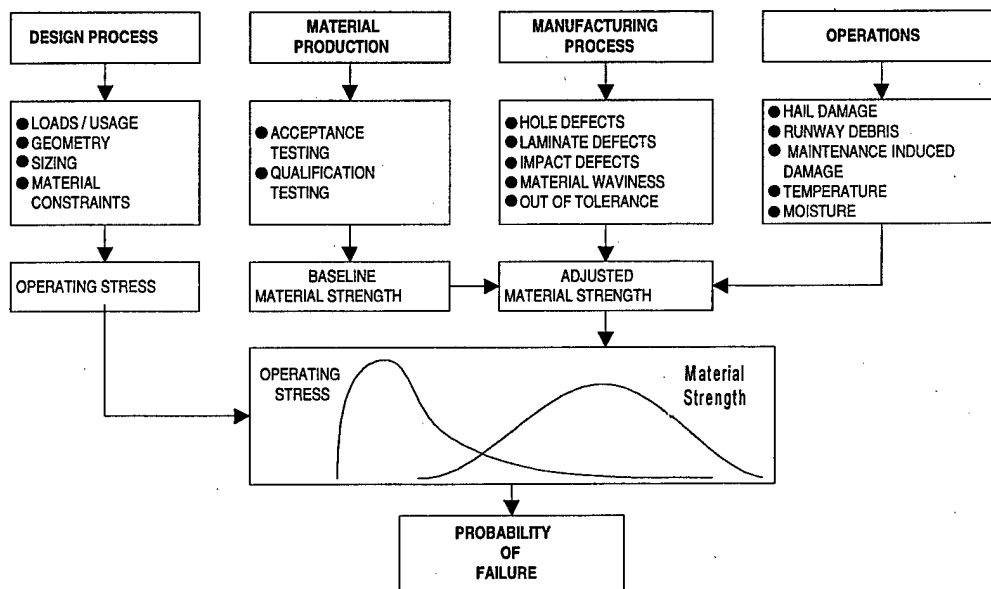


FIGURE 5-1. OVERVIEW OF NGCAD PROBABILISTIC DESIGN MODEL

trial, the result of the design process is to yield a maximum operating stress distribution, while the other three components work together to yield a material strength distribution. As explained above, numerical integration of the product of the maximum operating stress PDF and the material strength CDF determines PF for each Monte Carlo trial. PF is determined by averaging the results from Monte Carlo trials.

5.2.1 Design Process.

The NGCAD probabilistic design model is directly related to the structural analysis of the component, performed external to the probabilistic model. Applied loads, part geometry, and material properties are input to a finite element model to yield nodal deflections and internal loads. From this, failure criteria are applied and margins of safety generated from deterministic composite structural analysis methods. Normally, this procedure is repeated until the structure is optimized within the usual design constraints.

Margins of safety are a key input to the probabilistic analysis. They are used to determine the design limit stress level at each analysis location. Predicted maximum load distributions are established from load factor n_z exceedance data; this defines the shape of the maximum operating stress PDF through scaling of the Maximum n_z per flight PDF. Knowing the n_z level corresponding to design limit load, a scale factor ($n_z \rightarrow$ stress) is used to convert the maximum n_z per flight PDF to engineering units consistent with those of the material strength PDF.

5.2.2 Material Production.

Material strength distributions are established from mechanical property tests performed on the specific material(s) used in the component(s). These are normally available from material qualification tasks performed early in the development program. Often, valuable data are also available from material acceptance testing as the program matures.

A key assumption in the probabilistic model is that component failure is directly related to a basic mechanical property for which ample data have been developed to accurately describe its statistical distribution. This is particularly important in the tails of the distributions since the structural failure probability is typically very small ($<10^{-8}$).

5.2.3 Manufacturing Process and Operations.

This portion of the model simulates activity encountered during production of parts that affects material strength. This is defined as manufacturing defects. A manufacturing defect has some quantifiable impact on basic material strength. The nature, severity, and frequency of defects must be investigated and defined. This is somewhat arbitrary because it is the purpose of the quality control process to identify and screen out defects. That is, it is the defect that escapes detection that is important to structural risk.

In operational use, the part geometry, location on the aircraft, failure data from similar aircraft, and the predicted environment are analyzed to determine the expected frequency of operational damage. The source of this damage is low energy impact, either from foreign objects (runway debris, hail) or maintenance. Damage size and severity data are analyzed and a single material

strength scale factor representing the distribution of strength reductions is chosen. The material strength is reduced according to the expected frequency, average effect on strength, and location on aircraft.

5.3 DETAILED DESCRIPTION OF NGCAD METHODOLOGY.

For a given location subject to a potential failure mode, the Monte Carlo simulation does the following:

- Adjusts stress and strength PDFs due to randomly selected effects
- Calculates probability of failure via Romberg integration
- Calculates an average probability of failure from all trials

Figure 5-2 shows a detailed flowchart of the NGCAD methodology, with each significant flowchart element assigned a number. Each box will be discussed in this section. Note that figure 5-1 is a high-level depiction of this flowchart.

Box 1—Load Requirements. The design service life and design usage are based on usage requirements, typically stipulated in terms of:

- Total flight hours
- Total number of flights
- Total number and type of landings
- Total service years
- Mission profiles (divided into segments [taxi, ascent, cruise, etc.] with associated duration, altitude, speed and weight)
- Mission mix or number of flights of each mission

Box 2—Exceedance Data. The load spectrum for each mission segment is characterized by a table of occurrences of a load parameter. The normal load factor at the aircraft center of gravity, n_z , is commonly used. A table of occurrences is made by summing the occurrences per mission segment. These are plotted to form an exceedance graph. An example for positive maneuver loads is shown in figure 5-3(a). This shows the number of times in which specified values are exceeded during a specific time period. The time period is picked such that if measurements were taken again during an equal number of flight hours, the exceedance spectrum would theoretically be the same. Once the service life summary, mission profiles, and load factor spectra are defined, the load spectrum can be generated at specific locations on the aircraft using transfer functions based on load paths, material properties, and geometry.

NGCAD PROBABILISTIC DESIGN MODEL FOR EACH STRUCTURAL COMPONENT, K = 1, ..., M

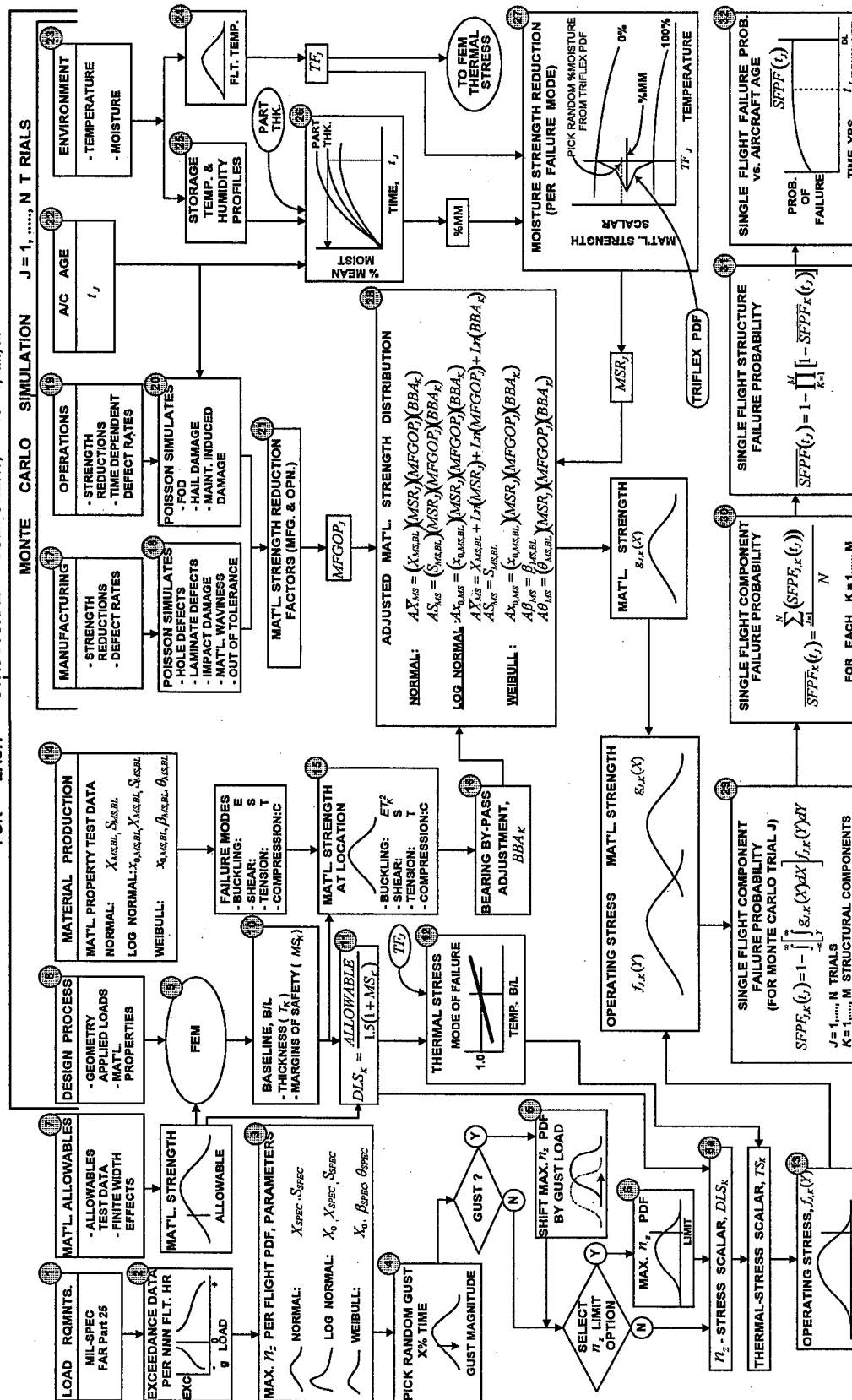
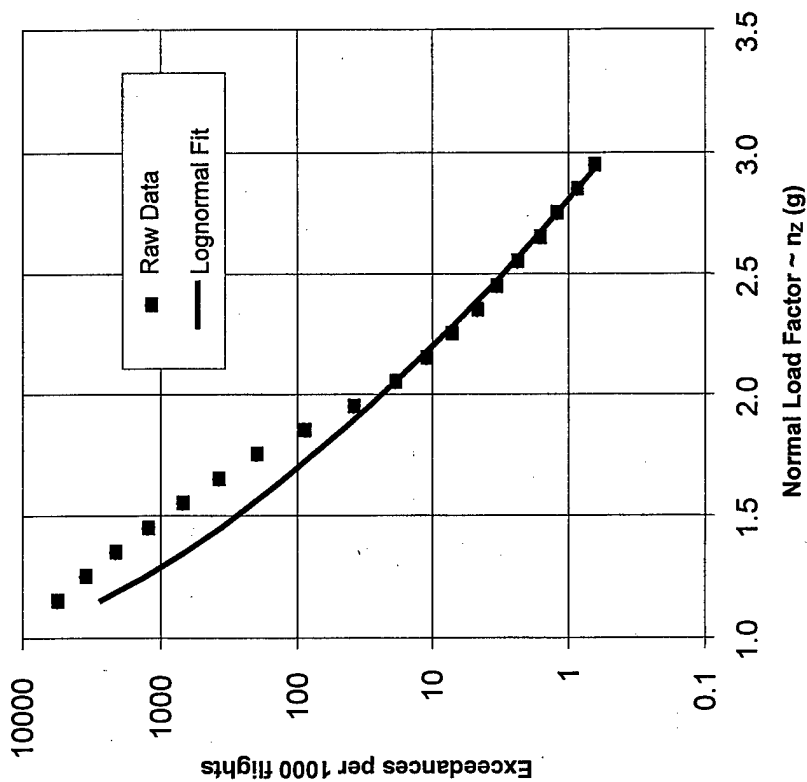
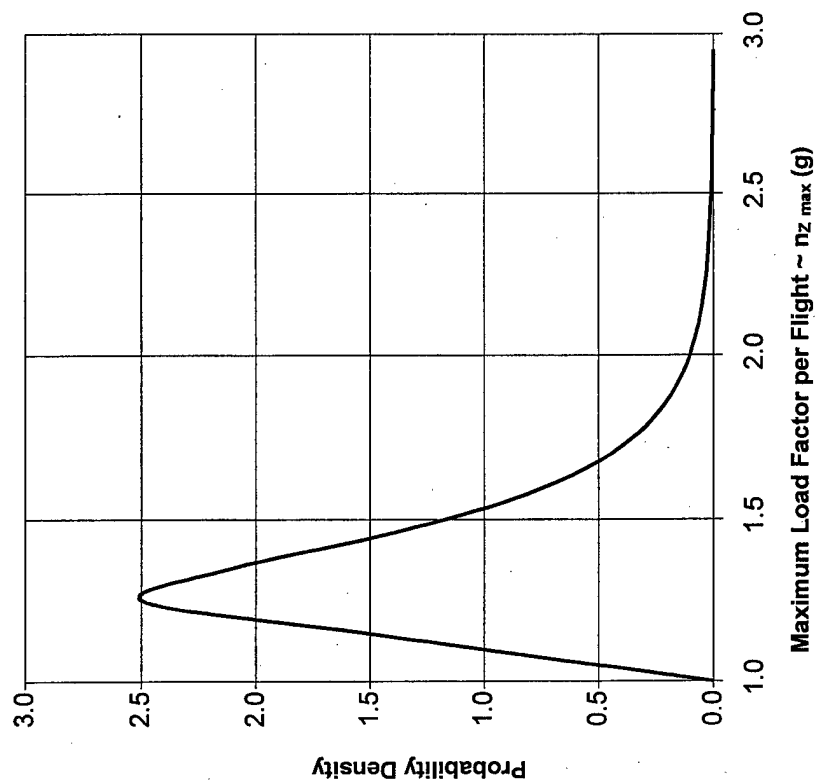


FIGURE 5-2. NGCAD PROBABILISTIC DESIGN MODEL FLOWCHART



(a) Positive Maneuver n_z -Exceedance Data and Lognormal Fit



(b) $n_{z_{max}}$ Per Flight PDF: Lognormal: $\mu = -1.0664$, $\sigma = 0.5368$, $t_0 = 1.0$

FIGURE 5-3. CONVERSION OF n_z EXCEEDANCE DATA TO $n_{z_{max}}$ PER FLIGHT PDF

Box 3—Max n_z per Flight PDF Parameters. Once the load factor spectrum is defined, it is converted to a probability distribution function (PDF) of the maximum n_z per flight. The Poisson distribution is used for this. This PDF represents the distribution of the probability of achieving maximum load factor levels during a single flight and is shown in figure 5-3(b). One procedure to obtain this PDF from the exceedance curve (figure 5-3(a)) is illustrated by the following example. The Microsoft EXCEL spreadsheet analysis for the Lear Fan 2100 aircraft is shown in table 5-2.

Columns A and B are a table of exceedances provided as input data. Column C is the CDF obtained to calculate the probability of a given load level being the maximum during a single flight by using the Poisson distribution. That is, the parameter λ is defined as the expected number of times the load factor n_{zi} will be exceeded during a single flight.

TABLE 5-2. LEAR FAN 2100 CURVE FITTING OPTIMIZATION

A	B	C	D	E	F	G
n_z	No. of Exceedances per 1000 Flights	Poisson CDF	Optimized CDF	No. of Exceedances per 1000 Flights	Error Term	PDF
1.00	Infinity	0.00000	0	Infinity		0
1.15	5626.69	0.00360	0.06087	2799.04	0.00654	1.49622
1.25	3515.89	0.02972	0.27563	1288.69	0.01511	2.48931
1.35	2126.35	0.11927	0.51235	668.74	0.02279	2.12247
1.45	1237.13	0.29022	0.69117	369.37	0.02882	1.45814
1.55	696.11	0.49852	0.80867	212.36	0.03290	0.92312
1.65	379.17	0.68443	0.88184	125.75	0.03455	0.56712
1.75	199.23	0.81936	0.92659	76.25	0.03291	0.34593
1.85	88.90	0.91494	0.95391	47.19	0.01992	0.21179
1.95	38.38	0.96235	0.97070	29.74	0.00489	0.13084
2.05	18.94	0.98124	0.98113	19.05	0.00000	0.08177
2.15	11.16	0.98890	0.98768	12.39	0.00188	0.05175
2.25	7.27	0.99276	0.99186	8.18	0.00350	0.03318
2.35	4.70	0.99531	0.99455	5.47	0.00950	0.02155
2.45	3.39	0.99662	0.99631	3.70	0.00511	0.01417
2.55	2.39	0.99761	0.99747	2.53	0.00444	0.00943
2.65	1.63	0.99837	0.99825	1.75	0.02231	0.00635
2.75	1.22	0.99878	0.99877	1.23	0.00067	0.00432
2.85	0.87	0.99913	0.99913	0.87	0.00108	0.00297
2.95	0.65	0.99935	0.99938	0.62	0.01445	0.00206
				Error Sum	0.26139	
				Parameters	$\mu = -1.0664$ $\sigma = 0.5368$	

Therefore the values in column B are divided by 1000 to get the Poisson expectation in terms of per flight. Mathematically, Column C value = $e^{(-0.001 \times \text{column B value})}$.

Based on the discussion of the Poisson distribution in section 3.6.3, for each load level i , $e^{-\lambda_i}$ thus represents the probability that n_{zi} will not be exceeded, hence the probability that the maximum n_z lies between 1.0 g and n_{zi} during the flight. Therefore $e^{-\lambda_i}$ is the value of $n_{z_{max}}$ per flight cumulative distribution function (CDF) at n_{zi} , or equivalently, the area under the $n_{z_{max}}$ per flight PDF between 1.0 g and n_{zi} . This process is repeated for as many n_{zi} values as necessary to adequately define the CDF.

To choose the best distributional fit of the CDF, the distribution parameters are optimized via built-in Microsoft EXCEL (Solver) routines, minimizing the objective function denoted Error Term in column F. (Note in the lognormal case shown, the third parameter is $n_z = 1$, so only μ and σ are given). This error term is defined as

$$\text{Column F value} = [\text{LN}(\text{column B}) - \text{LN}(\text{column E})]/\text{LN}(\text{column B}),$$

where column E values are the fitted exceedances per 1000 flight values generated by using the optimized lognormal parameters shown at the top of the figure, and are calculated by

$$\text{Column E value} = 1000 \times \text{LN}(\text{Column D value})$$

Column D values are generated by the equation for the CDF of a lognormal distribution with optimized parameters mean and sigma. The EXCEL spreadsheet has an internal function named LOGNORMDIST to generate the CDF in column D, given parameters μ and σ . If the fit were perfect, the values of column D would match exactly those in column C and the error sum, being minimized, would be zero.

In this example, the optimized parameters were $\mu = -1.0664$ and $\sigma = 0.5368$, while as mentioned above, the third parameter was set to 1.0. The resulting PDF, using these three parameters, is graphically shown in figure 5-3(b). This goodness-of-fit test is performed with normal, lognormal, and Weibull PDFs, the one with the least error sum is used. The third parameter of the Weibull and lognormal distributions is $n_z = 1$, i.e., the maximum load factor experienced during any time interval will always exceed $n_z = 1$ (level flight).

Box 4—Gust Loading. Gust loading is implemented as an event that occurs a portion of the flight time. From the input of probability of a gust occurring (e.g., 10%), a uniform distribution is defined to delineate between a gust and no-gust situation. Similarly, a probability level is given for the percentage of up vs. down gust, represented by another uniform distribution. That is, given that a gust occurs, there will be a percentage breakdown defined between up and down gusts.

To illustrate, suppose the probability of a gust occurring is 10%, and the probability of a down gust (given a gust has occurred) is 20%. In the Monte Carlo simulation, a random draw is made from a uniform [0,1] distribution: if the value lies between 0 and 0.1, the effect of gust will be implemented in the Monte Carlo trial. Then, another draw is made (uniform [0,1] distribution) to decide whether it is an up or down gust. Should that value lie between 0 and 0.2, the event will be modeled as a down gust.

Box 5—Distribution Shift Due to Gust. A random draw from a normal, Weibull, lognormal, or uniform gust load PDF is used to model the effect of gust. The effect of the gust load is to shift

the load factor distribution either in a positive or negative direction by an amount equal to the random draw.

In the NGCAD simulation, gust occurrence is superimposed on the maximum n_z during the flight. It would be unrealistic and too conservative to superimpose severe gust loads (up to 2 g's for the Lear Fan) on the maximum n_z during the flight. Instead, the gust magnitude PDF is defined as a uniform distribution from 0.1 g to 0.3 g, since the mean of the gust spectrum is about ~0.2 g and three is only a small deviation about this mean (0.1 g). Certainly, the user could input a n_{zmax} per flight PDF which corresponds to the gust exceedance spectrum, but to add this to the maneuver n_{zmax} per flight PDF would be unrealistically severe.

Box 6—Load Truncation. This box represents an option to truncate the load factor distribution. If unbounded, the load factor extends beyond that which is physically possible for the aircraft to achieve. If selected, truncation should be based upon performance attributes of the aircraft coupled with engineering judgment. Assessment of the Lear Fan 2100 wing was performed with the maximum load factor distribution truncated at ultimate load, which corresponded to approximately 5 g's at the aircraft center of gravity (c.g.). It may be of interest to the user to generate PF versus truncation level.

Box 6A—Conversion to Stress. This step represents the conversion from aircraft performance parameter to stress at the point under consideration. It is assumed to be a linear scale factor developed from deterministic structural analysis.

Box 7—Material Allowables. Development of material allowables is an important component of the NGCAD probabilistic methodology. A number of issues must be addressed when generating allowables, including number of batches and specimens per batch. In addition, because of the anisotropic characteristic of composites, difficulty in testing (in particular, compression), and the presence of more manufacturing process variables, there is often significant batch-to-batch variation. Material data developed at the coupon level often require adjustments, such as finite width correction.

Boxes 8 and 9—Design Process and Finite Element Model (FEM). The finite element model used to determine the response of the structure (deflections and internal loads) to externally applied loads requires (1) design geometry to establish a grid of nodal elements and primary load paths, (2) constraints to specify boundary conditions and symmetry, (3) externally applied loads as input to the model, and (4) material properties and thickness to define structural flexibility.

The FEM step is actually the result of detailed structural analyses which normally use the finite element models for primary inputs. Structural analysis identifies the predicted failure modes and quantifies the margin between applied loads and stresses and allowable loads and stresses. The margin of safety from this step establishes the relationship between stress and aircraft performance parameters such as n_z . The FEM is also useful to determine the state of stress throughout the component, thus guiding the selection of critical points for probabilistic analysis.

Box 10—Deterministic Baseline Parameters. The FEM is iterated until optimized (outside the probabilistic program), given design and manufacturing constraints. The resulting thickness and margin of safety (defined as $[\text{Allowable Strength}/\text{Ultimate Stress}-1]$) for the critical failure

modes at each node are designated as baseline thickness and baseline margin of safety for the subsequent probabilistic analysis.

Box 11—Design Limit Stress (DLS) Calculation. From the material allowable and margin of safety at each probabilistic analysis point (both inputs to the program), the design limit stress (DLS) is established. This is derived from the formula for margin of safety described above (Box 10), along with the definition of ultimate stress = 1.5 times the design limit stress. This is a very important part of the probabilistic analysis, as the DLS value is used in conjunction with the n_z value corresponding to the design limit condition. For example, the Lear Fan design limit load corresponds to 3.5 g.

The maximum n_z per flight PDF is thus converted to maximum stress per flight PDF (σ_{\max}) by way of a scale factor (denoted DLS on the flowchart), calculated as

$$n_{z \max} \rightarrow \sigma_{\max} \text{ scale factor} = [\text{DLS}]/[n_z \text{ level associated with DLS}]$$

This effectively changes the units on the horizontal axis without changing the form of the PDF. The parameters of the original load factor PDF are thus modified to reflect the linear correspondence between n_z and stress, as well as ensure the area under the PDF remains at 1.

Box 12—Thermal Stress. A provision is made to account for thermal stress at the component location. Calculation of thermal stress levels and their effect is done outside the program. During Monte Carlo simulation, a single temperature is randomly selected from the flight temperature profile (Box 25) distribution. If this temperature causes a thermal stress in addition to mechanical stress, it is represented by a factor (denoted TS on the flowchart) which adjusts (scales) the σ_{\max} per flight distribution. A table of temperature vs. thermal stress factor must be input to the program.

Box 13—Operating Stress PDF. The σ_{\max} per flight PDF is fully defined at this point, and is in the same units as the material strength PDF to enable integration. The distribution thus starts out as an $n_{z \max}$ per flight PDF and is translated should a gust condition be encountered, truncated should the $n_{z \max}$ limit option be chosen, and scaled to the same units as the material strength PDF.

Box 14—Material Production. For each distinct failure mode, sufficient test data should be obtained to define pertinent material property statistical distributions. MIL-HDBK-17 prescribes that 30 data points is a sufficient sample size to determine a stable mean, standard deviation, and a B-basis material allowable. Obviously, the larger the sample size, the greater the certainty in the statistical distribution assigned to the material property. This is discussed further in section 3 of this report.

Once the data has been obtained, it is screened for outliers and a goodness-of-fit test performed to find which distribution is most appropriate. The test is called the Anderson-Darling goodness-of-fit test and is recommended by MIL-HDBK-17 for use in generating design allowables. Spreadsheet optimization routines, such as those in Microsoft EXCEL, can also be used to evaluate goodness-of-fit and distribution parameters.

One difficulty in using a 3-parameter lognormal or Weibull distribution is in defining the third parameter, which is where the distribution begins. That is, there is zero probability that the strength, for the particular failure mode, will ever fall below that value. This is usually a difficult decision, thus the caution. Of course, one conservative option involves setting the third parameter (the starting point) to zero; this is what is recommended in MIL-HDBK-17.

Box 15—Spatial Distribution of Material Strength. In-plane shear, tension, and compression failure modes are modeled by sample data from coupon testing. There is no coupon test directly applicable to buckling strength, but since the equation for flat plate buckling strength (used to approximate the panel) contains a linear expression for the compression modulus, E_c , test data from these coupon level tests are used. Because critical buckling strength is also proportional to the square of part thickness, the factor t^2 is also used, so that buckling strength is modeled by an expression Et^2 . Thus, the buckling strength is proportional to the compression modulus E and to the square of the thickness $F_{cr} \sim E_c t^2$. This distribution can then be scaled and shifted as necessary to account for manufacturing and operational defects, as well as temperature and moisture effects.

Box 16—Bearing Bypass Adjustment. If there are analysis locations which have significant bearing stress and there is sufficient test data to calculate a material strength reduction factor, the material strength PDF can be adjusted (scaled) accordingly. As an example, a probabilistic analysis was performed on a wing structure where there was a 35% tension strength reduction at a fastener hole location with significant bearing stress.

The program assumes the effect will be predetermined (i.e., done outside the program) from test data of failure stress vs. bearing stress. That is, a series of locations defined by x and y coordinates are entered and, given a bearing stress at a particular location, the knockdown (scale) factor is determined by interpolation between the input x and y coordinates. This scale factor is denoted BBA in the flowchart.

Boxes 17 and 18—Manufacturing Defect Simulation. Types of manufacturing defects must be chosen which affect the material strength for the failure modes being analyzed. Occurrence rates for each type of manufacturing defect are generated outside the program and used with Monte Carlo simulation to account for the presence of undetected manufacturing defects. Defect size/severity data are analyzed and a single material strength scale factor representing the distribution of strength reductions is chosen. The material strength is adjusted (reduced) according to the expected frequency, average effect on strength, and location on the aircraft. These rates, based on the manufacturer's data, are input to the program, per defect type, as the expected number of defects per square foot of material.

Coupled with location area, probabilities of having a defect can be determined via use of the Poisson distribution. That is, using Poisson theory, the probability that one or more defects will occur is the quantity one minus the probability of having no defects. Mathematically,

$$P(1 \text{ or more defects}) = 1 - P(\text{no defects})$$

where

$$P(\text{no defects}) = e^{(- \text{defect rate} \times \text{location area})}$$

For example, if the manufacturing defect rate for waviness is input as 0.02 defects per square foot, and the area of the location of interest is 2 ft², then the probability of having a defect (calculated inside program) would be $P(1 \text{ or more defects}) = 1 - e^{-0.02 \times 2} = 0.0392$. During Monte Carlo simulation, numbers are generated from zero to one. A number between zero and 0.0392 would indicate a waviness defect at that location, and the material strength would be reduced (scaled) in accordance with table 5-1.

Boxes 19 and 20—Operational Damage Simulation. Occurrence rates for each type of operational damage are generated outside the program and used with Monte Carlo simulation to account for operational damage. These rates, usually based on data from similar aircraft, should be researched thoroughly, as operational damages typically lead to severe strength reductions and can produce relatively high probabilities of failure. Damage size and severity data is analyzed and a single material strength scale factor representing the distribution of strength reductions is chosen. The material strength is reduced according to the expected frequency, average effect on strength, and location on the aircraft. These rates are input, per defect type, as the expected number of defects per square foot of material per flight hour of operation. From Phase I of the Northrop Grumman Probabilistic Design project, funded by the FAA, the data shown in table 5-3 was obtained from two major commercial aircraft carriers. Portions of these data were used to develop program inputs for operational damage rates.

TABLE 5-3. OPERATIONAL DAMAGE; SOURCE: TWO U.S. AIRLINES (1993)

	Carrier A	Carrier B	Total
No. Flight Hours	2,005,896	1,691,775	3,697,671
No. Maintenance Induced Damages	585	491	1076
No. Lightning Strikes	60	51	111
No. Bird Strikes	4	3	7
No. Hail Storms	5	1	6

These data were used to generate rates in terms of number of occurrences per FH. Then, approximate dimensions (surface areas that would see the different types of damage) of a typical aircraft flown by these carriers were used to develop rates in terms of number of occurrences per FH per ft². With these rates, along with location area and analysis time (e.g., 15,000 FH), probabilities of having damage can be determined via use of the Poisson distribution, similar to the handling of manufacturing defects. The probability that one or more defects will occur is the quantity one minus the probability of having no defects. Mathematically,

$$P(1 \text{ or more defects}) = 1 - P(\text{no defects})$$

where $P(\text{no defects}) = e^{(- \text{defect rate} \times \text{location area} \times \text{analysis time})}$

For example, if the operational defect rate for hail damage is input as 1×10^{-8} defects per square foot per flight hour, the location area is 2 ft², and the analysis time is 20,000 FH, then the probability of having a defect (calculated inside the program) would be

$$P(1 \text{ or more defects}) = 1.0 - e^{-1 \times 10^{-8} \times 2 \times 20,000} = 0.0004$$

During Monte Carlo simulation, a number chosen between zero and 0.0004 would indicate hail damage at that location, and the material strength would be reduced (scaled) in accordance with table 5-1.

Box 21—Material Strength Reduction Factors. It is possible that two types of manufacturing defects can occur at a location within the same Monte Carlo trial; logic is written into the program to choose the more severe reduction of the various defect types. Similar program logic is written for operational damage. It is further possible that a manufacturing defect as well as operational damage can occur at a location within the same Monte Carlo trial. Rather than superimpose the manufacturing and operational reduction factors, the program will choose the defect with the most severe strength reduction. The strength reduction scale factor, representing manufacturing defects and operational damage, is denoted MFGOP in the flowchart.

The program output lists, for each major structural component (consisting of several locations), the number of each type of manufacturing and operations damage defect that was modeled. Also listed via a table is the numbers of times each defect type was overridden by a more severe defect type, as described above. This enables verification that the program is modeling defects accurately.

Box 22—Aircraft Age. This probabilistic analysis can be run for any aircraft age, from zero flight hours to an analysis at the end of its life to find the single-flight probability of failure. The difference between a single-flight probability of failure for a new aircraft versus an aircraft at the end of its life is due to moisture absorption (into resin) and operational damage found to be a function of aircraft age. There is currently no provision to automatically run the analysis at different analysis times (aircraft ages), therefore the analysis time must be input and program rerun for each unique age.

The basic material strength is assumed to be independent of aircraft age; fatigue is not a failure mode considered. There has been much research into mathematical modeling of delamination growth as a function of age, similar to the modeling of fatigue in metals. While laboratory testing may validate certain growth models, actual aircraft historical usage has not (to date) borne out the steady cycle-by-cycle growth of delaminations to some critical size whereupon component failure results.

Box 23—Operating Environment. It is well known that organic matrix composites are susceptible to temperature and moisture, causing significant degradation of some of their mechanical properties. For carbon/epoxy, the moisture absorbed is contained in the resin matrix. External surfaces in direct contact with the environment absorb or desorb moisture almost immediately, while moisture flow into or out of the laminate interior occurs relatively slowly. The moisture diffusion rate is many orders of magnitude slower than the heat flow associated with thermal diffusion, but even relatively thick structure can become saturated within a few years.

The rate of moisture absorption is controlled by the material property called moisture diffusivity, which is primarily a function of temperature. Figure 5-4 illustrates this temperature dependence, showing a family of moisture gain curves obtained at several different temperatures. The percent moisture content in a given laminate is a function of relative humidity to which it is exposed.

The maximum moisture content is a little over 1%; this is typical for most organic matrix composites, given enough time to reach moisture equilibrium from realistic service exposure.

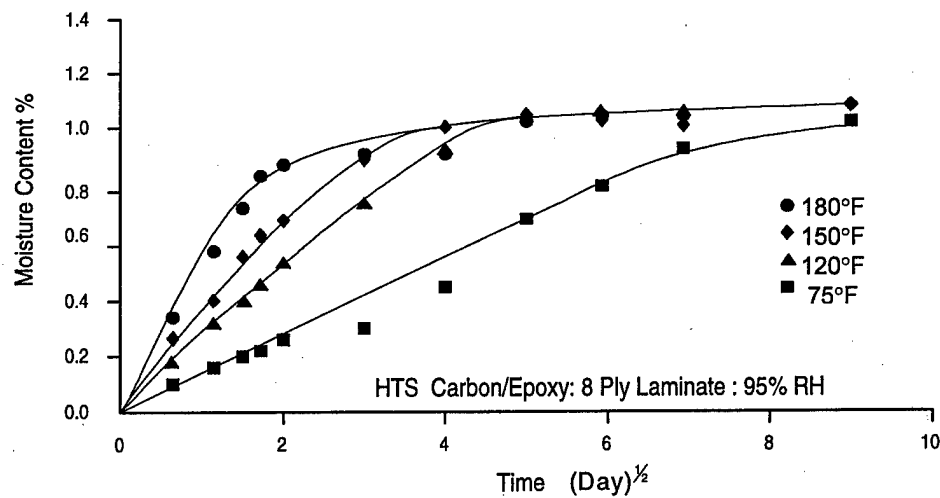


FIGURE 5-4. TYPICAL MOISTURE ABSORPTION RESPONSE [90]

Degradation of mechanical properties is primarily due to the reduction of matrix mechanical properties and interface bonding strength between fibers and matrix. The carbon fibers themselves are insensitive to hygrothermal effects. Moisture in the organic matrix lowers the temperature at which the matrix starts to soften. Therefore matrix-dominated mechanical properties (compression) tend to significantly decrease with increasing moisture content and increasing temperature (figure 5-5).

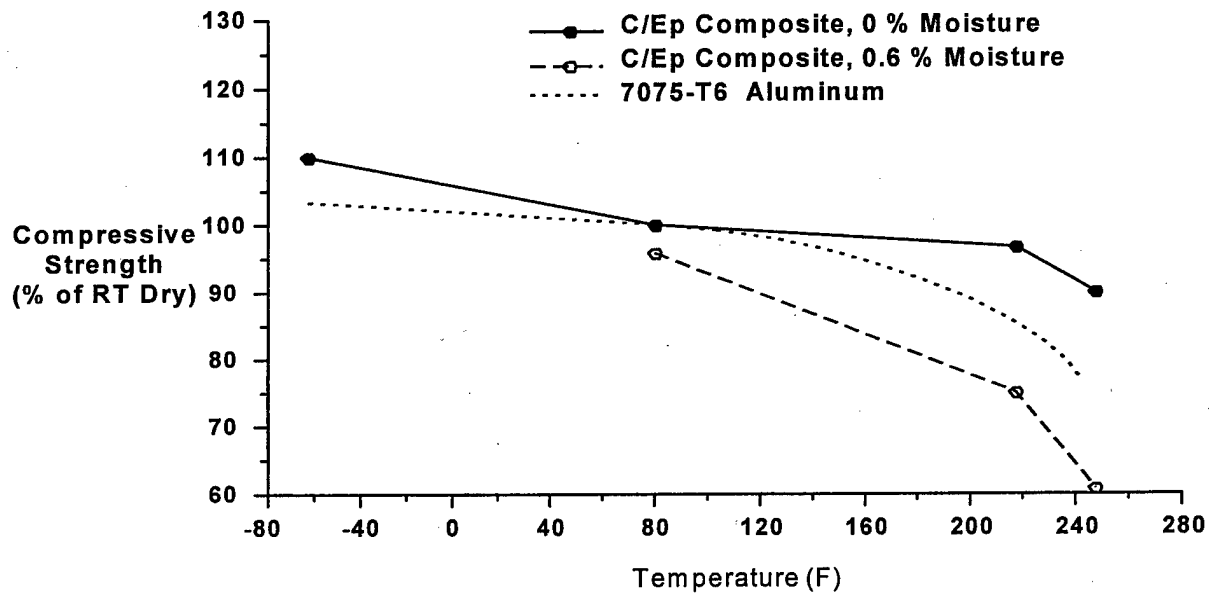


FIGURE 5-5. EFFECT OF TEMPERATURE AND MOISTURE ON COMPRESSION STRENGTH [90]

Box 24—Flight Temperature Distribution. Altitudes and times of individual segments of each mission can be utilized, when available, to obtain the time distribution of structural temperature in flight. Then either a discrete or continuous distribution can be used to represent the expected flight temperature frequency during a single flight. Of course, a continuous distribution should be truncated on both ends, but this is not a limitation.

By creating a probability distribution from the mission profile data, temperature is modeled independently of the time into the mission. That is, temperature is randomly chosen from the probability distribution within each Monte Carlo trial; these trials do not conform to any time sequence of any particular mission. The randomly chosen temperature is that which exists during the maximum maneuver, $n_{Z_{max}}$. The temperature distribution is based on pooled mission profile time-at-altitude data, coupled with assigning average temperature-at-altitude values, thus all possible temperatures are accounted for. It is assumed that $n_{Z_{max}}$ could occur at any of these temperatures, so Monte Carlo simulation considers them all and calculates an average probability of failure over all values of temperature.

The temperature chosen in each simulation is input to calculate thermal stress changes (described in Box 12) and to adjust material strength for hygrothermal laminate effects.

Box 25—Storage Environment. Laminate moisture absorption will occur throughout the aircraft's life cycle. If the laminate is exposed to the sun or other heat sources, there can be a significant increase in structural temperature. A relationship between ambient temperature and structural surface temperature is used to determine the structure temperature profile. It is therefore desirable to obtain ambient temperature and relative humidity profiles (hourly data for a year period is preferable) for the primary base location, calculate the structural temperature profile, and compute the percent moisture absorbed as a function of time. This ambient temperature and relative humidity data can be obtained from Surface Airways Hourly data [91], available from the U.S. Department of Commerce, via the National Climatic Data Center.

A computer program was used incorporating the mass diffusion theory following Fick's Law, which is a moisture analog to thermal diffusion. The program uses the Surface Airways Hourly data as input, as well as laminate thickness and boundary conditions. This program is not a part of the Probabilistic Design computer program.

Box 26—Moisture Absorption Model Output. The result of the moisture absorption program runs is to generate a family of moisture absorption vs. time curves, each corresponding to a laminate thickness. Obviously, the lower curves represent thicker laminates. The probabilistic design program is run at a certain time, in years, representing aircraft age. As seen in the flowchart, the laminate thickness, for this given age, will have an average percent moisture absorbed value. This number is actually percent weight gain of the laminate. Should the actual part thickness lie between two thickness curves, linear interpolation is performed to establish the percent moisture absorbed.

Box 27—Strength Reduction due to Environment. The temperature chosen from Monte Carlo sampling of the flight temperature distribution identifies the point along the abscissa of the

material strength scalar vs. temperature graph. A triflex distribution is defined, anchored at the dry (set to 0%, or 0.0) and wet (set to 100%, or 1.0) curves.

The triflex distribution, developed at Northrop Grumman, is a modified triangular distribution, defined by four parameters: (1) minimum value (0 representing the dry curve), (2) maximum value (1.0 representing the wet curve), (3) the mode (highest point), and (4) shape factor. The percent moisture absorbed, given aircraft age and laminate thickness, is defined (done automatically) to be the mode of this triflex distribution. The shape factor is defined by the user to adjust the shape (steep, shallow) around the mode; its role is similar to how a beta distribution uses a shape parameter to adjust the variance.

Monte Carlo simulation is used to randomly pick from this distribution; the value chosen represents the actual moisture content, which determines the material strength scalar. This value is therefore a function of base temperature and relative humidity, flight temperature, laminate thickness, and aircraft age. This process accounts for the hygrothermal effects on the laminate. Denoted MSR in the flowchart, it scales the material strength distribution in accordance with table 5-1.

Box 28—Adjusted Material Strength Distribution. The material strength distributions originate from material coupon test data and are subsequently scaled by the (1) bearing by-pass factor (2) temperature or moisture factor, and (3) manufacturing or operations factor. The mathematical procedures of scaling the distributions are shown in table 5-1.

Box 29—Component Failure Probability (per Monte Carlo Trial). The computer program presently has the capability to integrate combinations of normal, lognormal, and Weibull probability distributions. The integrations are carried out using Romberg integration techniques and are described in reference 90. For each unique combination of stress and strength distribution, the double integration formula for probability of failure is transformed to a single integral.

Truncation of distributions is accounted for in the integration limits. That is, truncating the applied stress distribution at a particular load level is modeled by a change to the upper limit (as opposed to infinity or the integration limits computed by computational limitations). Doing this, however, requires a correction to the calculated probability of failure value. This correction is accomplished by changing the upper bound of the numerical integration by dividing the probability of failure by the area under the stress PDF curve up to the stress truncation level. In most cases, this area is very close to 1.

The exact forms of the integration formulae will not be given here for all combinations of stress and strength PDF; only the case of a lognormal stress PDF combined with a normal strength PDF will be considered. For this choice, the PDFs of the two distributions are

$$f(s) = \frac{1}{\sigma_s(s-s_0)\sqrt{2\pi}} e^{-\frac{1}{2}\left(\frac{\ln(s-s_0)-\mu_s}{\sigma_s}\right)^2} \quad g(t) = \frac{1}{\sigma_t\sqrt{2\pi}} e^{-\frac{1}{2}\left(\frac{t-\mu_t}{\sigma_t}\right)^2}$$

After a change of variables, the resulting equation for probability of failure is

$$PF = \int_A^B \frac{1}{\sqrt{2\pi}} \exp\left\{-\frac{1}{2}Z^2\right\} \Phi\left(\frac{s_0 + e^{\sigma_s Z + \mu_s} - \mu_t}{\sigma_t}\right) dZ,$$

where

$$Z = \frac{\ln(s - s_0) - \mu_s}{\sigma_s},$$

and where the integration limits are

$$A = -\sqrt{-2\ln[\sqrt{2\pi}(P_0)]} \quad \text{and} \quad B = +\sqrt{-2\ln[\sqrt{2\pi}(P_0)]},$$

in which P_0 is normalizing factor which is set to 1×10^{-40} to insure that the integration is performed over a region which includes all values of the integrand $\geq 1 \times 10^{-40}$.

The total number of integrations performed is determined as follows:

$$\text{Total no. of integrations} = [\text{no. of M.C. trials}] \times [\text{no. of locations}] \times [\text{no. of failure modes}] \times [\text{no. of thickness sensitivity values}]$$

A case with either a small number of locations or Monte Carlo trials can be run to assess the average time taken for each integration. Then the approximate total amount of time required to perform larger-scale analyses can be assessed.

Box 30—Component Failure Probability (per Location). For each location, the number of Monte Carlo simulations usually produces a corresponding number of unique probabilities of failure. Since the objective is to get one answer per location, an arithmetic average is used to determine an average probability of failure for each location.

Box 31—Total Structure Failure Probability. To get a probability of failure for a group of locations, or for an entire structure, the structural locations are considered to be in series; that is, failure of any one location will lead to structural failure of the whole assembly. That is, no load path redundancy or redistribution is assumed. This is usually a conservative approach.

As an example, take a system comprised of two independent elements in series, each having a probability of failure of 1%. To find the probability of failure of the system, we calculate 1 minus the probability that both elements will survive (i.e., the product of the probabilities of the survival of each of the two elements), as follows:

$$PF_{TOT} = 1 - (1 - 0.01) \times (1 - 0.01) = 1 - (0.99)(0.99) = 0.0199$$

Box 32—Failure Probability vs. Aircraft Age. Because of the time dependence of environmental conditioning of the composite structure and of undetected operational damage, the single-flight probability of failure could change over time. To create a curve of SFPP vs. time, the program must be rerun with the different analysis times as input.

5.4 ADDITIONAL PROBABILITY CALCULATIONS.

The result from the NGCAD probabilistic methodology is the single-flight probability of failure (P_{SF}). Given P_{SF} , the following equation is used to determine the probability of failure (P_S) for a single aircraft during its design lifetime:

$$P_S = 1 - \prod_{i=1}^K (1 - P_{SF_i}),$$

where K is the total number of flights during a design lifetime. If P_{SF_i} is constant (independent of time), this becomes

$$P_S = 1 - (1 - P_{SF_i})^K$$

5.5 DESCRIPTION OF PROGRAM OUTPUT.

Tables 5-4 through 5-6 show examples of program output: table 5-4 is a probability of failure summary by location and major structural component; while tables 5-5 and 5-6 summarize the number of defects chosen via simulation for each major component.

5.5.1 Failure Probability Summary (Table 5-4).

The probability of failure for each major component is obtained by assuming all locations are independent no load path redundancy. The component probability of failure is obtained using a series calculation described above in Box 31, using the failure probabilities of all failure modes within the components. Similarly, the probability of failure for the total structure is a series calculation using the failure probabilities of the components. In table 5-4, locations are grouped into high- and low-strain points (from deterministic stress analysis) on the upper and lower skins, denoted USH and LSH, respectively.

TABLE 5-4. EXAMPLE PROBABILITY OF FAILURE LISTING

Loc	Failure Modes		Total
	Compression Strength	Tensile Strength	
Tot	0.471E-09	0.508E-10	0.519E-09
USH	0.468E-09		0.468E-09
LSH		0.508E-10	0.508E-10
USH	Compression Strength	Tensile Strength	Total
1	0.411E-09		0.411E-09
2	0.135E-12		0.135E-12
3	0.109E-10		0.109E-10
4	0.466E-10		0.466E-10
5	0.517E-13		0.517E-13
LSH	Compression Strength	Tensile Strength	Total
6		0.236E-10	0.236E-10
7		0.447E-11	0.447E-11
8		0.923E-11	0.923E-11
9		0.736E-11	0.736E-11
10		0.606E-11	0.606E-11

The columns contain failure probabilities per failure mode, and the Total column is a series calculation of the individual failure mode failure probabilities. That is, we assume each failure mode to be independent from one another. At the top of this output file, the total failure probability for each failure mode is given. This enables assessment of the relative contribution of each failure mode to the total failure probability.

5.5.2 Defect Summaries.

The top part of the table 5-5 gives a summary of the total number of defects from all locations, per failure mode, for each type of defect used. The Occurred column represents the total number of occurrences of that defect type from the Poisson distribution model within the Monte Carlo simulation, while the Used column represents those defects that were actually used to scale the strength distribution. The difference in these two values comes from the fact that if several defect types are chosen within the Monte Carlo trial at a specific location, the effects will not be compounded; the defect with the most severe effect will be chosen, and the less severe defect types are ignored.

TABLE 5-5. MANUFACTURING DEFECT SUMMARY

	Total	Defects	Compression Strength		Tensile Strength	
			Occurred	Used	Occurred	Used
All Locations	9718	9651	7895	7833	1823	1818
Hole	3476	3469	2517	2511	959	958
Laminate	3497	3313	3229	3190	125	123
Impact	548	548	399	399	149	149
Waviness	1450	1406	1059	1058	349	348
Tolerance	932	915	691	675	241	240
Upper Skin High Strain	7895	7833	7895	7833		
Hole	2517	2511	2517	2511		
Laminate	3229	3190	3229	3190		
Impact	399	399	399	399		
Waviness	1059	1058	1059	1058		
Tolerance	691	675	691	675		
Lower Skin High Strain	1823	1818			1823	1818
Hole	959	958			959	958
Laminate	125	123			125	123
Impact	149	149			149	149
Waviness	349	348			349	348
Tolerance	241	240			241	240

The number of defects, per failure mode, are summed from all locations within each major structural component. The Total column represents the arithmetic sum of defects from the failure mode columns. Note that since the impact defect has the most severe effect, it will be used every time, as can be seen in the defect numbers.

Similar output shows the operational defects chosen from the simulation. The layout is similar to the manufacturing defect summary, where the total number of defects chosen from the Monte

Carlo simulation are summarized taking into account all locations that define each major structural component.

Blank entries indicate that the defect type was not specified for that failure mode, while zeroes (not shown) would indicate that the number of Monte Carlo trials was not enough for the defect to occur. From Poisson distribution rates, it is possible (and very important) to determine how many trials will be needed to ensure each defect (and its effect) is accurately represented in the simulation.

5.6 EXAMPLE PROBLEM.

The following example problem illustrates the methods used in the NGCAD probabilistic approach. Monte Carlo simulation is used to model the effects of gust on the applied stress distribution and manufacturing defects on the component strength distribution, then numerical integration is used to calculate the probability of failure for each simulation.

The maximum stress during a single flight for a given aircraft structural component is a random quantity which follows a normal distribution with a mean of 2000 psi and a standard deviation of 500 psi. The strength of the component is also a random quantity and follows a normal distribution with a mean of 4000 psi and a standard deviation of 1000 psi. There is a 50% chance that a positive gust will occur during the maximum stress excursion and cause the stress to increase by 200 psi. The expected number of undetected manufacturing defects for this component is 1. Note that this is a mathematical expectation, not a probability, thus there could be 0, 1, 2, 3, etc., manufacturing defects. It is surmised that if at least one defect exists, the basic strength of the component will be reduced by 20%.

What is the single-flight probability of failure, if failure is defined as the component's maximum stress exceeding its strength?

5.6.1 Theoretical Background.

As discussed earlier in this section, the single-flight probability of failure is the product of the maximum stress per flight probability density, $f(s)$, and the material strength cumulative probability, $G(s)$, integrated over the region in which $f(s)$ is defined:

$$\text{SFPP} = \int_{\Omega_f} f(s) G(s) ds$$

Figure 5-6 shows the PDFs for the applied stress and component strength in units of ksi. Figure 5-7 shows the applied stress PDF and the component strength CDF. The CDF is the probability that the strength is less than the given value, i.e., the area under the PDF from negative infinity to the given value (hence the term cumulative). It follows that the CDF is asymptotic to 0 and 1 in the negative and positive directions, respectively.

Figure 5-8 shows the product of the stress PDF and the strength CDF; the area under this curve is the probability of failure, thus the product is referred to as the integrand.

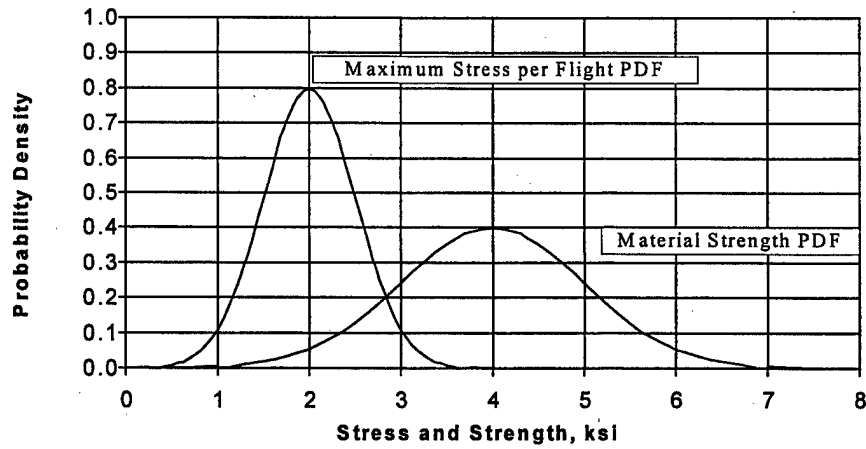


FIGURE 5-6. BASIC STRESS AND MATERIAL STRENGTH PROBABILITY DENSITY FUNCTIONS

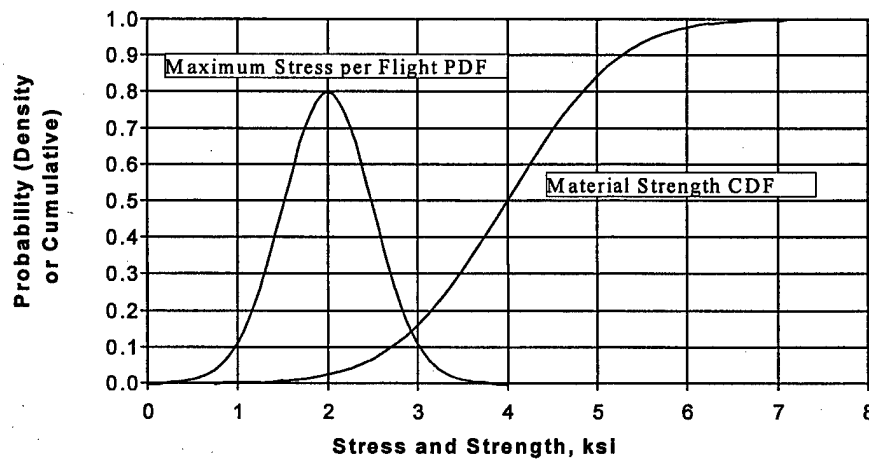


FIGURE 5-7. APPLIED STRESS PDF AND MATERIAL STRENGTH CDF

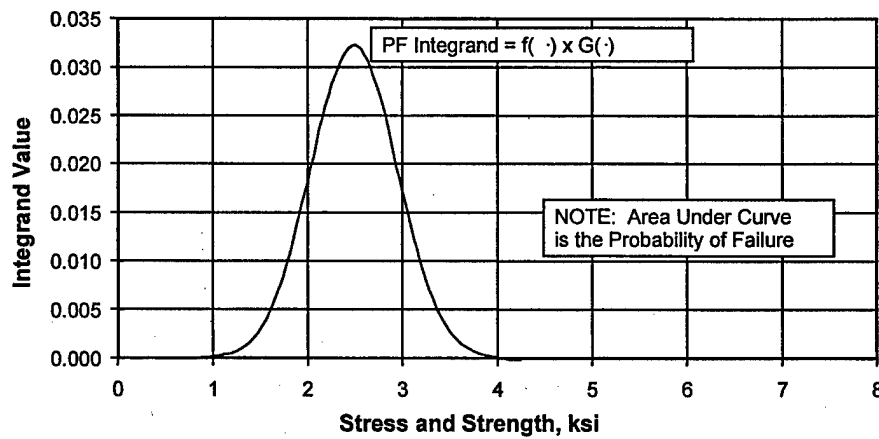


FIGURE 5-8. INTEGRAND: PRODUCT OF APPLIED STRESS PDF AND MATERIAL STRENGTH CDF

For the case where both the maximum stress per flight and material strength are independently and normally distributed, the SFPF is straightforward and can be found in any reliability textbook which addresses the load-strength interference problem:

$$\text{SFPF} = \Phi[(\mu_s - \mu_t)/(\sigma_s^2 + \sigma_t^2)^{1/2}] \quad (5-1)$$

where

Φ \equiv standard normal cumulative distribution function

$\mu_s, \sigma_s \equiv$ mean, standard deviation of the stress PDF

$\mu_t, \sigma_t \equiv$ mean, standard deviation of the strength PDF

Since a similar derivation of an equation for SFPF is not straightforward for all combinations of probability distributions, an alternate mathematical derivation is demonstrated for the normal-normal case, which is representative of the derivation used for the other distribution combinations.

$$f(s) = \frac{1}{(2\pi)^{1/2} \sigma_s} \exp\left[-\frac{1}{2} \left(\frac{s - \mu_s}{\sigma_s}\right)^2\right]$$

$$G(s) = \Phi\left(\frac{s - \mu_t}{\sigma_t}\right)$$

Then

$$\text{SFPF} \equiv \int_{\Omega_f} f(s) G(s) ds = \frac{1}{(2\pi)^{1/2} \sigma_s} \int_{-\infty}^{\infty} \exp\left[-\frac{1}{2} \left(\frac{s - \mu_s}{\sigma_s}\right)^2\right] \Phi\left(\frac{s - \mu_t}{\sigma_t}\right) ds$$

Substituting variables, let $Z = (s - \mu_s)/\sigma_s \Rightarrow s = \sigma_s Z + \mu_s \Rightarrow ds = \sigma_s dZ \Rightarrow dZ = ds/\sigma_s$

New integration limits: $s \rightarrow -\infty \Rightarrow Z \rightarrow -\infty$

$s \rightarrow +\infty \Rightarrow Z \rightarrow +\infty$

The transformed expression for SFPF is thus:

$$\text{SFPF} = \frac{1}{(2\pi)^{1/2}} \int_{-\infty}^{\infty} \exp\left(-\frac{1}{2} Z^2\right) \cdot \Phi\left(\frac{\sigma_s Z + \mu_s - \mu_t}{\sigma_t}\right) dZ = \int_{-\infty}^{\infty} \phi(Z) \cdot \Phi\left(\frac{\sigma_s Z + \mu_s - \mu_t}{\sigma_t}\right) dZ \quad (5-2)$$

where $\phi \equiv$ standard normal probability density function.

This formula is used in the NGCAD program to calculate SFPF, where the stress and strength are normally distributed. Formulas for combinations of normal, lognormal, and Weibull stress and strength distributions are similarly derived and used; the resulting equations are listed in table 3-5.

In this example, equations 5-1 and 5-2 will be employed separately to attain the identical solution for SFPP. A Microsoft EXCEL spreadsheet will also be included to demonstrate trapezoidal integration and verify the Romberg integration of equation 5-2.

5.6.2 Solution.

In this example, for each Monte Carlo simulation, there are four possible outcomes of the two independent events (gust and manufacturing defect) which must be considered in determining the SFPP:

- No gust, no manufacturing defect
- Gust, no manufacturing defect
- No gust, manufacturing defect
- Gust, manufacturing defect

Each outcome's probability of occurrence is the product of the probabilities of the independent events that define the outcome. The probability of the event gust is 0.5, hence the probability of the event no gust is also 0.5. For manufacturing defects, more explanation is required. Recall the expected number of defects is 1. Assuming the occurrence of defects can be modeled as a Poisson process, the probability of no manufacturing defect is $\exp(-1) \approx 0.368$, hence the probability of manufacturing defect (actually 1 or more defects) is $1 - \exp(-1) \approx 0.632$. (Recall that for this problem, existence of any number of defects reduces the material strength by 20%, regardless of how many.)

Thus, the outcome probabilities (Pr_i , $i=1$ to 4) are:

- No gust, no manufacturing defect: $0.5 \times 0.368 = 0.184 = Pr_1$
- Gust, no manufacturing defect: $0.5 \times 0.368 = 0.184 = Pr_2$
- No gust, manufacturing defect: $0.5 \times 0.632 = 0.316 = Pr_3$
- Gust, manufacturing defect: $0.5 \times 0.632 = 0.316 = Pr_4$

Note that these probabilities sum to 1, as they encompass all possible outcomes. After calculating each outcome's SFPP and weighing it by its probability of occurrence, the sum constitutes the solution to the problem. Mathematically,

$$SFPP = Pr_1 \times SFPP_1 + Pr_2 \times SFPP_2 + Pr_3 \times SFPP_3 + Pr_4 \times SFPP_4$$

We know the Pr_i probabilities for each scenario; the SFPP can be calculated by using equations 1 or 2. The use of equation 2 will be demonstrated by running the NGCAD probabilistic analysis program.

Solution via equation 1: $SFPP_i = \Phi[(\mu_s - \mu_t)/(\sigma_t^2 + \sigma_s^2)^{1/2}]$

$$SFPP = \sum_i (Pr_i \times SFPP_i) = 0.0945$$

Solution via equation 2: $SFPF_i = \int_{-\infty}^{+\infty} \phi(Z) \cdot \Phi[(\sigma_s Z + \mu_s - \mu_t)/\sigma_t] dZ$

Table 5-6 shows the resultant failure probabilities associated with each of the four outcomes.

TABLE 5-6. FAILURE PROBABILITIES ASSOCIATED WITH OUTCOMES

Outcome (i)	μ_s	σ_s	μ_t	σ_t	Pr_i	$SFPF_i$
1	2000	500	4000	1000	0.184	0.0368
2	2200	500	4000	1000	0.184	0.0537
3	2000	500	3200	800	0.316	0.1017
4	2200	500	3200	800	0.316	0.1446

The NGCAD program was run to demonstrate the Monte Carlo simulation integration of equation 2. An input file was set up to create basic stress and strength PDFs identical to Outcome no. 1 above (no gust, no defects $\Rightarrow \mu_s=2000, \sigma_s=500, \mu_t=4000, \sigma_t=1000$).

To understand the following steps to create this applied stress input, the reader needs to fully understand the steps in defining the applied stress distribution, as shown in figure 5-2. A normal distribution was input for the n_{zmax} per flight PDF with the mean = 2 and the standard deviation = 0.5. Then, a stress/ n_z scale factor of 1000 was forced by setting Design Factor (DF) = 1.5, Allowable = 9000, Margin of Safety (MS) = 1.0, and the n_z corresponding to 100% Design Limit Stress (n_zDLS) = 3.0, as per the relation

$$\text{Stress}/n_z = \text{Allowable}/[DF(1+MS)]/n_zDLS = 9000/1.5[1+1]/3 = 1000$$

This produces the desired parameters ($\mu_s=2000, \sigma_s=500$) for basic maximum stress per flight PDF and is verified in the program output (at the end of this example). The component strength PDF is input directly.

To include the effects of gust, the input included (1) probability of gust occurring (0.5), (2) probability of down gust given that gust occurs (0.0, hence ensuring up gust only), and (3) the probability distribution for the shift in the input n_{zmax} PDF when gust occurs (Uniform[0.2,0.2]). Based on these inputs and the stress/ n_z scale factor of 1000, a positive shift of 200 in the stress PDF will occur when gust is sampled during Monte Carlo simulation (during approximately half the trials). To include the effects of undetected manufacturing defects, a manufacturing defect rate of 1.0 and a strength reduction factor of 0.8 were input. As described above, there is ~63.2% chance during a given Monte Carlo trial that at least one defect will occur and the basic material strength PDF will be scaled by 0.8.

Initially, the program was run with only 10 Monte Carlo trials. With the random number seed selected, this was enough to demonstrate the numerical integration results for the four possible outcomes. Results are summarized in table 5-7.

TABLE 5-7. RESULTS CORRESPONDING TO THE FOUR OUTCOMES

Outcome (i)	MC Trial No.	Fraction of Trials (Fr_i)	SFPF _i
1	5	0.1	0.0368
2	1,4	0.2	0.0537
3	2	0.1	0.1017
4	3,6-10	0.6	0.1446

$$SFPF = \sum(Fr_i \times SFPF_i) = 0.1113$$

Two points are evident from these results. First, there is excellent agreement between the SFPF_i values here and the those for equation 1, demonstrating the accuracy of Romberg integration applied to equation 2. Second, the number of Monte Carlo trials (10) is obviously insufficient to accurately simulate the individual outcome probabilities. (Compare Fr_i values in this table to Pr_i values in the previous table.) More trials are necessary to converge to the "exact" solution achieved with equation 1. In fact, convergence becomes evident at approximately 1000 trials as shown in table 5-8.

TABLE 5-8. FAILURE PROBABILITIES ASSOCIATED WITH M.C. TRIALS

MC Trials	SFPF
10	0.111335
100	0.104170
1000	0.094854
10,000	0.094032
100,000	0.094316
"Exact"	0.094483

Figure 5-9 shows the PDFs describing the maximum stress per flight for the "gust" and "no gust" cases and the component strength PDFs for the "manufacturing defect" and "no manufacturing defects" cases. Figure 5-10 is the integrand per equation 2 for the outcome where neither gust nor manufacturing defect occur. Table 5-9 shows a spreadsheet application (using Microsoft EXCEL software) of the trapezoidal rule to estimate the area under the SFPF integrand curve for comparison with Romberg integration results from the NGCAD program. Recall that Romberg integration is an extended version of the trapezoidal rule.

Appendix A shows the NGCAD program output (including an echo of the input data), with the number of Monte Carlo trials set to 10.

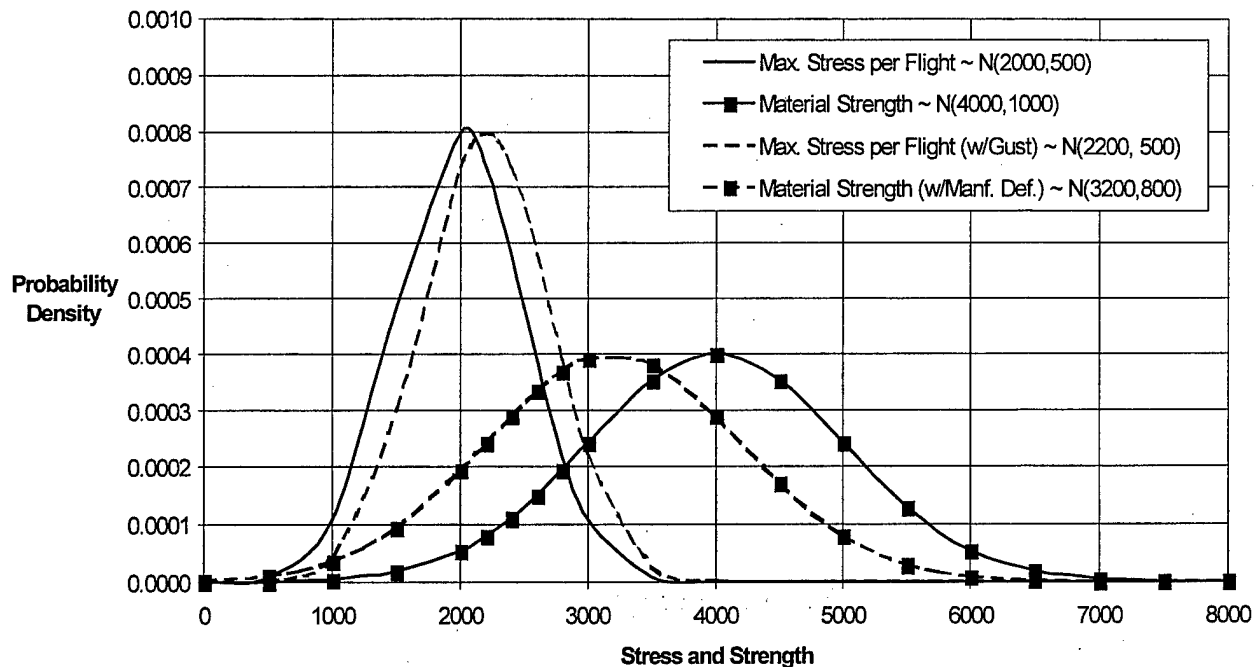


FIGURE 5-9. MAXIMUM STRESS AND COMPONENT STRENGTH PDFs

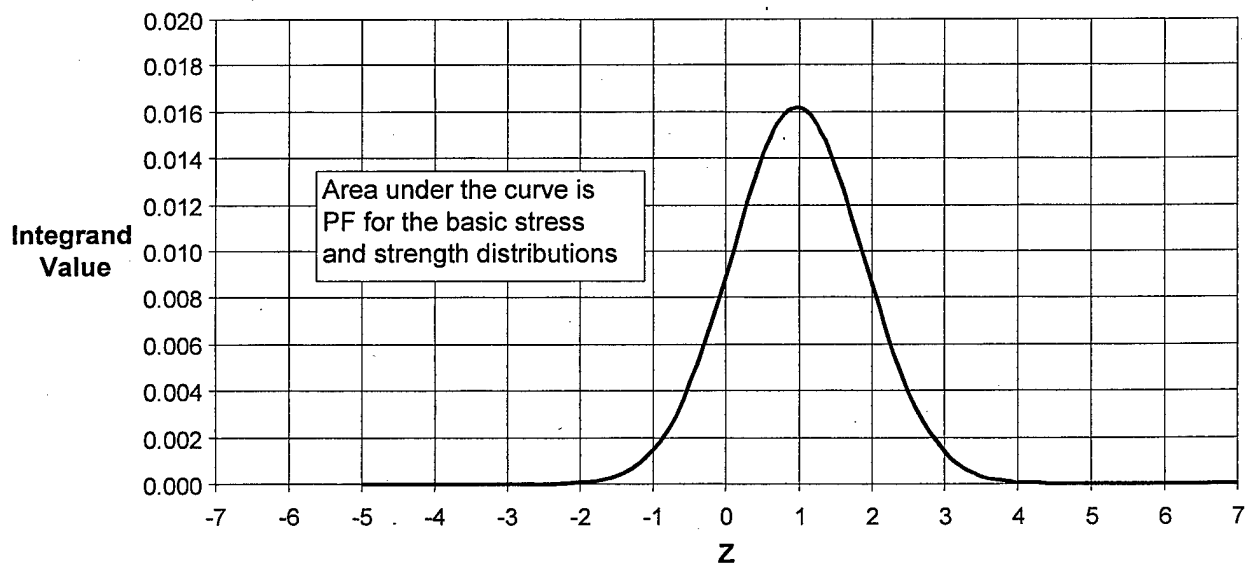


FIGURE 5-10. INTEGRAND FOR OUTCOME NO. 1: NO GUST, NO DEFECT

TABLE 5-9. TRAPEZOIDAL RULE CALCULATION (NO GUST, NO DEFECT)

PF integrand for Normal-Normal Case			
	Stress (s)	Strength (t)	
P1=	2000	4000	
P2=	500	1000	Trapezoidal
	Z	f(Z)	Area
	-3.0	1.03117E-06	
	-2.8	2.66736E-06	3.69853E-07
	-2.6	6.56713E-06	9.23448E-07
	-2.4	1.53896E-05	2.19567E-06
	-2.2	3.43277E-05	4.97173E-06
	-2.0	7.2886E-05	1.07214E-05
	-1.8	0.000147312	2.20198E-05
	-1.6	0.000283424	4.30735E-05
	-1.4	0.000519109	8.02532E-05
	-1.2	0.000905144	0.000142425
	-1.0	0.001502561	0.000240771
	-0.8	0.002374755	0.000387732
	-0.6	0.003573528	0.000594828
	-0.4	0.005120207	0.000869373
	-0.2	0.006985726	0.001210593
	0.0	0.009075962	0.001606169
	0.2	0.011229375	0.002030534
	0.4	0.013232044	0.002446142
	0.6	0.014850298	0.002808234
	0.8	0.015874891	0.003072519
	1.0	0.016165394	0.003204028
	1.2	0.015681827	0.003184722
	1.4	0.014493701	0.003017553
	1.6	0.012763631	0.002725733
	1.8	0.01071086	0.002347449
	2.0	0.008565951	0.001927681
	2.2	0.006529457	0.001509541
	2.4	0.004744401	0.001127386
	2.6	0.003286584	0.000803098
	2.8	0.002170837	0.000545742
	3.0	0.001367392	0.000353823
	3.2	0.000821505	0.00021889
	3.4	0.000470817	0.000129232
	3.6	0.000257452	7.28269E-05
	3.8	0.000134346	3.91798E-05
	4.0	6.69151E-05	2.01261E-05
	4.2	3.18191E-05	9.87342E-06
	4.4	1.44482E-05	4.62673E-06
	4.6	6.26615E-06	2.07143E-06
	4.8	2.59632E-06	8.86247E-07
	5.0	1.02801E-06	3.62433E-07
		sum (~SFPP) =	0.036819

6. BENEFITS OF PROBABILISTIC ANALYSIS.

Uncertainties in the definition of loads, geometry, assembly procedures, manufacturing processes, engineering models, material properties, and maintenance or operational environments as well as uncertainties in testing lead to uncertainty in structural design and ultimately safety. There have been many probabilistic analysis tools developed, but in general they are difficult for nonstatistical experts to understand and implement and have not been universally accepted by the engineering community. This does not mean that probabilistic analysis methods are without merit. There is ongoing effort to refine the methods and improve the user-friendliness and flexibility of associated computer programs.

A list of benefits was obtained by reviewing nearly 100 technical reports on probabilistic methods published through 1996; these were written by both developers and application engineers. The following list is the authors' consensus of perceived benefits:

- a. *Enables quantification of the design risk or reliability.* The classical deterministic analysis approach accounts for design uncertainties via an uncertainty factor multiplying the maximum expected stress. Probabilistic analysis, on the other hand, models most or all design parameters as being variable and combined with established structural analysis, yields a quantitative measure of reliability. This is obviously advantageous if reliability is specified as a basic contractual requirement. NASA design requirements for future space vehicles and structures are expected to be specified in reliability terms [93].

There have been structural reliability requirements imposed on military aircraft in the past, but the reliability values generated from such analyses are generally based on historical data from field maintenance data on aircraft with similar design features. A simplified, constant failure rate math model is usually employed, similar to established reliability analysis methods for avionics and electrical components. The techniques used to assess structural reliability are typically not tied to structural analysis methods. Employing probabilistic methods will aid reliability engineers in improving their analyses.

- b. *Identifies regions of high risk in a design.* The total structural risk is typically a function of a series of reliability values at specific locations within the structure. Should a particular region be shown to drive the overall risk, measures can be taken to reduce that risk via design change, and/or manufacturing inspection procedures can be implemented to minimize the occurrence of defects in critical zones.
- c. *Allows determination of design variable importance to reliability.* The reports were unanimous in identifying this benefit of probabilistic analysis. A powerful attribute of probabilistic analysis is the information gained in understanding the interactions, effects, and sensitivities of design variables. This information can be used to optimize testing for various purposes and can highlight the need to tighten (or relax) design or manufacturing tolerances. For instance, if it was shown that minor variation in stringer thickness had a major effect on resultant stress, tightening tolerances may be advantageous. Most probabilistic analysis software provides an output of design parameter sensitivity.

- d. *Provides a means to compare competing designs.* In addition to comparing overall reliability values of competing designs, the probabilistic analysis can point out specific features or locations in which the reliability significantly differs among designs. This can increase the understanding of the structure's behavior and lead to design improvements.
- e. *Provides a metric for design optimization.* Aerospace structures are operated in harsh and uncertain environments and yet must meet minimum weight, high performance, and stringent reliability requirements. Safety must be maintained at a high level. Reduced weight tends to reduce reliability and therefore must be implemented judiciously. Probabilistic analysis provides the measure of structural reliability, which can then be optimized by changing certain design variables. That is, design parameters are varied to minimize weight, but the overall reliability must meet a specified level.
- f. *Can reduce unnecessary conservatism.* This is particularly true with composite aircraft structure design, which is governed by compounded conservatism illustrated by the following criteria:
- Worst case temperature and moisture
 - Worst case damage, undetected
 - Reduced design allowables

This approach translates to a design philosophy that assumes the structure will simultaneously experience the worst case temperature, moisture, and damage conditions and will be composed of low-strength material. These worst case assumptions often lead to an excessively conservative design. The probabilistic analysis approach accounts for the expected occurrence of such events and combines them statistically.

- g. *Provides a means to establish optimum inspection intervals.* The worldwide trend of operating military and commercial aircraft beyond their original design life has introduced new structural integrity concerns arising from aging. This calls for extensive inspection. The main motivation for inspection is uncertainty arising from load predictions, analysis models, and material parameters. Probabilistic analysis treats uncertainties in a consistent manner, modeling parameters such as initial flaw size, load spectrum variation, crack growth model parameters and crack detection probability, and can be used to optimize the time interval for crack detection in metals.

Note: Establishing inspection intervals for composite material designs is driven by different phenomena than crack growth. Various approaches have been applied to model delamination growth as a function of time (cycles). Delamination growth is a very complex failure mechanism and is highly dependent on the structural geometry, making these theories difficult to apply.

- h. *Provides a means to establish warranties and spare parts policy.* Probabilistic analysis provides a means to estimate the frequency of failures and thus can provide valuable input to the warranting of parts. Associated with this is the estimate of the number of spares needed.

Incorporating probabilistic methods eventually leads to a better design approach in that the engineer develops a more comprehensive understanding of the problem encompassing many disciplines. The probabilistic evaluation gives the designer an idea of the inherent risk, but just as important, provides a means of evaluating design parameter sensitivities. In general, probabilistic methods require more detailed analysis, which can ultimately lead to an improved, more efficient design.

7. GROUND RULES, CONSIDERATIONS, AND LIMITATIONS.

The goal of a probabilistic engineering analysis applied to an aerospace structure is to define accurately the reliability of the design, expressed in terms of a per flight or per lifetime basis. Such knowledge would be invaluable to the designer, producers, operators, and certifying agencies of aerospace structures. This goal is often very difficult to achieve because of the number of potential variables involved in the calculations.

Some of the reasons for this difficulty are discussed in this section. These discussions are not meant to discount the potential value of probabilistic methods, nor to discourage the continued development of these tools, but to be realistic about the expectations and identify opportunities for continued effort.

A list of ground rules, considerations and limitations for the application of probabilistic analysis was obtained by reviewing nearly 100 technical papers on probabilistic methods published through 1996; these were written by both developers and application engineers. The following list, in no particular order, is the authors' consensus of ground rules, considerations, and limitations:

- a. *Knowledge of engineering and statistical theory required.* Currently, to use probabilistic methods, a fundamental knowledge of probability theory and statistics is required on the part of the application engineer. More advanced statistical knowledge is highly desirable because the underlying probability theory of many of these methods is complex. Of equal or greater importance than statistical knowledge is that application engineers fully understand structural design concepts. The optimal application engineer is an experienced structural analyst/design engineer with a good understanding of statistics.

An alternate, though less desirable approach is to form a team consisting of structural and statistics experts. Crucial aspects of each field would be discussed by the team and potential design implications researched.

- b. *Lack of sufficient statistical data.* Probabilistic analysis typically uses interpolations, extrapolations, small data samples, and therefore has inherent error. This can lead to an analysis full of assumptions about the nature of design variables and subsequently impacts analysis accuracy.

Some authors assert that small amounts of data can be used to perform the probabilistic analysis. Should the analysis show a design parameter to be a driver, it is contended that additional testing can be specified to better characterize the variable. This is idealistic; in the real world, external factors force compressed development schedules, and cost is always an issue. Thus additional testing must be justified by the increased benefits obtained. A method to help quantify uncertainties of probabilistic analysis and to rationally assess the risk of accepting the results is to establish confidence bounds for the reliability values generated.

- c. *Legal issues.* Legal implications of probabilistic methods are unclear at this time. The risk level associated with deterministic design has never been quantified, even though it

exists. As such the establishment of a threshold value for a socially acceptable risk level has been avoided. Probabilistically designed products require establishment of reliability/failure criterion and thus the acknowledgment of the existence of some finite failure probability, which could have a myriad of associated legal ramifications. Governmental certifying agencies along with producers will be required to establish minimum design reliability values.

- d. *Additional time and resources required.* Significant time is needed to build the probabilistic models, especially if integrated with existing structural analyses, which themselves are very time consuming. Depending on the type of analysis method used (described in section 3), running the probabilistic analysis may require significant computer resources.
- e. *Design certification.* Ideally, reliability analysis values should be verified by hardware demonstrations. Currently, there is no commonly accepted method established to certify an aerospace structure, given it has been designed to a certain reliability level. How does one demonstrate a structural probability of failure of 1×10^{-9} ? Most authors agree that this issue is a major roadblock to incorporation of the probabilistic methodology. This is why many suggest the best use for probabilistic analysis is as a tool for identifying design parameter sensitivities and contribution to reliability for proposed or existing designs.
- f. *Accounting for the unknowns.* Because an uncertainty factor may not be used in probabilistic analysis, the application engineer must be certain he has accounted for all scenarios, variables, and interaction of failure modes. The purpose of the uncertainty factor associated with deterministic methods is to account for an under-strength airframe as well as inadvertent overloads caused by load and strength variation as well as non-structural factors (to a certain extent) such as pilot error or a freak maintenance accident. Currently no known probabilistic structural analysis methods inherently take into account nonstructural contributions to failure. An analogous approach should be developed for probabilistic methods. Chamis [94] wrote a paper addressing the human factor in structural reliability.

In addition, significant weight growth typically occurs over the lifetime of an aircraft due to design modifications and avionics upgrades. This issue requires attention when designing a structure initially to a target reliability level. That is, it may be prudent to anticipate weight growth and design to a value greater than the target reliability value to account for expected reliability degradation due to weight growth.

- g. *Tail Sensitivity.* When predictions of structural behavior are required in the high reliability range (approx. 0.99999 or greater), it is necessary to use parametric modeling methods since sufficiently large data sets are usually not available. This involves fitting parametric functions to the data and choosing the one with the best fit. These parametric functions permit extrapolation from available data to ranges outside the data, but if the probability of failure is extremely small, this extrapolation will be substantial. Slight deviation from the assumed model in tail regions can have a dramatic effect on high

reliability estimates [95]. The estimated reliability therefore depends strongly on the parametric function.

With respect to the use of parametric models, one well known statistician [96] wrote "all models are wrong, but some are useful," meaning that no parametric statistical model should be accepted uncritically. Breiman [97] writes "the probability of failure $P_f = 1 \times 10^{-6}$ has an Alice in Wonderland flavor and should be banned from nonfiction literature." Obviously this is a well-known issue in probabilistic analysis. It should be the obligation of the analyst to investigate consequences of departures from the parametric model employed.

- h. *Different approaches available.* As expounded in section 3, there are competing techniques for performing probabilistic structural analyses, and due to technique or model assumptions, they often yield different results. Each approach has its advantages as well as shortcomings as far as accuracy, run time, and ease of implementation. Reference 98 provides an excellent discussion of these issues associated with the commonly used probabilistic methods. Obviously, accuracy should be the primary goal and compromised only if run time and implementation hardships are encountered. Many problems with computational speed have been dealt with due to enormous increases available with parallel processing on workstations, enabling Monte Carlo simulation methods to become more feasible.
- i. *Existing failure mode model must exist.* The first step in probabilistic analysis is to identify all the modes of failure, ways in which the structure might fail to fulfill its intended purpose. Since probabilistic methods do not provide this identification, an existing method to model the failure mode must be used. For instance, modeling fracture, fatigue, flaw growth, etc., can be accomplished using existing structural models and building a probabilistic framework around them. Probabilistic analysis, therefore, does not introduce any new structural analysis techniques but depends heavily on using state-of-the-art methods; they are at the heart of the analysis.
- j. *Modeling the system.* Component reliability in its simplest form addresses individual, independent failure modes. In reality, multiple failure modes or sites as well as multiple interacting failure modes most likely are involved in structural failure. Furthermore, structural redundancy and damage progression may also be important. These issues bring in the need to model system reliability, especially if dependence exists. Several research papers [99 through 101] have focused on probabilistic methods to model system reliability, simulating a sequence or interaction of individual component failure modes.

In summary, probabilistic analysis methods, to be useful, must be embraced by the design and analysis engineering community. They cannot remain in a research team project with an associated aura of statistical mystique, with the rest of the engineering department left to be impressed with the complex math and promises, yet uninterested because there is nothing they can experiment with. A user-friendly and flexible application tool must be provided to engineers, i.e., something they can experiment with on a limited scale, for probabilistic methods to advance outside the research arena.

In addition, recognition of the value of probabilistic methods by academia and inclusion of engineering curriculum based on fundamental statistical and probabilistic principles would help facilitate long-term growth of this discipline. It will be of great help if future aerospace engineers entering the work force are familiar with fundamental statistical and probabilistic principles. Also of help would be the establishment of documented, standardized probabilistic analysis procedures to uniformly guide engineers.

8. REFERENCES.

1. Bernstein, P.L., Against the Gods: The Remarkable Story of Risk, John Wiley & Sons, 1996.
2. Pugsley, A.G., "A Philosophy of Aeroplane Strength Factors," Report and Memorandum No. 1906, British Aeronautical Research Committee, 1942.
3. Freudenthal, A.M., "The Safety of Structures," Paper No. 2296, American Society of Civil Engineers: Transactions, 1945.
4. Weibull, W., "A Statistical Distribution Function of Wide Applicability," Journal of Applied Mechanics, Vol. 18, 1951.
5. Freudenthal, A.M., "Safety and the Probability of Structural Failure," Paper No. 2843, American Society of Civil Engineers: Transactions, 1954.
6. Freudenthal, A.M., Garrelts, J.M., and Shinozuka, M., "The Analysis of Structural Safety," Journal of the Structural Division, ASCE, Vol. 92, No. ST1, February 1966.
7. Cornell, C.A., "Bounds on the Reliability of Structural Systems," Journal of the Structural Division, ASCE, Vol. 93, No. ST., February 1967.
8. Lind, N.C., "The Design of Structural Design Norms," Journal of Structural Mechanics, Vol. 1, No. 3, 1973.
9. Hasofer, A.M. and Lind, N.C., "Exact and Invariant Second-Moment Code Format," Journal of the Engineering Mechanics Division, ASCE, Vol. 100, No. EM1, February 1974.
10. Muller, G.E. and Schmid, C.J., "Factor of Safety - USAF Design Practice," AFFDL-TR-78-8, Wright Patterson Air Force Base, 1978.
11. FAA Statistical Handbook of Aviation: Calendar Year 1993, U.S. Department of Transportation, FAA APO-95-5.
12. Evans, M., Hastings, N., and Peacock, B., Statistical Distributions, John Wiley & Sons, New York, 1993.
13. Fox, E.P. and Safie, F., "Statistical Characterization of Life Drivers for a Probabilistic Design Analysis," AIAA-92-3414.
14. King, R.L., "The Determination of Design Allowable Properties for Advanced Composite Materials," GEC Journal of Research, Vol. 5, No. 2, 1987.

15. Wagner, H.D., Phoenix, S.L., and Schwartz, P., "A Study of Statistical Variability in the Strength of Single Aramid Filaments," Journal of Composite Materials, Vol. 18, July 1984.
16. Nakayasu, H., Murotsu, Y., Mori, K., and Kase, S., "Effect of Distribution and Sample Size in Material Testing on Probabilistic Design of Structure," ICQC, TS. D1-20, Tokyo, 1978.
17. Aerospace Information Report 5080, "Integration of Probabilistic Methods into the Design Process," SAE, 1997.
18. Kapur, K.C. and Lamberson, L.R., "Reliability in Engineering Design," John Wiley & Sons, New York, 1977.
19. Wirsching, P.H., "Literature Review on Mechanical Reliability and Probabilistic Design," Probabilistic Structural Analysis Methods for Select Space Propulsion System Components (PSAM), NASA Contractor Report 189159, Vol. III, 1992.
20. Metropolis, N. and Ulam, S., "The Monte Carlo Method," Journal of the American Statistical Association, 44, N 247, 335-341, 1949.
21. Sobol, I.M., A Primer for the Monte Carlo Method, CRC Press, Inc., 1994.
22. Shooman, M.L., Probabilistic Reliability: An Engineering Approach, McGraw-Hill Book Company, New York, 1968.
23. Mahadevan, S., "Modern Structural Reliability Methods," NASA Marshall Space Flight Center, October 1994.
24. Rosenblatt, M., "Remarks on a Multivariate Transformation," Annals of Mathematical Statistics, Vol. 23, No. 3, pp. 470-472, 1952.
25. Wu, Y.-T., "Computational Methods for Efficient Structural Reliability and Reliability Sensitivity Analysis," AIAA-93-1626-CP, 1993.
26. Box, G.E.P. and Draper, N.R., Empirical Model-Building and Response Surfaces, John Wiley & Sons, New York, 1987.
27. Montgomery, D.C., Design and Analysis of Experiments, 3rd Edition, John Wiley & Sons, New York, 1984.
28. Myers, R.H. and Montgomery, D.C., Response Surface Methodology, John Wiley & Sons, New York, 1995.
29. Box, G.P. and Behnken, D.W., "Some New Three-Level Designs for the Study of Quantitative Variables," Technometrics, 2, pp. 455-475, 1960.

30. Montgomery, D.C. and Peck, E.A., Introduction to Linear Regression Analysis, John Wiley & Sons, New York, 1992.
31. Eric P. Fox of Pratt & Whitney, "Methods of Integrating Probabilistic Design Within an Organization's Design System Using Box-Behnken Matrices," published by the American Institute of Aeronautics and Astronautics, AIAA-93-13809-CP.
32. Liu, P.-L. and Der Kiureghian, A., "Optimization Algorithms for Structural Reliability Analysis," Report No. UCB/SESM-86/09, Department of Civil Engineering, University of California, Berkley, CA, July 1986.
33. Nikolaidis, E., Ruiz, R.H., and Maglaras, G., "Evaluation of Methods for Reliability Assessment When Random Variables Are Correlated," AIAA-95-1312-CP, 1995.
34. Wu, Y.T. and Wirsching, P.H., "New Algorithm for Structural Reliability Estimation," Journal of Engineering Mechanics, ASCE, Vol. 113, No. 9, September 1987, pp. 1319-1336.
35. Breitung, K., "Asymptotic Approximations to Multinormal Integral," Journal of Engineering Mechanics, Vol. 110, No. 3, pp. 357-366.
36. Aerospace Information Report 5083, "Engineering Probabilistic Methods," SAE, 1996 (Draft).
37. Henley, E.J. and Kumamoto, H., Reliability Engineering and Risk Assessment, Prentice-Hall, Inc., Englewood Cliffs, N.J., 1981.
38. Torng, T.Y., Wu, Y.-T., and Millwater, H.R., "Structural System Reliability Calculation Using a Probabilistic Fault Tree Analysis Method," AIAA-92-2410-CP, 1992.
39. Lincoln, J.W., "Method for Computation of Structural Failure Probability for an Aircraft," ASD-TR-80-5035, July 1980.
40. Lincoln, J.W., "Risk Assessment of an Aging Aircraft," Journal of Aircraft, Vol. 22, No. 8, August 1985, pp. 687-691.
41. Abernathy, R.B., Breneman, J.E., Medlin, C.H., and Reinman, G.L., "Weibull Analysis Handbook," AFWAL-TR-83-2079, November 1983.
42. Shiao, M.C. and Chamis, C.C., "Probabilistic Evaluation of Fuselage-Type Composite Structures," NASA TM-105881, November 1992.
43. Shiao, M.C., Abumeri, G.H., and Chamis, C.C., "Probabilistic Assessment of Composite Structures," AIAA-93-1441-CP, 1993.

44. P.N. Murthy and Chamis, C.C., "Probabilistic Analysis of Composite Material Structure," NASA Tech Briefs, November 1995, pp. 60-61.
45. P.N. Murthy, "ICAN - Second-Generation Integrated Composite Analyzer," NASA Tech Briefs, November 1995, pp. 60-61.
46. Liaw, D.G., Singhal, S.N., Murthy, P.N., and Chamis, C.C., "Quantification of Uncertainties in Composites," AIAA-93-1440-CP, 1993.
47. Shah, A.R., Singhal, S.N., Murthy, P.N., and Chamis, C.C., "Probabilistic Simulation of Long Term Behavior in Polymer Matrix Composites," AIAA-94-1445-CP, 1994.
48. Shah, A.R., Murthy, P.N., and Chamis, C.C., "Effect of Cyclic Thermo-Mechanical Load on Fatigue Reliability in Polymer Matrix Composites," AIAA-95-1358-CP, 1995.
49. Shiao, M.C., Singhal, S.N., and Chamis, C.C., "Network Based Parallelism of Probabilistic Composite Structural Analysis," AIAA-95-1259-CP, 1995.
50. Singhal, S.N., Abumeri, G.H., Shiao, M.C., and Chamis, C.C., "Probabilistic Assessment of Tailored Composite Structures," AIAA-94-1418-CP, 1994.
51. Chamis, C. and Minnetyan, L., "Probabilistic Evaluation of Bolted Joints in Polymeric Structures," Paper Number 25, AGARD Conference on Bolted/Bonded Joints in Polymeric Composites, Florence, Italy, September 1996.
52. Thacker, B.H. and Senseny, P.E., "Probabilistic Structural Analysis of Deep Tunnels," Probabilistic Methods in Geomechanics, AMD Vol. 134, ASME, 1992, pp. 1-13.
53. Wu, Y.-T., Journal, A.G., Abramson, L.R., and Nair, P.K., "Uncertainty Evaluation Methods for Waste Package Performance Assessment," NUREG/CR-5639, U.S. Nuclear Regulatory Commission, January 1991.
54. Wu, Y.-T., Torng, T.Y., Millwater, H.R., Fossum, A.F., and Rheinfurth, M.H., "Probabilistic Methods for Rotordynamic Analyses," SAE-911110, April 1992.
55. Wu, Y.-T., "Development of a Probabilistic Design Methodology and Code Framework," presented at the FAA Technical Interaction Workshop on Development and Application of Probabilistic Risk Assessment Methodologies for Aircraft Safety Evaluations, October 1996.
56. "Review of the Probabilistic Failure Analysis Methodology and Other Probabilistic Approaches for Application in Aerospace Structural Design," Technical Paper, NASA Marshall Space Flight Center, 1993.
57. Moore, N.R., Ebberle, D.H., Newlin, L.E., Sutharshana, S., and Creager, M., "An Improved Approach for Flight Readiness Certification - Methodology for Failure Risk

Assessment and Application Examples," Jet Propulsion Laboratory Report under NASA RTOP 553-02-01, May 1992.

58. Newlin, L. et al., "Probabilistic Low-Cycle Fatigue Failure Analysis Applicable to Liquid Propellant Rocket Engines," Proceedings of the AIAA/ASME/ASCE/AHS/ASC 31st Annual Structures, Structural Dynamics, and Materials Conference, 1990, Part 2, pp. 1115-1123.
59. Sutharshana, S. et al., "Probabilistic High-Cycle Fatigue Failure Analysis Applicable to Liquid Propellant Rocket Engines," Proceedings of the AIAA/ASME/ASCE/AHS/ASC 31st Annual Structures, Structural Dynamics, and Materials Conference, 1990, Part 2, pp. 1105-1114.
60. Sutharshana, S., Grigoriu, M., Moore, N., and Fox, E., "Computational Methods for Probabilistic Flaw Propagation Analyses," presented at the Structures Congress '91, ASCE, 1991.
61. Shiao, M.C., Nagpal, V.K., and Chamis, C.C., "Probabilistic Structural Analysis of Aerospace Components Using NESSUS," AIAA 88-2373, 1988.
62. Shiao, M.C. and Chamis, C.C., "Probability of Failure and Risk Assessment of Propulsion Space Components," NASA Technical Memorandum 102323, 1989.
63. Newell, J.F., Rajagopal, K.R., and Ho, H., "Probabilistic Structural Analysis of Space Propulsion System Turbine Blades," AIAA 89-1372-CP, 1989.
64. Chamis, C.C. and Cruse, T.A., "Probability Approach for Strength Calculations," presented at the AGARD Structures and Materials Panel Workshop, 70th SMP Meeting, Sorrento, Italy, April 1990.
65. Thacker, B.H., McClung, R.C., and Millwater, H.R., "Application of the Probabilistic Approximate Analysis Method to a Turbopump Blade Analysis," AIAA-90-1098-CP, 1990.
66. Khalessi, M.R., Wu, Y.-T., and Torng, T.Y., "A New Most-Probable-Point Search Procedure for Efficient Structural Reliability Analysis," Proceedings of the 32nd Structures, Structural Dynamics, and Materials Conference, AIAA/ASME/ASCE/AHS/ASC, Part 2, April 1991, pp.1295-1304.
67. Torng, T.Y., Lin, H.-Z., Chang, C., and Khalessi, M.R., "Development of the Integrated Probabilistic Analysis Software Package, FEBREL-MSC/NASTRAN," AIAA-95-1260-CP-1995.
68. Khalessi, M.R., Lin, H.-Z., and Collier, M.A., "Probabilistic Transient Dynamic Impact Analysis of PA103E2 Insensitive Munitions Container," AIAA-95-1265-CP, 1995.

69. Minnetyan, L., Singhal, S.N., and Chamis, C.C., "Probabilistic Simulation of Progressive Fracture in Bolted-Joint Composite Laminates," NASA-TM-107207, May 1996.
70. Thomas, M., "Aerospatiale Method for Selection of Service Inspection Intervals," presentation to MIL-HDBK-17 committee, March 1995.
71. Tisseyre, M., Plantec, J.Y., Beaufils, J.Y., and Boetsch, R., "Aerospatiale Probabilistic Methods Applied to Aircraft Maintenance," Durability and Structural Reliability of Airframes, 1994.
72. Tropis, A., Thomas, M., Bounie, J.L., and Lafon, P., "Certification of the Composite Outer Wing of the ATR72," Aerospatiale report, 1993.
73. Adamson, J.D., "The Probabilistic Design system Development Experience," AIAA 94-1444, 1994.
74. Fox, E.P., "Method of Integrating Probabilistic Design Within an Organization's Design System Using Box-Behnken Matrices," AIAA 93-1380-CP, 1993.
75. Fox, E.P., "The Pratt & Whitney Probabilistic Design System," AIAA-94-1442-CP, 1994.
76. Fox, E.P., "Issues in Utilizing Response Surface Methodologies for Accurate Probabilistic Design," AIAA-96-1496-CP, 1996.
77. Lykins, C., Thomson, D., and Pomfret, C., "The Air Force's Application of Probabilistics to Gas Turbine Engines," AIAA-94-1440-CP, 1994.
78. McKnight, R.L., Bechtel, G.S., and Cook, T.S., "Probabilistic Turbine Blade Tip Durability Analysis," AIAA-93-1383-CP, 1993.
79. Verderaine, V., "First-Order Reliability Application and Verification Methods for Semi-Static Structures," Journal of Spacecraft and Rockets, Vol. 31, No. 6, pp. 1050-1053, 1994.
80. Verderaine, V., "Illustrated Structural Application of Universal First-Order Reliability Method," NASA Technical Paper, 1994.
81. Verderaine, V., "Structural Deterministic Safety Factors Criteria and Verification," NASA Technical Paper, 1993.
82. Brown, A.M. and Ferri, A.A., "Development of a Probabilistic Component Mode Synthesis Method for the Analysis of Non-Deterministic Substructures," NASA-Technical Memorandum 111870, 1995.

83. Ekstrom, J.L., Allred, and Sauvageau, D.R., "Applying Design to Reliability Techniques to a Composite Solid Rocket Motor Case," AIAA-91-1033-CP, 1991.
84. Stroud, W.J., Davis Jr., D.D., Maring, L.D., Krishnamurthy, T., and Elishakoff, I., "Reliability of Stiffened Structural Panels: Two Examples," NASA Technical Memorandum 107687, December 1992.
85. Stroud, W.J. and Nikolaidis, E., "Reliability-Based Structural Optimization: A Proposed Analytical-Experimental Study," NASA Technical Memorandum 109055, December 1993.
86. Sobel, L., Buttutta, C., and Suarez, J., "Probabilistic and Structural Reliability Analysis of Laminated Composite Structures Based on the IPACS Code," AIAA-93-1444-CP, 1993.
87. Ushakov, A., Kuznetsov, A.A., Stewart, A., and Mishulin, I.B., "Probabilistic Design of Damage Tolerant Composite Aircraft Structures," Final Report under Annex 1 to Memorandum of Cooperation AIA/CA-71 between the FAA and Central Aero-Hydrodynamic Institute (TsAGI), 1996.
88. Bucher, C.G. and Bourgund, U., "A Fast and Efficient Response Surface Approach for Structural Reliability Problems," Structural Safety, 7, pp. 57-66, 1990.
89. Abdi, F., "Concurrent Probabilistic Simulation of High Temperature Composite Structural Response," NASA-CR-198502, July 1996.
90. Carnahan, B., Luther, H.A., and Wilkes, J.O., "Applied Numerical Methods," John Wiley & Sons, New York, 1969.
91. "Surface Airways Hourly and Airways Solar Radiation," TD-3280, National Oceanic and Atmospheric Administration, November 1989.
92. MIL-HDBK-17, Polymer Matrix Composites, Volume 1, Guidelines, February 1992.
93. Ryan, R.S. and Townsend, J.S., "Application of Probabilistic Analysis and Design Methods in Space Programs," Journal of Spacecraft and Rockets, Vol. 31, No. 6, November-December 1994.
94. Chamis, C.C., "Probabilistic Simulation of the Human Factor in Structural Reliability," AIAA-93-1495-CP, 1993.
95. Neal, D.M., Matthews, W.T., and Vangel, M.G., "Model Sensitivity in Stress-Strength Reliability Computations," presented at the ARD 36th Conference on the Design Experiments in Army Research, Development and Testing, MTL TR 91-3, January 1991.

96. Box, G.E.P., Robustness in the Strategy of Scientific Model Building, Robustness in Statistics, R.L. Launer and G.N. Wilkinson, eds., Academic Press, Inc., New York, 1979.
97. Breiman, L. and Stone, C., "Broad Spectrum Estimates and Confidence Intervals for Tail Quantiles," Technical Report No. 46, Stat. Dept., University of California, Berkeley, CA, 1985.
98. Ebberle, D.H., Newlin, L.E., Sutharshana, S., and Moore, N.R., "Alternative Computational Approaches for Probabilistic Fatigue Analysis," AIAA-95-1359-CP, 1995.
99. Shiao, M.C. and Chamis, C.C., "Reliability of Composite Structures With Multi-Design Criteria," AIAA-94-1382-CP, 1994.
100. Mahadevan, S. and Chamis, C.C., "Structural System Reliability Under Multiple Failure Modes," AIAA-93-1379-CP, 1993.
101. Wu, Y.-T., "An Adaptive Importance Sampling Method for Structural System Reliability Analysis," presented at the ASME Winter Annual Meeting, 1992.

APPENDIX A—NGCAD PROGRAM OUTPUT

See discussion in section 5.

Northrop Grumman Proprietary

Probabilistic Design - Monte - Version: 16-JUL-1997 at 11:00

Run date: 16-SEP-1997 14:57:34

*** MONTE OUTPUT FILE ***

Echoing Input Data:

J.D. Narciso

Example Problem #1 - Normal/Normal, Gust and Manufacturing defects

9/16/97

01 Main counters

- 1 Number of locations
- 1 Number of thickness sensitivities
- 1 1 Beginning and Ending Thickness sensitivities
- 6 Number of failure modes
- 10 Number of Monte Carlo iterations

02 Flight and Lifetime Information

- 30.000000 Analysis: Start time (in years)
- 30.000000 Analysis: End time (in years)
- 1000.000 Average number of flight hours per year
- 1.000 Average number of hours per flight

03 Output Generation Control Flags

Detailed Output Specifications:

- Y Output details for each PF computed
- Y Output details for each AVEPF computed

Graphics Output Indicator Flags:

- 0 Count of specification lines
- Location Sets: Count = 1
- All: Count of range specification lines = 1
- LOC: 1--> 1

04 Miscellaneous Information

PROG_VER = NEW

- 1234567 Random number generator seed
- N Truncation is NOT being used
- 1.0000 Averaging class value (for AVEPF computations)
- 1.5000 Design Factor
- 1 Major Aircraft Components
- ALL_LOC Name of Major Aircraft Component 1
- .10000000E+03 Weight of Major Aircraft Component 1
- 001 001 Location range

```

=====+=====+=====+=====+=====+=====+=====+=====
05  Location Information
-----+-----+-----+-----+-----+-----+-----+-----
Baseline Thickness for each Location: Baseline Thickness = .100000 :
Locations ( 1 to 1)
Area for each Location:
Area = 1.000000 : Locations ( 1 to 1)

=====+=====+=====+=====+=====+=====+=====+=====
06  Thickness Sensitivity Information
-----+-----+-----+-----+-----+-----+-----+-----
100.00

=====+=====+=====+=====+=====+=====+=====+=====
07  Failure Mode Information
-----+-----+-----+-----+-----+-----+-----+-----
Count of Failure Mode Usage Definition Blocks = 1
Block 1 : Usage flags = N N N N N Y
Range: Loc = ( 1 to 1)
Failure Mode Type Codes:
Failure Mode 1: CM
Failure Mode 2: SM
Failure Mode 3: TM
Failure Mode 4: CS
Failure Mode 5: SS
Failure Mode 6: TS

=====+=====+=====+=====+=====+=====+=====+=====
08  Margins of Safety
-----+-----+-----+-----+-----+-----+-----+-----
Baseline MOS = 1.000000: Loc ( 1 to 1) FM 1-6( 0 0 0 0 0 1)
Alternate Margins of Safety:
None are used

=====+=====+=====+=====+=====+=====+=====+=====
09  Material Strength Allowables
-----+-----+-----+-----+-----+-----+-----+-----
Material Strength Allowables:
Allowable = 9000.000000 : Loc ( 1 to 1) FM 1-6( 0 0 0 0 0 1)

=====+=====+=====+=====+=====+=====+=====+=====
10  Operation STRESS Distribution Information
-----+-----+-----+-----+-----+-----+-----+-----
Count of Operation Distribution Definition Blocks = 1
Block 1 : Maximum-Nz PDF and related data
NORMAL : Mean = 2.00000 Sigma = .50000
3.0000 Number of Gs equal to 100% DLS
Count of range specification lines = 1
Range: Locations ( 1 to 1) Failure Modes 1-6( 0 0 0 0 0 1)

=====+=====+=====+=====+=====+=====+=====+=====
11  Material STRENGTH Distribution Information
-----+-----+-----+-----+-----+-----+-----+-----
Count of Material Strength Distribution Definition Blocks = 1
Block 1
NORMAL : Mean = 4000.00000 Sigma = 1000.00000
Count of range specification lines = 1

```

Range: Locations (1 to 1) Failure Modes 1-6(0 0 0 0 0 1)
 Material Strength Knock-down Factors:
 Strength Knockdown Factor = 1.000000 : Loc (1 to 1) FM 1-6(0 0
 0 0 0 1)

14 Gust Effects Information

"Gust" Usage Flag : Y
 Probability of Gust Occurring : .50000
 Probability of Down vs Up Gust: .00000
 UNIFORM : [.200000, .200000]
 UNIFORM : [.200000, .200000]

15 Manufacturing Defects Information

Manufacturing Defects Usage Flag: Y
 Count of Manufacturing Defect Types = 1
 Type 1: Delam
 Generic Manufacturing Defect Rates:
 Loc 1 to 1: Rates = 1.00000
 Manufacturing Defect Reduction Factors:
 Failure Mode 1(CM) : .000000
 Failure Mode 2(SM) : .000000
 Failure Mode 3(TM) : .000000
 Failure Mode 4(CS) : .000000
 Failure Mode 5(SS) : .000000
 Failure Mode 6(TS) : .800000

18 OTHER Mandatory Distributions

Count of Skin/Temp Distribution Definition Blocks = 1
 Block 1
 DISCRETE : Beg Index = 1 End Index = 2 Interpolation =0
 1) -65.000000 .500000 CumVal: .50000
 2) 160.000000 .500000 CumVal: 1.00000
 Count of range specification lines = 1
 Range: Locations (1 to 1)
 Average Moisture Content % Distribution:
 Assumed distribution type = TRIFLEX
 Min, Max, Rho: 0.000000000000000E+000 1.000000000000000
 1.000000000000000E-001

19 Risk Driver Analysis

PERFORM-RISK-ANALYSIS 0
 PRINT-ALL 0
 PRINT-RATIO 0
 GUST 0
 TEMPERATURE/MOISTURE 0
 MFG-DEFECTS 0
 OPR-DEFECTS 0
 END

```
=====+=====+=====+=====+=====+=====+=====
20 Declaration of Effects Used
-----+-----+-----+-----+-----+-----+-----
```

```
GUST 1
TEMPERATURE/MOISTURE 0
MFG-DEFECTS 1
OPR-DEFECTS 0
END
```

```
=====+=====+=====+=====+=====+=====+=====
00 END OF FILE
-----+-----+-----+-----+-----+-----+-----
```

Data from Input File Successfully Retrieved:

No Errors Detected

Gust is on (per input data)

Temperature/Moisture is off (per input data)

Mfg Defects are on (per input data)

Opr Defects are off (per input data)

No graphics data will be saved

Pre-Computing for Locations ...

Sensitivity(1) = 100.0% Location(1) [Thk= .1000] Failure Mode(6) = TS

MOS(K,J) for output reporting only = 1.00000000

```
>>> THICKNESS 1 LOCATION 1 FAILURE MODE 6"TS" MCI 1
STRENGTH: NORMAL : 4000.00000 1000.00000 .00000 .00000
STRESS : NORMAL : 2000.00000 500.00000 .00000 .00000
DN-GUST: UNIFORM : 200.0000000 200.0000000 .0000000 .0000000
UP-GUST: UNIFORM : 200.0000000 200.0000000 .0000000 .0000000
Iteration 1): Time = 360.0 Temp = -65.0
Event type = GUST : SHIFT = 200.00000
STRESS : NORMAL : 2200.00000 500.00000 .00000 .00000
Mfg Defect Scale Factor = 1.0000000000000000
Event type = DEFECT: SCALE = 1.00000
STRENGTH: NORMAL : 4000.00000 1000.00000 .00000 .00000
Integration Limits : ILA = -.14915625E+02 ILB = .13504404E+02
Iteration 1) : PF = .5370230737E-01
```

```
>>> THICKNESS 1 LOCATION 1 FAILURE MODE 6"TS" MCI 2
STRENGTH: NORMAL : 4000.00000 1000.00000 .00000 .00000
STRESS : NORMAL : 2000.00000 500.00000 .00000 .00000
DN-GUST: UNIFORM : 200.0000000 200.0000000 .0000000 .0000000
UP-GUST: UNIFORM : 200.0000000 200.0000000 .0000000 .0000000
Iteration 2): Time = 360.0 Temp = 160.0
Event type = GUST : SHIFT = .00000
STRESS : NORMAL : 2000.00000 500.00000 .00000 .00000
Mfg Defect Scale Factor = 8.000000000000000E-001
Event type = DEFECT: SCALE = .80000
STRENGTH: NORMAL : 3200.00000 800.00000 .00000 .00000
Integration Limits : ILA = -.12412500E+02 ILB = .13504404E+02
Iteration 2) : PF = .1016870095E+00
```

```
>>> THICKNESS 1 LOCATION 1 FAILURE MODE 6"TS" MCI 3
STRENGTH: NORMAL : 4000.00000 1000.00000 .00000 .00000
```

STRESS : NORMAL : 2000.00000 500.00000 .00000 .00000
 DN-GUST: UNIFORM : 200.0000000 200.0000000 .0000000 .0000000
 UP-GUST: UNIFORM : 200.0000000 200.0000000 .0000000 .0000000
 Iteration 3): Time = 360.0 Temp = -65.0
 Event type = GUST : SHIFT = 200.00000
 STRESS : NORMAL : 2200.00000 500.00000 .00000 .00000
 Mfg Defect Scale Factor = 8.000000000000000E-001
 Event type = DEFECT: SCALE = .80000
 STRENGTH: NORMAL : 3200.00000 800.00000 .00000 .00000
 Integration Limits : ILA = -.12812500E+02 ILB = .13504404E+02
 Iteration 3) : PF = .1445727829E+00

>>> THICKNESS 1 LOCATION 1 FAILURE MODE 6"TS" MCI 4
 STRENGTH: NORMAL : 4000.00000 1000.00000 .00000 .00000
 STRESS : NORMAL : 2000.00000 500.00000 .00000 .00000
 DN-GUST: UNIFORM : 200.0000000 200.0000000 .0000000 .0000000
 UP-GUST: UNIFORM : 200.0000000 200.0000000 .0000000 .0000000
 Iteration 4): Time = 360.0 Temp = 160.0
 Event type = GUST : SHIFT = 200.00000
 STRESS : NORMAL : 2200.00000 500.00000 .00000 .00000
 Mfg Defect Scale Factor = 1.000000000000000
 Event type = DEFECT: SCALE = 1.00000
 STRENGTH: NORMAL : 4000.00000 1000.00000 .00000 .00000
 Integration Limits : ILA = -.14915625E+02 ILB = .13504404E+02
 Iteration 4) : PF = .5370230737E-01

>>> THICKNESS 1 LOCATION 1 FAILURE MODE 6"TS" MCI 5
 STRENGTH: NORMAL : 4000.00000 1000.00000 .00000 .00000
 STRESS : NORMAL : 2000.00000 500.00000 .00000 .00000
 DN-GUST: UNIFORM : 200.0000000 200.0000000 .0000000 .0000000
 UP-GUST: UNIFORM : 200.0000000 200.0000000 .0000000 .0000000
 Iteration 5): Time = 360.0 Temp = -65.0
 Event type = GUST : SHIFT = .00000
 STRESS : NORMAL : 2000.00000 500.00000 .00000 .00000
 Mfg Defect Scale Factor = 1.000000000000000
 Event type = DEFECT: SCALE = 1.00000
 STRENGTH: NORMAL : 4000.00000 1000.00000 .00000 .00000
 Integration Limits : ILA = -.14515625E+02 ILB = .13504404E+02
 Iteration 5) : PF = .3681912260E-01

>>> THICKNESS 1 LOCATION 1 FAILURE MODE 6"TS" MCI 6
 STRENGTH: NORMAL : 4000.00000 1000.00000 .00000 .00000
 STRESS : NORMAL : 2000.00000 500.00000 .00000 .00000
 DN-GUST: UNIFORM : 200.0000000 200.0000000 .0000000 .0000000
 UP-GUST: UNIFORM : 200.0000000 200.0000000 .0000000 .0000000
 Iteration 6): Time = 360.0 Temp = 160.0
 Event type = GUST : SHIFT = 200.00000
 STRESS : NORMAL : 2200.00000 500.00000 .00000 .00000
 Mfg Defect Scale Factor = 8.000000000000000E-001
 Event type = DEFECT: SCALE = .80000
 STRENGTH: NORMAL : 3200.00000 800.00000 .00000 .00000
 Integration Limits : ILA = -.12812500E+02 ILB = .13504404E+02
 Iteration 6) : PF = .1445727829E+00

>>> THICKNESS 1 LOCATION 1 FAILURE MODE 6"TS" MCI 7
 STRENGTH: NORMAL : 4000.00000 1000.00000 .00000 .00000
 STRESS : NORMAL : 2000.00000 500.00000 .00000 .00000

DN-GUST: UNIFORM : 200.0000000 200.0000000 .0000000 .0000000
 UP-GUST: UNIFORM : 200.0000000 200.0000000 .0000000 .0000000
 Iteration 7): Time = 360.0 Temp = -65.0
 Event type = GUST : SHIFT = 200.00000
 STRESS : NORMAL : 2200.00000 500.00000 .00000 .00000
 Mfg Defect Scale Factor = 8.000000000000000E-001
 Event type = DEFECT: SCALE = .80000
 STRENGTH: NORMAL : 3200.00000 800.00000 .00000 .00000
 Integration Limits : ILA = -.12812500E+02 ILB = .13504404E+02
 Iteration 7) : PF = .1445727829E+00

>>> THICKNESS 1 LOCATION 1 FAILURE MODE 6"TS" MCI 8
 STRENGTH: NORMAL : 4000.00000 1000.00000 .00000 .00000
 STRESS : NORMAL : 2000.00000 500.00000 .00000 .00000
 DN-GUST: UNIFORM : 200.0000000 200.0000000 .0000000 .0000000
 UP-GUST: UNIFORM : 200.0000000 200.0000000 .0000000 .0000000
 Iteration 8): Time = 360.0 Temp = -65.0
 Event type = GUST : SHIFT = 200.00000
 STRESS : NORMAL : 2200.00000 500.00000 .00000 .00000
 Mfg Defect Scale Factor = 8.000000000000000E-001
 Event type = DEFECT: SCALE = .80000
 STRENGTH: NORMAL : 3200.00000 800.00000 .00000 .00000
 Integration Limits : ILA = -.12812500E+02 ILB = .13504404E+02
 Iteration 8) : PF = .1445727829E+00

>>> THICKNESS 1 LOCATION 1 FAILURE MODE 6"TS" MCI 9
 STRENGTH: NORMAL : 4000.00000 1000.00000 .00000 .00000
 STRESS : NORMAL : 2000.00000 500.00000 .00000 .00000
 DN-GUST: UNIFORM : 200.0000000 200.0000000 .0000000 .0000000
 UP-GUST: UNIFORM : 200.0000000 200.0000000 .0000000 .0000000
 Iteration 9): Time = 360.0 Temp = 160.0
 Event type = GUST : SHIFT = 200.00000
 STRESS : NORMAL : 2200.00000 500.00000 .00000 .00000
 Mfg Defect Scale Factor = 8.000000000000000E-001
 Event type = DEFECT: SCALE = .80000
 STRENGTH: NORMAL : 3200.00000 800.00000 .00000 .00000
 Integration Limits : ILA = -.12812500E+02 ILB = .13504404E+02
 Iteration 9) : PF = .1445727829E+00

>>> THICKNESS 1 LOCATION 1 FAILURE MODE 6"TS" MCI 10
 STRENGTH: NORMAL : 4000.00000 1000.00000 .00000 .00000
 STRESS : NORMAL : 2000.00000 500.00000 .00000 .00000
 DN-GUST: UNIFORM : 200.0000000 200.0000000 .0000000 .0000000
 UP-GUST: UNIFORM : 200.0000000 200.0000000 .0000000 .0000000
 Iteration 10): Time = 360.0 Temp = 160.0
 Event type = GUST : SHIFT = 200.00000
 STRESS : NORMAL : 2200.00000 500.00000 .00000 .00000
 Mfg Defect Scale Factor = 8.000000000000000E-001
 Event type = DEFECT: SCALE = .80000
 STRENGTH: NORMAL : 3200.00000 800.00000 .00000 .00000
 Integration Limits : ILA = -.12812500E+02 ILB = .13504404E+02
 Iteration 10) : PF = .1445727829E+00

Statistics Summary for Monte Carlo Iterations -
 Averages --> : Time = 360.0 Temp = 47.5 PF = .1113347444E+00
 Std Devs --> : Time = .0 Temp = 118.6 PF = .4584667141E-01

Probability of Failure:

Thickness Adjustment 1 = 100.0 Percent

Loc	Failure Modes						Total
	CM	SM	TM	CS	SS	TS	
Tot	.000000E+00	.000000E+00	.000000E+00	.000000E+00	.000000E+00	.000000E+00	
.111335E+00	.111335E+00						
All					.111335E+00	.111335E+00	
All	CM	SM	TM	CS	SS	TS	Total
1					.111335E+00	.111335E+00	

Summary of Manufacturing Defects for Thickness Adjustment 1: 100.0 Percent

(Occurred & Used)

	Total	CM	SM	TM	CS	SS	TS
ALL LOCs	7 7						7 7
Delam	7 7						7 7
All	7 7						7 7
Delam	7 7						7 7

Count of integrations = 10

Failure Mode "TS" Thickness = .1000000 Location = 1
 The number of Monte Carlo loop iterations = 10
 The average time = .360.0000
 The average temperature = 47.5000
 The average probability of failure = .11133474444779E+00

Manufacturing Defects:

Defect Type	R-factor	Occurred	Used
1) Delam	.800	7	7

Operational Defects:

Defect Type	R-factor	Occurred	Used
-------------	----------	----------	------

*** MONTE OUTPUT: END-OF-FILE ***

Elapsed time for this run is .0 minutes.

Grand total elapsed time for this run is .0 minutes.